# AIR FORCE INSTITUTE OF TECHNOLOGY

## AIR UNIVERSITY
## UNITED STATES AIR FORCE

PSYCHOLOGICAL CORRELATES OF A MODEL OF

THE HUMAN VISUAL SYSTEM

THESIS

GE/EE/71S-2 Arthur P. Ginsburg

## SCHOOL OF ENGINEERING



**WRIGHT-PATTERSON AIR FORCE BASE, OHIO**

# DISCLAIMER NOTICE

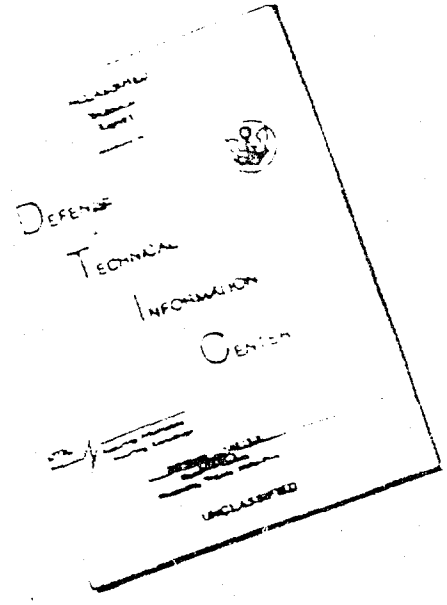


THIS DOCUMENT IS BEST QUALITY AVAILABLE. THE COPY FURNISHED TO DTIC CONTAINED A SIGNIFICANT NUMBER OF PAGES WHICH DO NOT REPRODUCE LEGIBLY.

# PSYCHOLOGICAL CORRELATES OF A MODEL OF THE HUMAN VISUAL SYSTEM

THESIS

GE/EE/71S-2

Arthur P. Ginsburg
2nd Lt USAF

Unclassified

Security Classification

DOCUMENT CONTROL DATA - R & D

(Security classification of title, body of abstract and indexing annotation must be entered when the overall report is classified)

1. ORIGINATING ACTIVITY (Corporate author)

Air Force Institute of Technology (AFIT-EN)
Wright-Patterson AFB, Ohio 45433

2a. REPORT SECURITY CLASSIFICATION

Unclassified

2b. GROUP

3. REPORT TITLE

Psychological Correlates of a Model of the Human Visual System

4. DESCRIPTIVE NOTES (Type of report and inclusive dates)

AFIT Thesis

5. AUTHOR(S) (First name, middle initial, last name)

Arthur P. Ginsburg
2nd Lt USAF

| 6. REPORT DATE | 7a. TOTAL NO. OF PAGES | 7b. NO. OF REFS |
|---|---|---|
| June 1971 | 116 | 52 |

| 8a. CONTRACT OR GRANT NO. | 9a. ORIGINATOR'S REPORT NUMBER(S) |
|---|---|
| b. PROJECT NO. | GE/EE/71S-2 |
| c. | 9b. OTHER REPORT NO(S) (Any other numbers that may be assigned this report) |
| d. | |

10. DISTRIBUTION STATEMENT This document has been approved for public release and sale; its distribution is unlimited.

11. SUPPLEMENTARY NOTES

Details of illustrations in this document may be better studied on microfiche

12. SPONSORING MILITARY ACTIVITY

13. ABSTRACT

A model of the human visual system is investigated for psychological correlates. A priori hypotheses from the model concerned with human identification of defocused letters as well as identification of rotated letters have been validated with the computer model. Gestalt principles of similarity, proximity, closure, and figure-ground perception as well as geometric illusions are explained in terms of spatial filter bandwidth using the optics homolog. The experimental results have allowed postulates which extend the model by means of another cortical transform and a spatial filter shape which is also psychologically correlated. It is further postulated that the human perceptual space is the image domain from spatially filtered transforms of object forms. It is concluded that the model provides a means of obtaining quantitative psychological correlates of the human visual system. Recommendations are made for additional investigations concerning psychological correlates.

DD FORM 1 NOV 65 1473

Unclassified

Security Classification

| KEY WORDS | LINK A | | LINK B | | LINK C | |
|---|---|---|---|---|---|---|
| | ROLE | WT | ROLE | WT | ROLE | WT |
| Pattern Recognition | | | | | | |
| Biological Model | | | | | | |
| Human visual System | | | | | | |
| Fourier Transform | | | | | | |
| Spatial Filtering | | | | | | |
| Computer Model | | | | | | |
| Fourier Optics | | | | | | |
| Psychological Correlates | | | | | | |
| Gestalt Principles | | | | | | |
| Geometric illusions | | | | | | |

# PSYCHOLOGICAL CORRELATES OF A MODEL OF THE HUMAN VISUAL SYSTEM

THESIS

Presented to the Faculty of the School of Engineering

of the Air Force Institute of Technology

Air University

in Partial Fulfillment of the

Requirements for the Degree of

Master of Science

by

Arthur P. Ginsburg, B. S.

2nd Lt USAF

Graduate Electrical Engineering

June 1971

## Preface

This thesis represents an exploratory investigation of the Kabrisky model of the human visual system with psychological correlates. There are many psychological theories that attempt to describe perceptual processes; however, these theories tend to be restrictive in scope as well as detail. It is not fully known what pattern information is necessary for human pattern identification or why the human visual system recognizes some patterns more readily at $0^{\circ}$ and $90^{\circ}$ than at $45^{\circ}$. Additionally, it is not known how the human visual system groups dot patterns into meaningful units or why the system fails with simple geometric illusions.

This investigation is concerned with these perceptual phenomena and attempts to offer a unified explanation of them in terms of the low-pass spatial filtering used by the model.

I gratefully acknowledge the stimulating environment as well as the advice and encouragement provided by Dr. Matthew Kabrisky during this research. Also acknowledged are the critical comments provided by Capt. Joseph Carl, Sqn. Ldr. Tony Gill, Capt. Larry Goble, and Mr. Frank Maher. I am also indebted to Dr. Hans Oestricher and Lt. Fred Howard for permitting me to use their laboratory facilities as well as Tom Herbert for providing the special spatial filters and Capt. Dennis Quine for the realization of most of the photographs appearing herein. Additionally, I thank the subjects who volunteered for the psychological experiments.

Finally, but certainly not least, I owe special appreciation to my sons, David and Richard, who patiently did without a father during this research period and to my wife, Mary, who spent many hours rechecking the voluminous subject data.

Arthur P. Ginsburg

Contents

## Contents

## List of Figures

# List of Tables

## Abstract

A model of the human visual system is investigated for psychological correlates. A *priori* hypotheses from the model concerned with human identification of defocused letters as well as identification of rotated letters have been validated with the computer model. Gestalt principles of similarity, proximity, closure, and figure-ground perception as well as geometric illusions are explained in terms of spatial filter bandwidth using the optics homolog. The experimental results have allowed postulates which extend the model by means of another cortical transform and a spatial-filter shape which is also psychologically correlated. It is further postulated that the human perceptual space is the image domain from spatially filtered transforms of object forms. It is concluded that the model provides a means of obtaining quantitative psychological correlates of the human visual system. Recommendations are made for additional investigations concerning psychological correlates.

# PSYCHOLOGICAL CORRELATES OF A MODEL OF THE HUMAN VISUAL SYSTEM

## I. Introduction

### Background

The way that the cortex processes human perceptual information is largely unknown. However, there have been numerous models proposed to explain possible cortical information processing of the human visual system. The two basic approaches that have been used to model nervous systems will be termed microscopic and macroscopic. The microscopic approach is concerned with the modeling of neurons into nerve nets or neuromimes to determine the operating principles of nervous systems, e.g., the McCullock and Pitts Model (Ref 43:145-172). The macroscopic approach is concerned with the basic structure of subsystems of the nervous system, e.g., the Kabrisky Model (Ref 26). The argument against the microscopic approach is humorously but cogently presented by Kabrisky in "Birds and Feathers - Neurons and Nervous Systems" (Ref 25). Based upon known anatomical and physiological data of the human visual system, Kabrisky investigated the mathematics that the infra-cortical structure could support. The validity of this approach is suggested by the fact that it worked. Improvements to the Kabrisky model by Radoy (Ref 42), Tallman (Refs 45 and 46), and Gill (Ref 15) have resulted in a pattern recognition algorithm based upon an adaptive low-pass spatially filtered Fourier transform that scales and classifies alpha-numeric and geometric patterns with more than 95% accuracy. Additionally, the Tallman-Radoy algorithm has been the basis for such diverse

classification problems as random one-dimensional waveforms, metal-crystal structure, speech recognition, and Chinese character recognition (Ref 16). Furthermore, the model has been extended by Blackford to include color pattern recognition capabilities with substantial success (Ref 5).

The demonstrated success of the Kabrisky model embodied by the Tallman-Raioy computer algorithm has led to a second look at the model and has prompted such questions as: Is the Kabrisky model conceptually valid? Can it provide metrics for human pattern recognition? Maher, in an initial psychological investigation of the Kabrisky model, correlated the computer model output with human output for the ranked similarity of animal forms (Ref 34). The resulting correlation coefficient of 0.961 supported the validity of the model. However, the model has prompted other hypotheses for psychological correlates. Kabrisky has suggested that cortical retention of "blurred" patterns is adequate for human identification (Ref 28:137). Additionally, the model's failure to classify patterns under rotation has suggested another correlate to human performance. This paper is concerned with exploratory investigations of these two hypotheses with the computer model. During this investigation, evidence for correlates with the Gestalt principles of perceptual organization and geometric illusions emerged and was pursued using a Fourier optics homolog. Furthermore, the model is extended with a different biologically realizable transform and spatial-filter shape.

Perhaps the greatest information concerning the perceptual organization of the human visual system has come from the psychologists. Their contribution in psychophysics, experimental paradigms, and data analysis has greatly advanced knowledge of human perception. Whereas

the psychologist cannot fully describe the mechanism for human perception, his procedures and observations offer significant clues to the engineer in designing and validating his model. Dodwell, in his book on visual pattern recognition, provides an excellent example of this approach as well as psychological theories of pattern recognition (Ref 11).

The major problem that the psychologists as well as the engineers have in pattern recognition research is that of defining a feature space in which like patterns or pattern elements cluster. Whereas the engineer is free to use any feature selection scheme that works, the psychologist is limited to metrics that must be correlated to human performance. It would entail a lengthy discussion to elaborate on the many proposed metrics of human pattern recognition; therefore, the reader is referred to an article by Brown and Owen, "The Metrics of Visual Form" (Ref 7). It is sufficient to note that to the author's knowledge, there exists no feature space that has been widely accepted based upon known metrics of visual form. A priori quantitative predictions in human perceptual research are still the exception rather than the rule. It would appear that a valid model of the human visual system would be a logical source for developing metrics of visual form. This paper will demonstrate that the low-pass spatially filtered transform domain may provide the feature space required to quantify metrics of visual form.

## Scope and Organization

The research approach reported in this paper has been that of a bioengineer interested in investigating a mathematical model of the human visual system against known psychological correlates. This is an

admittedly dangerous procedure due to the disparity of interpretations concerning psychological experimental results. However, there are gross perceptual phenomenona that have been repeatedly substantiated, e.g., human perceptual invariance to rotated patterns and Gestalt principles of perceptual organization. These perceptual phenomena have been widely studied, but the visual mechanism that produces them is not fully known. It is these gross perceptual phenomena that the author believes are important for an initial validation of a model of the human visual system. Therefore, rather than be concerned with a definitive psychological experiment to accept or reject a model (if there is one), the purpose of this investigation is to present evidence from disparate psychological experiments that when examined as a whole, will substantiate the model. This research is on an exploratory level and hopefully sets the groundwork for a more in-depth investigation of the model. This paper is also written in an attempt to bridge the gap between the bioengineer concerned with cortical models and the cognitive psychologist. With this in mind, detailed mathematical theory is omitted with a concomitant sacrifice of rigor for a more heuristic development. Adequate references are made for the reader interested in additional detail.

To orient the reader, the next section contains the biological background and assumptions as well as the mathematics of the model, computer and optics simulation, and spatial filtering. The following four sections are concerned with the experiments of the model against psychological correlates: recognition of defocused letters, recognition of rotated letters, Gestalt principles of perception, and geometric illusions. Each of these sections contains a brief introduction orienting the reader to the specific objectives of each experiment, followed by

methods, results, and discussions. The experimental results and psychological correlates that allow the model to be extended in terms of spatial filter shape are then presented, followed by an experiment they suggest. The Kabrisky model is then extended by means of another transform as well as correlated with a contemporary psychological theory of the human visual system. Finally, the paper will present the conclusions and recommendations. Subject data and computer data in graph as well as table form are contained in the appendices.

# II. The Kabrisky Model of the Human Visual System

## Introduction

This section contains an overview of the human visual system--the infra-cortical structure and the mathematics it could support. A heuristic approach to the cortical computations will lead to the normal form of the two-dimensional discrete Fourier Transform. Additionally, the computer simulation of the model as well as the optical homolog and spatial filtering are discussed.

## Biological Background

In modeling any complex system, certain assumptions must be made if the model is to be physically realizable. However, the use of assumptions is not necessarily a negative action; indeed, they may highlight the key concepts as well as important design areas for future developments. Therefore, Kabrisky's model of the human visual system assumes monocular, monochromatic, non-temporal as well as exclusively foveal vision. Since human pattern recognition is easily performed with the preceding constraints, the assumptions are conceptually valid and do allow a computer realizable approximation for a model of the human visual system.

All visual systems must initially encode the external visual field in a manner compatible to subsequent processing mechanisms. The retina of the eye, consisting of rods and cones, provides the initial encoding in the form of pulse-frequency electrical information. However, the retina does not provide uniform visual acuity. Greatest visual acuity is limited to the fovea--the retinal region containing the most dense populations of cones. The physical size of the central fovea is

approximately 24 seconds of arc, much smaller than approximately 160° of the total visual field (Ref 38). The foveal information, transmitted via the optic nerve and the lateral geniculate body, is mapped homeomorphically, i.e., adjacency is preserved at the primary visual cortex (Broadmann's area 17) as illustrated in Fig. 1. The importance of the

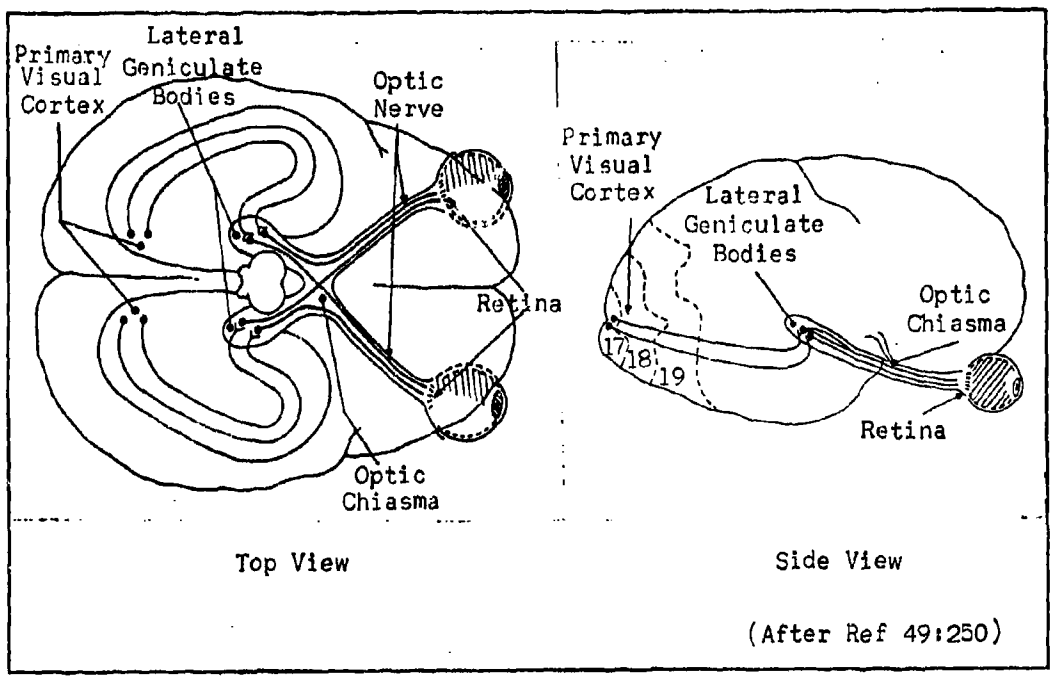


Fig. 1

The Human Visual System

foveal information is expressed by an apparent one-to-one mapping of the relatively small foveal image onto nearly half of the primary visual cortex (Ref 49:348). With the exception of some edge enhancement, little information is believed to occur from the fovea to the primary visual cortex (Ref 28:122 and Ref 50). Therefore, it appears that the pulse-frequency coded representation of the foveal visual field is mainly preserved at the primary visual cortex for higher cortical processing.

The human cortex is structurally a flat thin sheet, constructed of relatively independent small columnar units. Kabrisky calls these columnar units "basic computational units" or BCE's (Ref 26:39). Neurophysiological evidence confirming the existence of BCE's in cat and monkey cortex has come from experiments by Huble and Wiesel (Refs 23 and 50). Whereas the former physiology is well known, the details of the cortical connectivity must be conjectured. A glance at the cortical neural structure clearly reveals the problem. The dense and apparently random interconnectivity has not been amenable to known neurophysiological mapping techniques. Therefore, the mapping of this dense interconnectivity to different cortical areas can only be deduced from such experiments as that performed by Dusser de Barenne and McCulloch (Ref 12). When a pinhead strichnine spot was placed in the primary visual cortex (area 17), random strichnine spikes appeared in the association visual cortex (area 18). Whereas this seemingly random transmission from one cortical area to another suggests little to the physiologist, it suggests a mathematical transform correlate to the engineer.

Model Developments from the Biology

The preceding biological investigation led Kabrisky to conceptualize the cortical areas 17 and 18 as densely connected two-dimensional sheets as illustrated by Fig. 2. This conceptualization allowed Kabrisky to suggest that human two-dimensional pattern recognition could be based upon cross-correlation between area 17 and area 18. However, slight variations in the input pattern easily faults a pattern recognition scheme based upon cross-correlation. Additionally, a cross-correlation scheme requires a prohibitive amount of storage space for pattern memory. To overcome these problems, Kabrisky suggested the two-dimensional

Fourier transform as a possible cortical transform (Ref 26:82). Radoy demonstrated the validity of that concept in classifying simple patterns

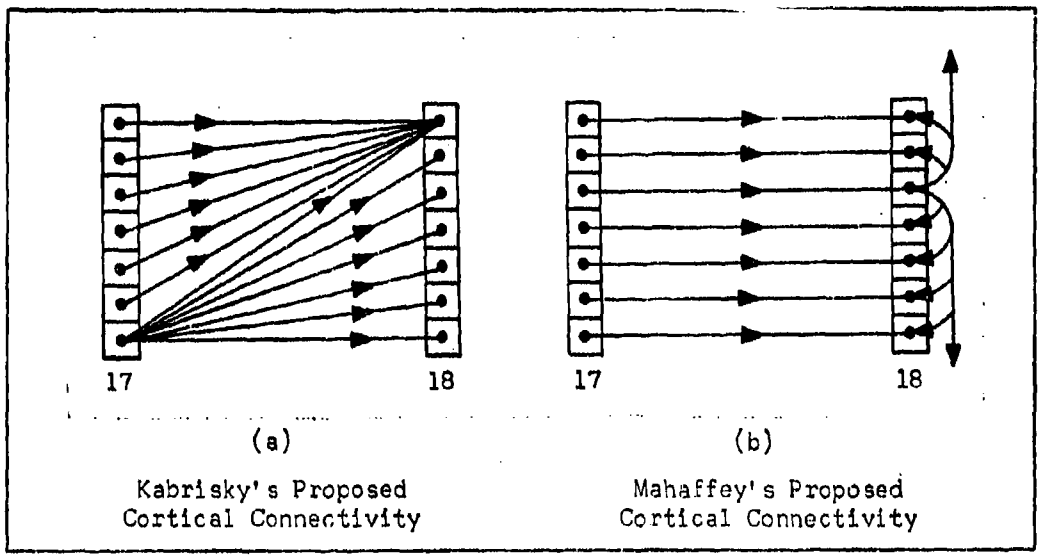


Fig. 2

The Kabrisky and Mahaffey Cortical Schemes
(Arrows Indicate Information Flow Direction)

with just the low spatial harmonics of the Fourier transform by cross-correlation in the transform domain (Ref 41). Tallman expanded Radoy's work and developed a pattern recognition scheme based upon low-pass adaptive spatial filtering (Refs 46 and 47). Gill, using a phychologically correlated moment technique, extended Tallman's algorithm to include pattern scaling (Ref 15).

It can be noted that the cortical scheme of the Kabrisky model could support other mathematical transforms. This observation led Carl to demonstrate that the sequency domain of the Walsh transform was qualitatively equal to the frequency domain of the Fourier transform in similar pattern recognition tasks (Ref 8). Subsequent investigations have led Kabrisky and Carl to report a class of densely connected transforms having unique sequency/frequency interpretations that are amenable

to low-pass spatial filtering techniques (Ref 29). Based upon a different interpretation of the cortical structure, Mahaffey has reported a less densely connected transform, illustrated by Fig. 2b, that does a Fourier-like transform on the surface of area 18 (Ref 33). It is intuitively satisfying to note that variations of mathematical transforms as well as cortical structure have yielded qualitatively similar results. Further research, primarily in the neurophysiological area, will be required to determine "the" human cortical transform or transforms.

Mathematics of the Model: the Fourier Transform

Consider a visual pattern composed of grey levels, pulse-frequency coded from the retina. The pulse-frequency coding can be considered to be a two-dimensional intensity sampling of the visual pattern. Without a loss of generality, let the sampled pattern, $p(x,y)$, be a two-dimensional square array over the visual field coordinates $(X,Y)$. Let $t(u,v,x,y)$ be some cortical function acting at a square BCE array $(U,V)$ between cortical areas 17 and 18, which when multiplied by $p(x,y)$, transforms $p(x,y)$ in some unique way. Thus, the transformed visual field at area 18 may be expressed as

$$P(u,v) = \sum_X \sum_Y p(x,y)\ t(u,v,x,y) \qquad (1)$$

Let the original visual pattern be obtained by an inverse transform $t^{-1}(u,v)$ such that

$$p(x,y) = \sum_U \sum_V P(u,v)\ t^{-1}(u,v,x,y) \qquad (2)$$

If one considers this inverse transformation to occur between area 18

and area 19, then the original pattern is now considered to be a reconstructed image at the higher cortical level. The advantages of transforming and reconstructing the pattern are realized when the transformed pattern is spatially filtered and this will be discussed in later sections. Whereas the reconstructed image is an isometry of the spatially filtered transform and adds no additional information for a pattern recognition algorithm, it does illustrate more meaningfully what the spatial filtering accomplishes with regard to the original pattern features.

Formalizing the preceding concepts in terms of matrix notation, let

$[p]$ = pattern matrix

$[T]$ = transform matrix

$[P]$ = transformed pattern matrix

where each matrix is an N×N square array.

Then by matrix multiplication

$$[P] = [T]\,[p]\,[T]^{T} \tag{3}$$

and if $[T]$ has an inverse, then the inverse transform is

$$[p] = [T]^{-1}\,[P]\,[T]^{-1} \tag{4}$$

If $[T]$ is based upon complex exponentials such that

$$[T] = \exp(-j\,\frac{2\pi uv}{N}) \tag{5}$$

then

$$[T]^{-1} = \frac{1}{N}\,[T]^{*} \tag{6}$$

where $[T]^*$ is the complex conjugate of $[T]$ and $[T]$ is the finite, discrete two-dimensional Fourier Transform of $[P]$ (Ref 29).

The two-dimensional finite, discrete Fourier Transform pair is usually expressed as

$$P(u,v) = \sum_{x=1}^{X} \sum_{y=1}^{Y} p(x,y) \exp\left[-j2\pi\left(\frac{xu}{X} + \frac{yv}{Y}\right)\right] \tag{7}$$

$$p(x,y) = \frac{1}{XY} \sum_{u=-U}^{U} \sum_{v=-V}^{V} P(u,v) \exp\left[j2\pi\left(\frac{xu}{X} + \frac{yv}{Y}\right)\right] \tag{8}$$

where $X = 2U + 1$, $Y = 2V + 1$ and $2\pi xu/X$, $2\pi yv/Y$ are the spatial frequencies (cycles per unit length) in the Fourier Transform plane. The properties of the Fourier Transform pair are fully discussed in Ref 46.

Let

$$z = 2\pi\left(\frac{xu}{X} + \frac{yv}{Y}\right) \tag{9}$$

Then, Eq (7) becomes

$$P(u,v) = \sum_{x=1}^{X} \sum_{y=1}^{Y} p(x,y) \exp(-jz) \tag{10}$$

Using Euler's Identity, Eq (10) becomes

$$P(u,v) = \sum_{x=1}^{X} \sum_{y=1}^{Y} p(x,y)(\cos z - j \sin z)$$

$$= \sum_{x=1}^{X} \sum_{y=1}^{Y} p(x,y) \cos z - j \sum_{x=1}^{X} \sum_{y=1}^{Y} p(x,y) \sin z \tag{11}$$

Thus, the Fourier Transform of an intensity pattern $p(x,y)$ can be

considered to be the summation of discrete points obtained from sine and cosine grids of varying frequency and orientations superimposed on the pattern $p(x,y)$, i.e., $P(u,v)$ is a weighted sum of $p(x,y)$. The specific weighting of $p(x,y)$ is determined by the transform. Kabrisky and Carl (Ref 29) have suggested that transforms need only two properties for useful image processing: 1) unique sequency/frequency interpretation and 2) dense connectivity whereby energy is localized, i.e., relatively few spectral components are large. Thus, the weighting process is indeed very special. In the case of the Fourier Transform, the pattern $p(x,y)$ is decomposed into a two-dimensional spectrum whereby each spectral component corresponds to the amount of energy contained in the pattern components. Furthermore, the energy from larger pattern features is localized in the lower spectral components (low spatial frequencies), whereas the energy from the smaller pattern features is found mainly in the higher spectral components (high spatial frequencies). This concept is illustrated in a later section.

## The Computer Model

The Tallman-Radoy computer algorithm utilized the preceding two-dimensional Fourier Transform to classify patterns using a linear decision function. The algorithm transforms patterns into the low-pass spatially filtered frequency domain and uses the minimum Euclidean distance between transformed patterns and stored prototypes to classify like patterns.

Tallman suggests to "visualize each pattern class as a many-faceted cloud in the image function space, whose faces are the linear hyperplanes corresponding to the Euclidean distance between prototypes of each class" (Ref 48:41). Since minimizing Euclidean distance maximizes correlation,

the Tallman-Radoy algorithm could also be considered as the cross-correlation of a spatially filtered pattern transform image with a stored prototype image.

The computer implementation of the Tallman-Radoy algorithm is illustrated by the flow diagram of Fig. 3 on page 15. Preprocessing consists of digitizing a pattern transparency onto magnetic tape by a PDP-1 computer-controlled Litton flying spot scanner. The digitized pattern is then processed by the Tallman-Radoy algorithm by an IBM 7094 digital computer. Briefly, the pattern is read-in, centered, energy normalized, and then scaled using the Gill scaling algorithm. The next procedures are to compute the pattern transform, spatial filter and dc normalize to correct for any scaling changes. The spatially filtered transform is now classified to a stored prototype. A correct pattern classification is acknowledged by computer print-out, whereas the prototype is updated if an incorrect classification occurs.

It is interesting to note that the centering process and the normalization process may be likened to human foveal centering and pupillary expansion, respectively.

The Optical Homolog

The optical processing model described herein is a homolog to the Kabrisky model. The optics fiber homolog that Radoy has suggested to mimic the visual pathways can also be achieved by collimated light (Ref 42:11-13). The following theoretical development parallels that by Pratt and Andrews (Ref 39).

Consider a coherent optical system illustrated by Fig. 4 on page 16. An object (pattern) in the xy-plane with transmittance $p(x,y)$ is illuminated by a coherent, collimated light beam normally provided by a

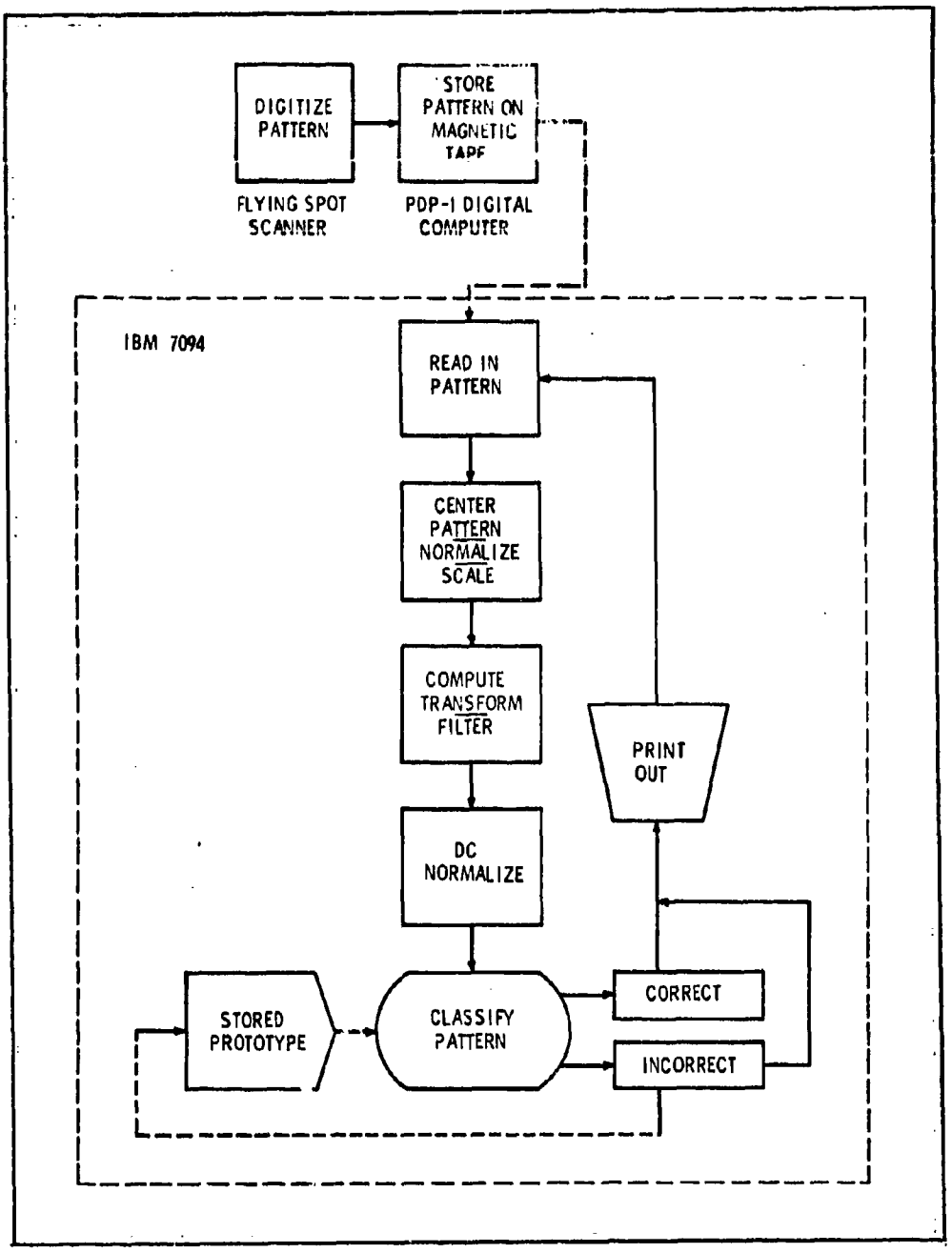


Fig. 3

Block Diagram of the Tallman-Radoy Algorithm with the Gill Scaling Routine

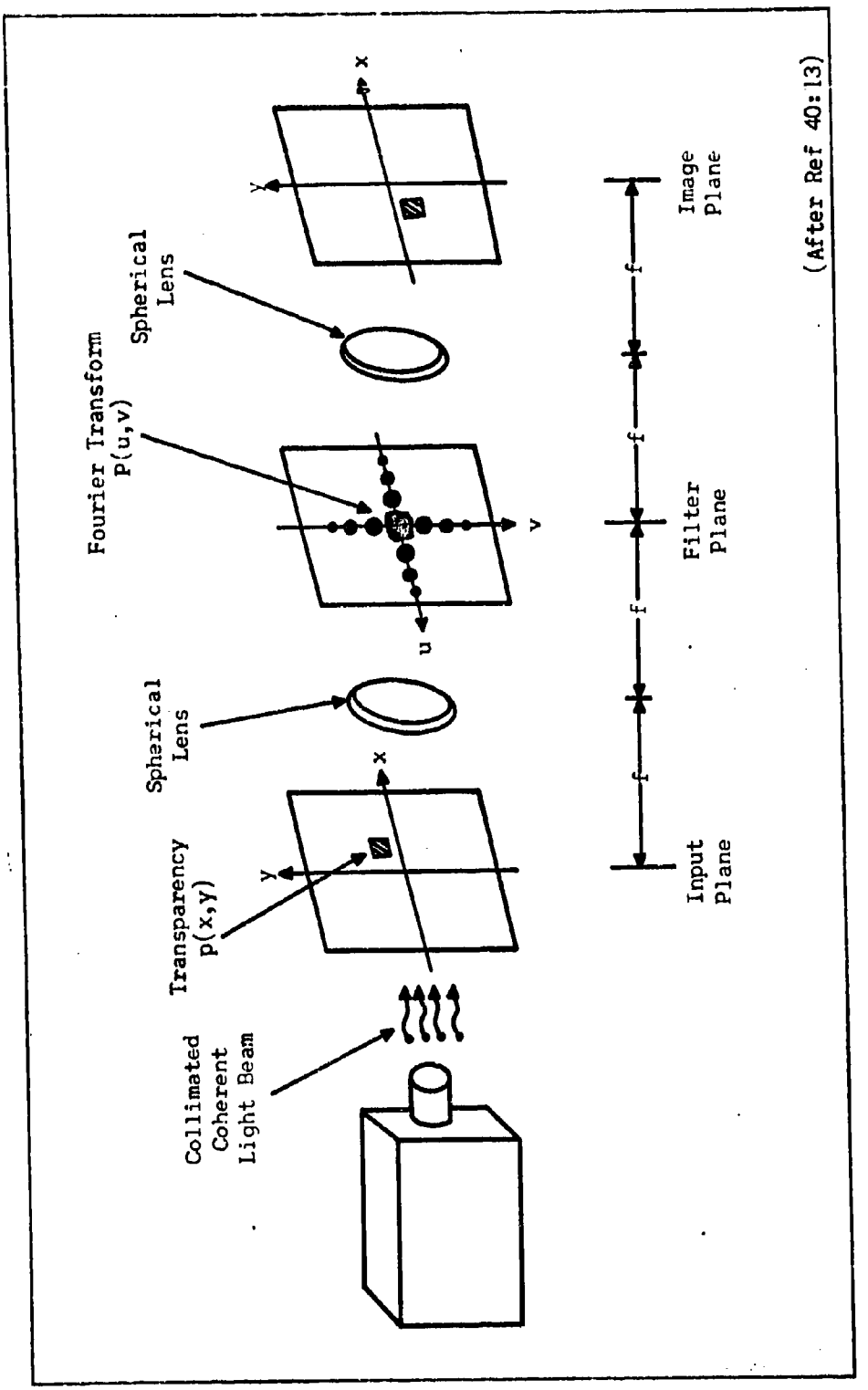


Fig. 4

A Coherent Optical System

laser. At the input plane the electric field amplitude of the light is proportional to $p(x,y)$. The first spherical lens produces an image of the object in the focal plane. The Kirchoff integral of diffraction theory describes the light electric field amplitude $P(u,v)$ in the filter plane and is given by the Fourier Transform equation

$$P(u,v) = \int_{x_o}^{X} \int_{y_o}^{Y} \left\{ p(x,y) \exp\left[ -J2\pi \left( \frac{xu + yv}{\lambda f} \right) \right] \right\} dxdy \qquad (12)$$

where $\lambda$ is the wavelength of the coherent light beam and $f$ is the focal length of the lens. The spatial frequencies in the Fourier Transform plane are given by $2\pi xu/\lambda f$, $2\pi yv/\lambda f$ and are measured in terms of cycles per unit length. An optically produced Fourier Transform as well as a three-dimensional amplitude graph of a Fourier transformed square is illustrated by Fig. 5 on page 18. A second spherical lens, inserted as in Fig. 4, will produce a second Fourier Transform that will reconstruct the image at the output plane.

Modification of the reconstructed image can be obtained by inserting a filter with a transmittance function $H(u,v)$ at the filter plane. The filter will modify the amplitude and phase of the light, thus modifying the spatial frequencies of the transformed pattern. As Pratt and Andrews point out, a major problem with conventional optical processes is the construction of filters with different transmittances (Ref 40:13). However, with computer simulation amplitude and phase functions of a filter are easily represented. Therefore, whereas the optical processing allows immediate viewing of a reconstructed image, precise control of the filtering process can be most easily attained by a computer simulation.

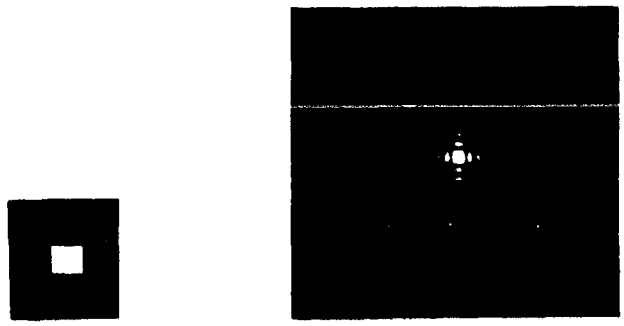

1/4 in.
Square

Diffraction Pattern
of 1/4 in. Square

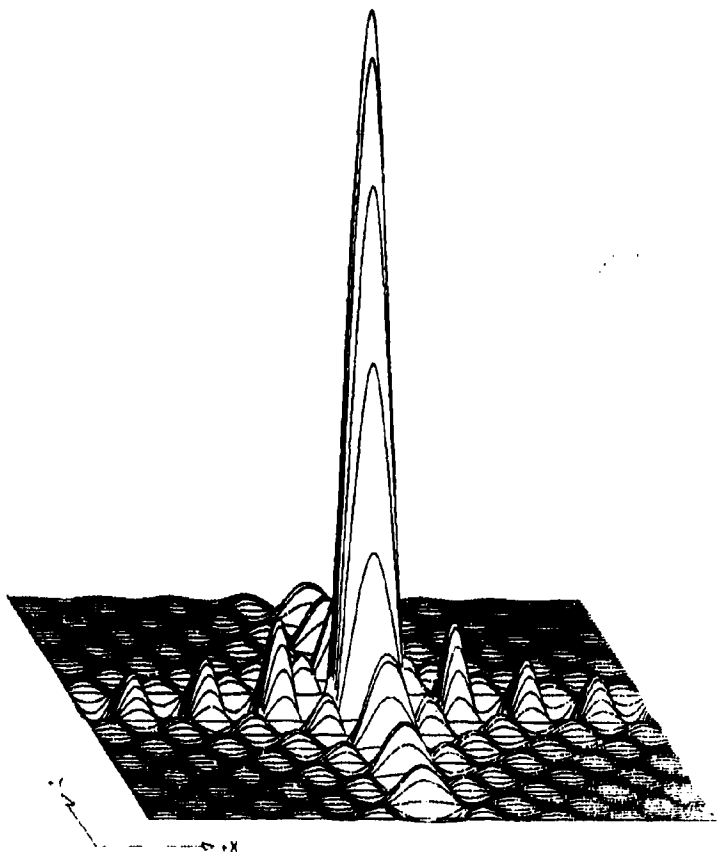


Three-Dimensional Diffraction Pattern of a Square

Fig. 5

Diffraction Patterns of a Square

The optical system used in this paper will be discussed in a later section.

Spatial Filtering

The spatial filtering techniques that have been eluded to in the previous sections are now discussed. It is the low-pass spatial filtering of the transformed pattern that has been mainly responsible for the success of the Tallman-Radoy algorithm in classifying patterns. The power of spatial filtering in the field of optics has been demonstrated by the Able-Porter experiments (Ref 18:143-146), O'Neill (Ref 37), Pratt and Andrews (Ref 40), and most recently by Lendaris and Stanley (Ref 31).

In terms of pattern classification, filtering may be generally defined as a process by which features relevant to the pattern class are separated from irrelevant features. For example, seriphs on any letter are an irrelevant feature with regard to letter identification. Low-pass spatial filtering of a Fourier transformed pattern does precisely this type of feature separation.

Spatial filtering is accomplished most easily in the frequency domain by describing the filter as a two-valued impulse response function:

$$H(u,v) = \begin{cases} 1 & \text{at some points } (u,v) \\ 0 & \text{elsewhere} \end{cases}$$

Therefore, a reconstructed image of a spatially filtered transform is given by:

$$p_r(x,y) = P\{P(u,v)\ H(u,v)\} \tag{13}$$

which is a simple multiplicative operation in the frequency domain. Low-pass spatial filtering of the Fourier transform is accomplished by

letting $H(u,v) = 1$ at the center portions of the transform and $H(u,v) = 0$ for the rest of the transform.

In terms of the biological model, assume a Fourier-like transform at cortical area 18. Spatial filtering can be conceptualized to occur by "pre-wired" cortical connections from area 18 to area 19 that transmit just parts of the transform. Additionally, a selective attention mechanism at a higher cortical level might learn to "pay attention to" different parts of the transform at area 18. Validity for concepts such as these awaits further experimentation.

The Tallman-Radoy algorithm accomplishes low-pass spatial filtering by computing only the lower spectral components of the transform. The computer model filter sizes are designated as 3×3, 5×5, 7×7, 9×9 which pass the dc and first, the dc through second, the dc through third, and the dc through fourth spatial harmonics, respectively, as illustrated by Fig. 6, page 21.

Low-pass spatial filtering of an optically produced Fourier Transform may be achieved by putting a mask filter in the focal plane where the transform occurs. The mask filter is simply a transparent portion of an opaque material which blocks the higher spatial frequencies from contributing to the reconstructed image. The mask filters are measured in microns ($\mu$) and for the half-inch patterns presented in this paper, a 100-$\mu$, 200-$\mu$, 300-$\mu$ mask filter passed the dc and first, the dc through third, the dc through fifth spatial harmonics, respectively. The effects of spatial filtering on the letter E are illustrated using optical techniques by Fig. 7, page 21. Consider the tremendous amount of redundant information that this pattern has in terms of spatial harmonics. The original letter has theoretically infinite spatial harmonics; nevertheless, only the dc and first harmonic are required for human as well as

machine identification. Later experiments will demonstrate even more convincingly the power of low-pass spatial filtering in regard to the Kabrisky model and psychological correlates.

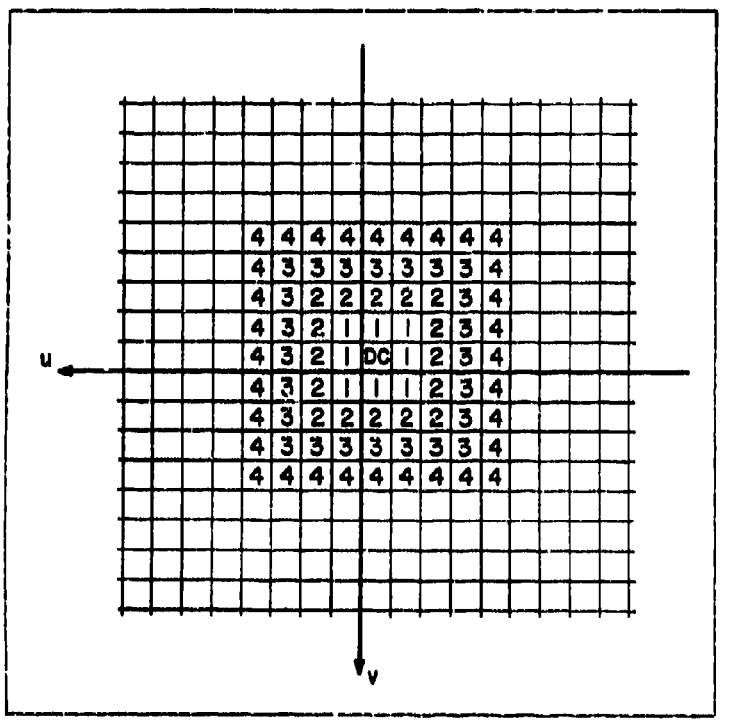


Fig. 6

Diagram of Low-Pass Spatial Filter

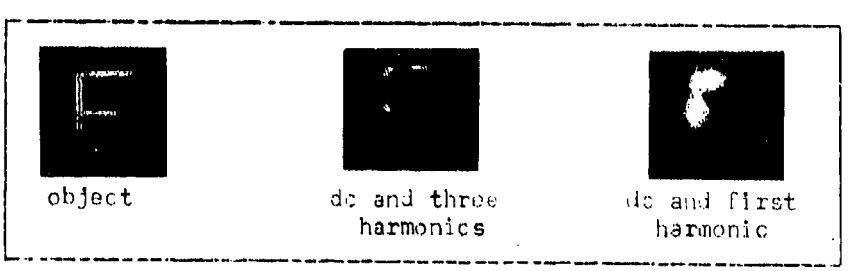


Fig. 7

Low-Pass Spatially Filtered Letter E

This concludes the introduction to the Kabrisky model and techniques used in the forthcoming experiments. However, subsequent experimental results will necessitate a return to spatial filtering theory.

## III. Identification of Defocused Letters Experiment

### Introduction

Tallman demonstrated that low-pass spatially filtered alphanumeric and geometric patterns could be correctly classified with a high degree of accuracy. This led to the hypothesis that human cortical retention of low-spatial frequency (blurred) patterns would also be adequate for identification (Ref 28:137). It is difficult to accurately correlate this hypothesis with previous psychological experimentation concerning defocused stimuli, due to the diverse defocusing schemes and different stimuli that have been used. However, this hypothesis does seem in opposition to statements such as Fredericksen's: "... when the stimulus is obscured and made ambiguous by being thrown out of focus, visual recognition is impaired" (Ref 14:1). That position implies the necessity of the high spatial frequencies that the model implies is redundant for pattern recognition.

This hypothesis was investigated by a learning task which required both long and short term memory and was based upon the span of perception method. Two subject groups were required to observe and report letter arrays--one group with normal letters and the other with defocused letters--under controlled conditions.

The span of perception method is perhaps one of the oldest psychological experimental methods. It requires the subject to report briefly presented stimulus containing multiple stimulus objects (Ref 45:902). Sperling, in investigating short term memory, demonstrated that the subjects' report of capital English letter arrays exposed for 50 msec. is invariant to letter arrays of over five letters and the spatial

arrangement of the letters (Ref 4:204). He summarized the experiment by stating: "When the subjects are asked to report all the letters of a stimulus, they can report only about five letters on the average" (Ref 4: 204). These results formed the basis of the learning task. The rational behind the experimental paradigm is that the high spatial frequencies missing from the defocused letters are redundant and should not detract from the letter identification and subsequent learning. Thus, implicit in the letter array learning is an investigation of the invariance of stimulus identification by means of different spatial frequency content. Consistent with psychological research methods, the null hypothesis is that there is no relationship between the mean learning performance with letter stimuli of high and low spatial frequency content.

Experimental Method

The subject population consisted of 10 males--nine graduate engineering students and one faculty professor, each having reported corrected or uncorrected 20/20 defect-free vision. Initially, five subjects were exposed to normal stimuli and five were exposed to defocused stimuli. The stimulus set consisted of 26, six-letter arrays (3×2) of capital, block, consonant English letters. The normal stimulus was 0.5-in. black letters on a white card which filled a 1.38 in. wide, 1.50 in. high array as Fig. 8a illustrates. The defocused stimulus was obtained by photographing optically defocused letters to approximately the fourth spatial harmonic. The fourth spatial harmonic was determined by defocusing a 0.5 in. letter V until a 0.125 in. cross section of the V could not be resolved. (The availability of the optics equipment that was used to obtain the reconstructed images reported in this paper was not known at this time.) Thus, the defocused stimulus was approximately

0.5 in. block letters on a transparent film which filled a 1.19 in. wide, 1.31 in. high array. The defocused stimulus was presented on a white card background as Fig. 8b illustrates.

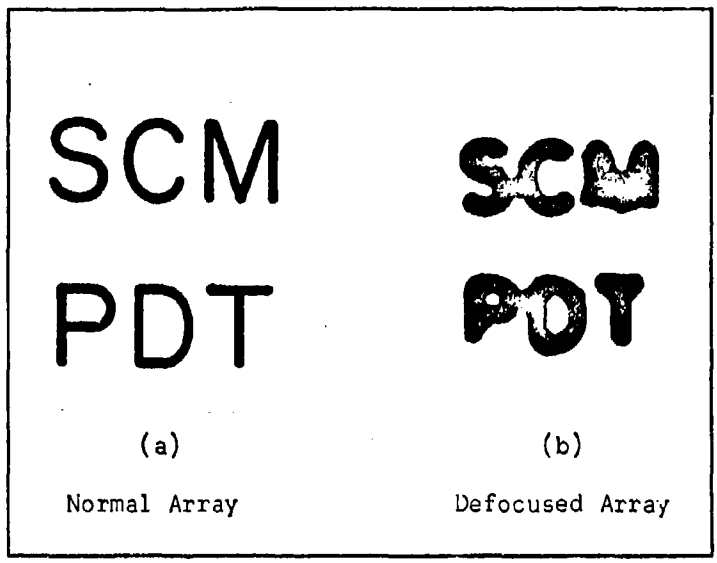


Fig. 8

Example of Normal and Defocused Letter Arrays Used for The Identification of Defocused Letters Experiment

The stimulus arrays were exposed in the Scientific Prototype (Model GB) three-channel tachistiscope shown in Fig. 9. The tachistiscope allowed precise control over stimulus exposure time (± 2%) and illumination. The luminance of the three tachistiscope channels was set at a mid-scale range of approximately 9 mL. throughout the experiment. Each subject received verbal instructions to give a forced whole response to the stimulus arrays by writing the letters he thought he saw during exposure in pre-printed 3×2 block arrays. The subject was instructed to focus on a black cross and then self-initiate the stimulus presentation by pressing a button. This initiated the stimulus presentation in the following paradigm:

1. white field pre-exposure with focusing cross for 0.5 sec.
2. stimulus array exposure for 50 msec.
3. white field post-exposure

The stimulus array was then changed as the subject wrote his response.

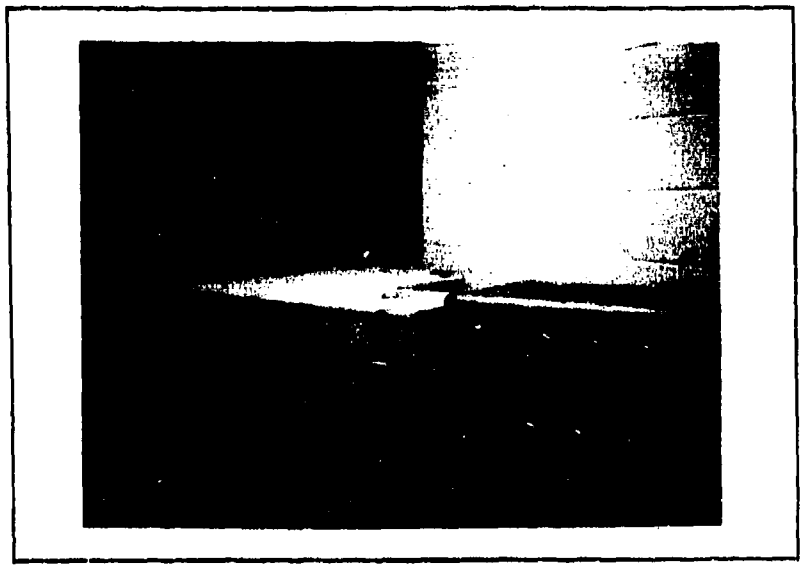

Fig. 9

Three-Channel Tachistiscope

Each subject was exposed to the same stimulus array sequence twice for three trials (Case 1). Three subjects from each group were exposed to the same stimulus arrays twice for five trials (Case 2). The stimulus arrays for each group were then switched--defocused for normal and normal for defocused--for four more trials (Case 3) resulting in a total of 20 trials.

Results

A correct subject response was considered to be a letter written in the correct array position with respect to the stimulus array. The mean

number of correct letters from all the subjects in each stimulus group per trial was plotted; the learning curves of Fig. 10 resulted. There is

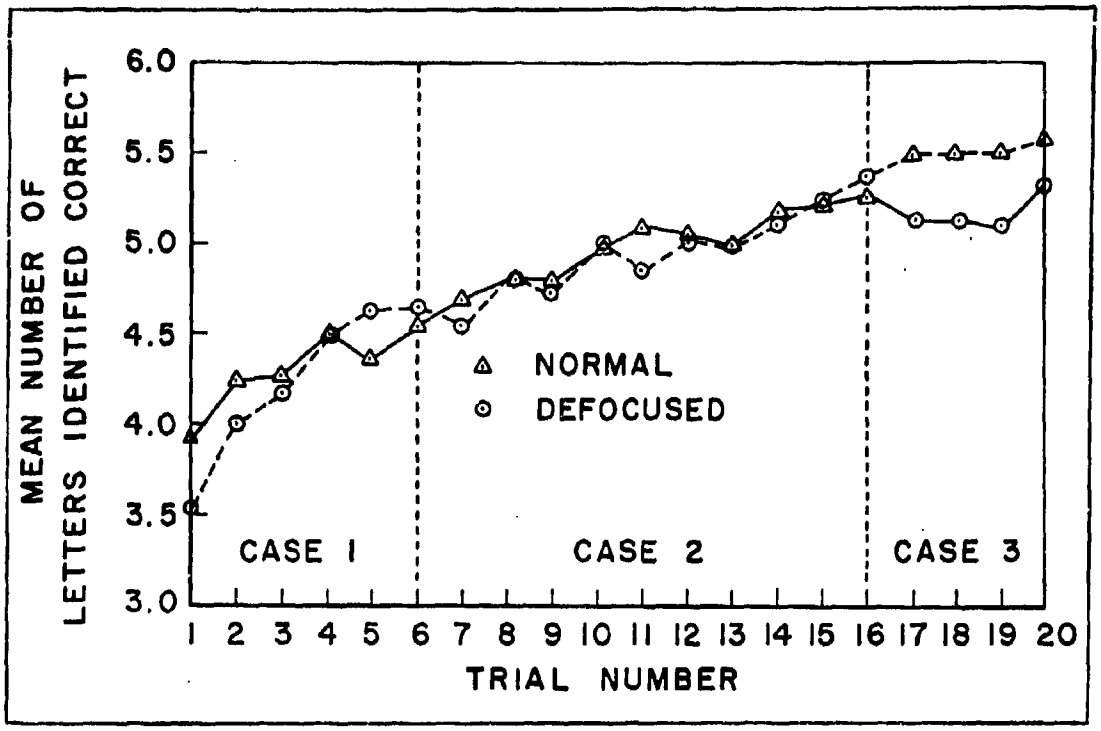


Fig. 10

Chart of Mean Number of Normal and Defocused Letters Identified Correct per Trial

less than one standard deviation of each group mean per trial, and the mean standard deviation for the 20 trials for the normal and defocused groups is 0.5552 and 0.4004, respectively. A t-test for the mean of two independent samples was computed to evaluate the mean performance of the two groups (Ref 43:165-169). The results are shown in Table I. Since the t statistics are much less than the significant values at the 0.2 level, it is concluded that there is no significant difference between the identification of the normal and defocused letters in this experiment and the null hypothesis is rejected. These results support

Table I

t-Test Results for Mean Letters Identified Correctly
for Normal and Defocused Letter Groups

| | Trials 1-6 | | Trials 1-20 | |
|---|---|---|---|---|
| | Stimuli | | | |
| | Normal | Defocused | Normal | Defocused |
| Sample Means | 4.2607 | 4.3230 | 4.8773 | 4.8427 |
| Sample Estimates of the Standard Deviations | 0.4486 | 0.2348 | 0.5522 | 0.4004 |
| Degrees of Freedom | 10 | | 38 | |
| t Statistic | 0.3015 ($p > 0.01 = 3.17$) | | 0.2269 ($p > 0.01 = 2.71$) | |

the validity of the initial hypothesis concerning the adequacy of cortical retention of blurred (low spatial frequency) patterns for pattern identification.

Discussion

These results should, perhaps, be qualified. To control the spatial frequency content of the defocused stimuli was difficult because of the photographic process used to generate them. However, comparison of the defocused letters with reconstructed image letters containing only the dc and first spatial harmonic obtained by optical Fourier transform techniques shows no significant differences as the letters "K" in Fig. 11 illustrates. This appears to be a good time to emphasize the difference between defocused stimuli and spatially filtered stimuli. It should be

noted that defocusing smears the higher spatial frequencies throughout the image plane, whereas low-pass spatial filtering of a transform

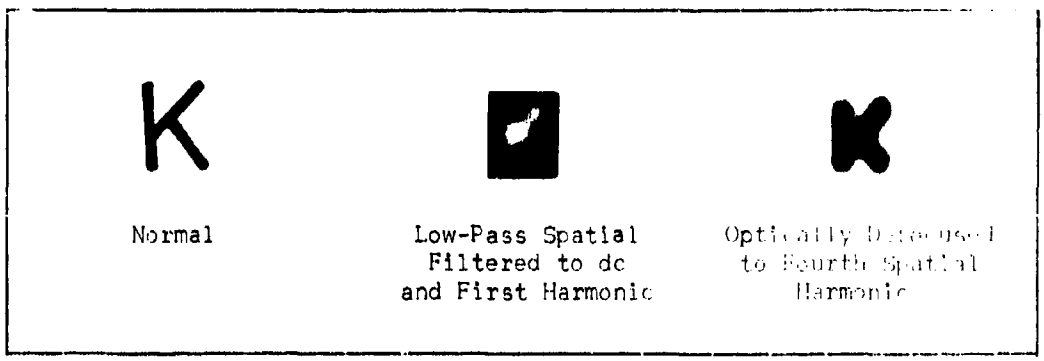


Fig. 11

Comparison of Defocused and Low-Pass Spatially Filtered Letter K

blocks the higher spatial frequencies from appearing in the reconstructed image. Other properties of the spatial filtering technique over defocusing will become apparent in more appropriate sections. Additional qualifications concerning this experiment include a single non-representative subject population and only one class of stimuli.

The experimental paradigm was devised to be consistent with the biological assumptions of the model. The tachistiscope viewing distance of the letter arrays was 42 in. Therefore, the visual angles of the normal and defocused letter arrays were $1^{o}\,53'$ and $1^{o}\,47'$, respectively, which are well under the $3^{o}\,20'$ parafoveal region reported by Polyak (Ref 38). This is consistent with the foveal assumptions of the model. The stimulus of 50 msec. is four times less than the minimum 200 msec. required for the voluntary eye scans (Ref 30:17). Therefore, the subjects were not able to "read" the letters individually but were forced

to input the letter arrays as a "whole." This point is important because it demonstrates that a feature selection process for human pattern identification can operate at a human cortical level that does not necessarily require the dissection of pattern features by eye scans for subsequent identification. Once again, this concept is compatible with the temporal assumptions of the model.

The results of this experiment tend to support the Gestalt concept that contour provides basic visual information (Ref 30:13). Another look at the stimulus arrays reveals that the characteristics of the normal and defocused letters obviate letter recognition based upon pattern template matching or edge detection. If contour were not the major factor in identifying the letters in the arrays, then one would expect that the detail and edge contrast difference between the two stimuli would have resulted in different learning curves. However, this was not the result. Therefore, it is suggested that the high spatial frequencies that do affect detail and edge contrast are redundant information for letter identification, whereas the low spatial frequencies that provide contour contain the necessary information for letter identification.

It is concluded that these results tend to validate the model and further investigation of pattern identification via spatial frequency content is warranted. Furthermore, it is suggested that stimulus content in terms of spatial frequencies would provide a more meaningful metric that appears lacking in previously reported psychological studies of ambiguous stimuli.

# IV. Letter Identification under Rotation Experiment

## Introduction

Attneave has pointed out that an adequate theory for human form perception should not only take into account the successful perceptual tasks humans perform, but it should also account for tasks under which humans fail (Ref 2:66). Specifically then, a valid model of the human visual system should provide a metric for invariance of form perception. One method for investigating this metric is pattern rotation. Human variance in recognizing rotated forms is well known and has been widely studied (Ref 11). Since the model also fails in recognizing rotated patterns, Kabrisky hypothesized that the invariance of pattern identification could be quantitatively described by the cross-correlation of the rotated low-pass spatially filtered pattern transforms with a reference transform (personal communication). The invariance of rotation could be measured by the minimum variance of the Euclidean distance between a reference and rotated pattern transform. It will be illustrated later that the circular letter O has low variance, whereas the angular letter Z has high variance.

The human visual system is spatially polarized with recognition thresholds for lines being dependent upon their vertical, horizontal, or diagonal orientation (Ref 30:29). Hake has summarized two recognition under orientation experiments--Fitts, et al., with a study of the Ohio State metric figures and Henle with a study of partially complete nonsense figures and alphabet letters (Ref 20:71-72). The Fitts study reported recognition performance of vertically oriented bilaterally symmetrical figures being superior to horizontally oriented figures.

Henle's results strikingly demonstrate that the recognition of letters is greatly dependent upon orientation. Thus, the invariance of rotation was investigated by correlating human identification errors of a rotated letter with Euclidean distance between the low-pass spatially filtered transform of the rotated letter obtained by means of the computer model. The rationale is that letters with high Euclidean variance under rotation should correlate with high human identification errors. The null hypothesis is that there is no correlation of letter rotation invariance between these two modalites.

Experimental Method

The subject population consisted of five naive right-handed male graduate engineering students with uncorrected 20/20 defect-free vision. The stimulus set was a 26-letter English alphabet of black, unfiltered, 0.5 in. high, 0.375 in. wide capital block letters, each on a white card. Photograph negatives of the letters were used as the computer stimulus. Each of the five subjects was evaluated for three trials, each trial having a different random arrangement of the 26 letters, providing a total of 15 trials.

The letters were exposed individually in a Scientific Prototype (Model GB) three-channel tachistiscope at angles of 0, 30, 60, 90, 120, and 150 degrees. The illumination of the tachistiscope channels was set at 9 mL. and remained constant throughout the experiment.

Each subject received verbal instructions that he would be shown any capital block English letter at any angle for a brief period of time and that he was to report verbally the letter that he thought was being presented. Upon request, the subject focused within a black circle and self-initiated the letter exposure by pressing a button.

An identification threshold for each subject at each trial was obtained by the method of limits. The presentation time was increased in 0.1 msec. increments from 1.5 msec. until the subject could correctly identify a letter presentation (G, R, B, for trials 1, 2, 3, respectively). The identification threshold time remained constant during each 26-letter trial. The average identification threshold time for the 15 subjects was 3.6 msec.

A subject report was required for each letter at each of the six angles. The letters were rotated counter-clockwise (with respect to the subject) from 150° to 0° in 30° increments using rotation rig mounted on the rear of the tachistiscope. A white card containing random block lines was exposed to the subject of the 0° letter presentation and a subject report was also required. The subjects usually guessed a letter for that presentation. This allowed a letter change to be made between exposures without disrupting the presentation rhythm. When each subject was queried as to the experimental paradigm after each trial, none reported a sequential rotation of exposed letters. This technique was used in lieu of a counter-balancing technique to obtain maximum data from a minimum number of available subjects. In addition, a counter-balancing technique was not used because the learning during the three trials was considered to be minimal and may have distorted the sensitive identification error differences between adjacent angular positions.

The Euclidean distance between each letter, referenced to itself at 0°, was obtained by using a modified Tallman-Radoy computer program using a Cooley-Tukey Fast Fourier Transform (Ref 9). Since the shape and size of the spatial filter would have a great effect upon the Euclidean distance values, four low-pass circle and square spatial filters were

used: 3×3, 5×5, 7×7, and 9×9. These are the same filter sizes that have been used for previous pattern classification schemes and by Maher's psychological correlate.

## Results

The total subject identification errors are presented in Table II on the following page. The values of Euclidean distance for each letter undergoing rotation for each filter shape and filter size is given in Appendix C. A one-way analysis of variance was computed to determine the homogeneity of the subject identification errors with respect to treatment (letter orientation) as well as subject population (Ref 43: 230-237). The results are listed in Table III on page 36. The significant results of the treatment indicate that the subject identification errors were due to the treatment, i.e., there is non-subject variability. The non-significant results of the subject population indicate that the identification errors came from a homogeneous population. These results validate the experimental paradigm and allow further analysis.

The Pearson product moment coefficient of correlation (r) was computed to correlate the total subject identification errors with the Euclidean distance of each letter at angles of 0, 30, 60, and 90 degrees. Angles of 120 and 150 degrees were not used because the maximum variance of Euclidean distance occurs in a 90° arc due to symmetry properties of the Fourier transform. (This property is illustrated by the fall-off of the Euclidean distance at 120° and 150° in the Appendix C tables.) The coefficient of determination (d), where $d = r^2$, is also computed for a more valid interpretation of the correlation coefficient (Ref 43:79). The level of significance of r and d was set as 0.20, a nominal level for exploratory research (Ref 43:155). The values of r and d for each

Table II

Total Subject Identification Errors for Each Letter at Angles of 0, 30, 60, 90, 120, and 150 Degrees from the Identification of Rotated Letters Experiment

| Letter | Total Identification Errors at Each Angle for Each Letter | | | | | |
|---|---|---|---|---|---|---|
| | 0° | 30° | 60° | 90° | 120° | 150° |
| A | 9 | 13 | 12 | 10 | 12 | 13 |
| B | 9 | 10 | 9 | 7 | 10 | 13 |
| C | 10 | 13 | 14 | 13 | 13 | 14 |
| D | 3 | 7 | 6 | 9 | 8 | 8 |
| E | 7 | 9 | 8 | 9 | 10 | 12 |
| F | 7 | 15 | 15 | 14 | 13 | 14 |
| G | 9 | 10 | 10 | 10 | 12 | 12 |
| H | 9 | 9 | 8 | 8 | 11 | 15 |
| I | 5 | 9 | 9 | 9 | 10 | 12 |
| J | 11 | 10 | 11 | 11 | 11 | 13 |
| K | 11 | 9 | 10 | 11 | 13 | 14 |
| L | 5 | 7 | 8 | 8 | 10 | 10 |
| M | 5 | 6 | 6 | 6 | 7 | 12 |
| N | 6 | 8 | 5 | 5 | 5 | 10 |
| O | 6 | 4 | 4 | 5 | 4 | 4 |
| P | 5 | 7 | 10 | 9 | 11 | 13 |
| Q | 12 | 14 | 15 | 14 | 14 | 14 |
| R | 8 | 8 | 11 | 12 | 11 | 13 |
| S | 6 | 7 | 6 | 6 | 11 | 11 |
| T | 7 | 9 | 10 | 11 | 11 | 11 |
| U | 2 | 3 | 4 | 4 | 5 | 7 |
| V | 7 | 7 | 5 | 4 | 7 | 11 |
| W | 3 | 5 | 5 | 3 | 7 | 10 |
| X | 8 | 6 | 7 | 7 | 10 | 12 |
| Y | 4 | 6 | 8 | 7 | 9 | 9 |
| Z | 4 | 6 | 7 | 7 | 12 | 12 |
| Total Errors | 178 | 217 | 223 | 219 | 254 | 299 |

Table III

Analysis of Variance with Respect to Treatment and
Subject Population of Identification of Rotated Letters Experiment

Analysis of Variance
with Respect to Treatment

| | Sum of Squares | DF | Mean Square | F Ratio |
|---|---|---|---|---|
| Between Groups | 1669.77 | 5 | 333.95 | 5.93* |
| Within Groups | 1351.60 | 24 | 56.32 | |
| TOTAL | 3021.37 | 29 | | |

*p > 0.05 = 2.62
p > 0.01 = 3.90

Analysis of Variance
with Respect to Subject Population

| | Sum of Squares | DF | Mean Square | F Ratio |
|---|---|---|---|---|
| Between Groups | 924.87 | 4 | 231.22 | 2.76* |
| Within Groups | 2096.50 | 25 | 83.86 | |
| TOTAL | 3021.37 | 29 | | |

*p > 0.05 = 2.76
p > 0.01 = 4.13

filter size and shape of each letter are shown in Table IV on the following page. The 3×3 square and the 5×5 square and circle filters have 14 letters above 0.80 when the correlation coefficient is used, whereas the 7×7 square and the 9×9 square and circle filter have 13 letters above 0.80 when the coefficient of determination is used. While the null hypothesis cannot be rejected for each letter, the large number of letters with correlations above 0.80 is significant and supports the validity of the model as providing a metric for human invariance of rotation.

Discussion. An underlying assumption for the use of the Pearson product-moment coefficient of correlation is that the relationship between the two variables be linear and, as a rule, linearity can be determined by inspecting a scatter diagram (Ref 19:98-103). But this is not meaningful with a small sample size such as four that was available in correlating each letter. Thus, the coefficient of correlation results must be tempered with assumed linearity between the two variables. However, the fact that the coefficients of determination were quantitatively similar to the coefficients of correlation and represent the proportion of the variance of a variable which may be predicted by another variable tends to substantiate the results. Other qualifications that should be included are a single non-representative subject population and only one stimulus class.

The seven letters that consistently have negative coefficient of correlations are found to have the highest identification errors at $0^{o}$ and $30^{o}$. It is believed that these errors are mainly due to the experimental paradigm and could be eliminated with a counter-balancing technique. For example, the letter X was frequently mistaken for the letter Z as was the letter V for the letter A. Additionally, Conrad has demonstrated

## Table IV

Correlation Coefficients (r) and Coefficients of Determination (d)
for Each Letter, Filter Size, and Filter Shape from
The Identification of Rotated Letters Experiment

| LETTER | 3 X 3 FILTER | | | | 5 X 5 FILTER | | | | 7 X 7 FILTER | | | | 9 X 9 FILTER | | | |
|---|---|---|---|---|---|---|---|---|---|---|---|---|---|---|---|---|
| | r | | d | | r | | d | | r | | d | | r | | d | |
| | CIRCLE | SQUARE | CIRCLE | SQUARE | CIRCLE | SQUARE | CIRCLE | SQUARE | CIRCLE | SQUARE | CIRCLE | SQUARE | CIRCLE | SQUARE | CIRCLE | SQUARE |
| A | .30 | .68 | .09 | .46 | .65 | .72 | .43 | .51 | .71 | .75 | .50 | .57 | .75 | .78 | .56 | .60 |
| B | -.69 | -.45 | .47 | .20 | -.38 | -.13 | .14 | .02 | -.53 | -.37 | .28 | .14 | -.50 | .48 | .25 | .23 |
| C | .74 | .93 | .55 | .86 | .87 | .87 | .77 | .76 | .87 | .92 | .76 | .85 | .90 | .91 | .81 | .82 |
| D | .84 | .87 | .70 | .76 | .87 | .83 | .75 | .69 | .89 | .86 | .80 | .73 | .89 | .89 | .80 | .78 |
| E | .54 | .73 | .29 | .53 | .70 | .70 | .49 | .49 | .73 | .73 | .54 | .53 | .76 | .75 | .57 | .57 |
| F | .57 | .91 | .33 | .83 | .88 | .91 | .77 | .83 | .94 | .97 | .89 | .95 | .96 | .97 | .91 | .94 |
| G | .77 | .92 | .59 | .85 | .89 | .92 | .79 | .85 | .86 | .93 | .75 | .87 | .90 | .91 | .81 | .83 |
| H | -.89 | -.56 | .79 | .31 | -.74 | -.63 | .55 | .40 | -.73 | -.70 | .54 | .49 | -.73 | .70 | .54 | .49 |
| I | .72 | .95 | .51 | .91 | .87 | .92 | .76 | .84 | .92 | .95 | .84 | .90 | .96 | .98 | .92 | .96 |
| J | .17 | .08 | .03 | .01 | .09 | .10 | .01 | .01 | .03 | .02 | .00 | .00 | -.03 | .07 | .00 | .01 |
| K | .02 | .25 | .00 | .06 | -.56 | -.72 | .31 | .52 | -.71 | -.77 | .51 | .59 | -.68 | -.66 | .47 | .43 |
| L | .99 | .98 | .99 | .95 | .99 | 1.00 | .99 | 1.00 | .99 | .99 | .99 | .98 | .99 | .98 | .98 | .97 |
| M | .85 | .96 | .72 | .93 | .98 | .97 | .96 | .95 | .97 | .97 | .95 | .95 | .99 | .98 | .97 | .96 |
| N | -.01 | -.51 | .00 | .26 | -.06 | -.13 | .00 | .02 | -.02 | .04 | .00 | .00 | .05 | .02 | .00 | .00 |
| O | -.37 | -.59 | .14 | .35 | -.55 | -.63 | .30 | .40 | -.50 | -.62 | .25 | .39 | -.60 | -.65 | .36 | .42 |
| P | .85 | .97 | .72 | .93 | .96 | .95 | .92 | .90 | .94 | .92 | .87 | .85 | .92 | .92 | .85 | .85 |
| Q | .85 | .86 | .72 | .75 | .87 | .90 | .76 | .82 | .89 | .92 | .79 | .85 | .91 | .92 | .82 | .84 |
| R | .98 | .91 | .95 | .83 | .29 | .37 | .09 | .13 | .67 | .61 | .45 | .37 | -.80 | -.73 | .64 | .54 |
| S | -.23 | -.06 | .05 | .00 | -.15 | -.14 | .02 | .02 | -.14 | .05 | .02 | .00 | -.06 | -.01 | .00 | .00 |
| T | .97 | .92 | .95 | .84 | .97 | .96 | .95 | .92 | .97 | .95 | .95 | .90 | .97 | .95 | .93 | .90 |
| U | .84 | .98 | .71 | .96 | .96 | .89 | .93 | .79 | .95 | .92 | .89 | .85 | .94 | .93 | .87 | .86 |
| V | -.80 | -.80 | .64 | .64 | -.61 | -.61 | .38 | .37 | -.53 | -.52 | .28 | .27 | -.55 | .61 | .30 | .38 |
| W | .10 | .58 | .01 | .34 | .83 | .89 | .69 | .80 | .66 | .70 | .44 | .49 | .68 | .65 | .46 | .42 |
| X | -.25 | -.68 | .06 | .46 | -.70 | -.74 | .49 | .55 | -.84 | -.89 | .70 | .79 | -.90 | -.90 | .81 | .81 |
| Y | .91 | .95 | .83 | .90 | .97 | .97 | .95 | .95 | .95 | .93 | .90 | .86 | .90 | .90 | .82 | .80 |
| Z | .83 | 1.00 | .68 | .99 | .98 | .99 | .97 | .97 | .99 | .99 | .99 | .99 | .99 | .99 | .97 | .98 |
| Number of r, d > 0.80 | 10 | 14 | 4 | 12 | 14 | 14 | 7 | 10 | 13 | 13 | 9 | 13 | 13 | 13 | 13 | 13 |

that acoustic confusions exist with visually presented letters, i.e., identification errors of letters may be a function of acoustic similarity as well as structural similarity (Ref 10). This is another factor which must be considered in human letter identification errors. However, a comparison with Conrad's table of listening errors with the confusion matrices of the identification errors shown in Appendix B reveals little similarity, and the identification errors reported in this paper will be mainly assumed to be due to structural similarity.

Analysis of the filter shape with respect to the coefficient of determination reveals that the square filter exceeded the circle filter in a number of letters with values above 0.80 for the 3×3, 5×5, and 7×7 filters. The results for the 9×9 square and circle filter were equal. This is to be expected; as the filter size is increased, the higher spatial frequencies added by the square corners become less significant. The ramifications of the square filter as optimal with respect to the circle filter will be discussed in a later section.

One final point is that the Euclidean distance variations of rotated patterns can be quantified in terms of statistical variance whereby

$$V = \frac{\Sigma x^2}{N} \tag{14}$$

where x = deviation from the sample mean and N = sample size. Hence, the variance over a 90° arc, computed for the Euclidean distance at 30°, 60°, and 90° for the letters O, I, and Z are 3.35, 49.45, and 109.36, respectively. This would appear to be a meaningful metric to be used in quantifying pattern shape variations under rotation. The disparity of variance between the letters O and Z is an intuitively satisfying result

since the letter O is circular (actually, it was slightly elliptical), whereas the letter Z is highly angular.

It is concluded that the correlation results support the validity of the model in providing a metric of human invariance of form perception under rotation and further investigation is warranted.

# V. Correlates to the Gestalt Principles of Perceptual Organization and Geometric Illusion

## Gestalt Principles of Perceptual Organization

Introduction. The Gestalt psychologists have long been concerned with perceptual organizations. Werthiemer, who initiated the Gestalt movement in psychology in 1923 argued that perceptual inputs are actively organized not passively detected (Ref 50). He went on to define the principles of organization; three of them are: proximity (closest elements form groups), similarity (similar elements form groups), and closure (fragments form wholes). Additionally, he noted that the effect of proximity is stronger than the effect of similarity. Another concern of the Gestalt psychologists has been perceptual figure-ground separation, whereby the figures in the visual field are perceived as a whole, separate from the remaining field. An electrical engineering analogy is the separation of signal from noise. An important point of these principles is that they are inadvertent concomitants to pattern identification. As Evans points out, the perceptual organization ... "is accomplished without any awareness on our part and we normally take it as given" (Ref 13:4).

The Gestalt principles are criticized mainly because they are intuitive descriptions that cannot identify the perceptual factors that cause them. While computer techniques such as Zahn's (Ref 52), have been used to describe some of these principles in a rigorous mathematical way, no one--to the author's knowledge--has provided a unified explanation of all these principles with a model such as that reported in this paper. If the model is valid, then it should explain the Gestalt principles in terms of the characteristics of low-pass spatially filtered

transforms. Therefore, an initial investigation of the Gestalt principles was undertaken using Fourier optics techniques.

Research Method. A KMS Industries two-lens optical correlator was arranged to perform the Fourier transform. A helium-neon laser provided the coherent light (wavelength = $6.328 \times 10^{-4}$ mm). One-half inch dot patterns, made from pin holes in aluminum sheets, were inserted in the object plane; spatial filtering was accomplished by mask filters in the focal plane; and the reconstructed image from the inverse spatially filtered Fourier transform was obtained at the image plane. The 200 $\mu$ and 300 $\mu$ square and circle mask filters pass the dc and first three and the dc and first five spatial harmonics, respectively, when referenced to a half-inch pattern size.

The reconstructed images were photographed with Polaroid 4×5 land film (type 55P/N) by a camera inserted in the image plane. Exposure times varied from $5 \times 10^{-3}$ sec. for the brighter images to 1 sec. for the weaker images, and the laser beam was attenuated with neutral density filters for the brightest images. The changes in exposure time and attenuation can be considered to be analogs to the energy normalization used by the computer model and pupillary control of the human eye. In the following photographs, the letters a, b, and c will denote the object pattern, spatially filtered transform, and the reconstructed image, respectively; photographs of images obtained with the spatial filter tilted 45° are indicated by bt and ct (in Figs. 12 through 18).

Optical low-pass spatial filtering is normally accomplished with circular spatial filters. However, the computer model has been using square spatial filtering and since the results of the invariance of form perception under rotation appeared more significant with a square filter, optical spatial filtering was accomplished with square spatial filters.

This decision was indeed fortunate for reasons that will become apparent later. The circle filters were constructed by holes punched in aluminum sheet metal, whereas the square filters were constructed using microphotography techniques.

Results. The gross features of the reconstructed image are little affected by the filter shape. This effect and the principle of closure and illustrated by Fig. 12, on the following page, with a dot G and dot form using 200 $\mu$ square and circle filters. The Gestalt "whole," a uniform distribution of object dots closing to form one group, is illustrated in Fig. 13. (The object dots were not perfectly uniform in size or arrangement, but they do convey the concept.) The principle of proximity is illustrated in Fig. 14, where uniformly shifted object dots form three groups. The principle of similarity is illustrated in Fig. 15 (on page 45), where two rows of small object dots between two rows of larger object dots form groups. The effect of proximity over similarity is illustrated by Fig. 16, with the grouping of dots and lines. Note the decreased effects of closure, proximity, and similarity when the filter is tilted 45°. These differences will be discussed later. The figure-ground principle is illustrated with a dot object R embedded in dot noise. Figure 17a contains large dot R with small dot noise, whereas Fig. 17b contains R and dot noise constructed with equal size dots. The figure-ground principle is also illustrated with the F/B object in Fig. 18. Note the brightness of the F versus the B due to similarity.

Discussion. The effects of spatial filtering on proximity are precisely those described by Hochberg and Handy, whereby proximity produces a commensurate intrarow increase in brightness differences which, in turn, produced alternating dark and light columns that reorganized perception from rows to columns (Ref 22).

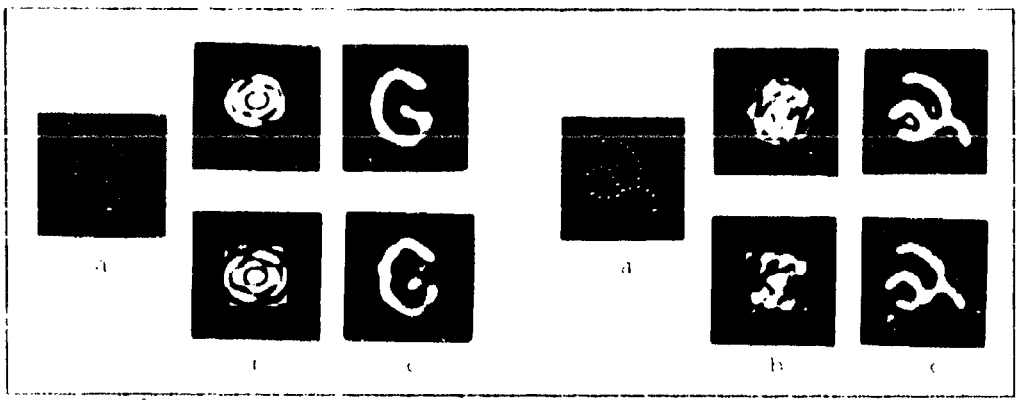

Fig. 12
Principle of Closure Illustrated by Dot G and Dot Form
(200 μ Circle and Square Filter)

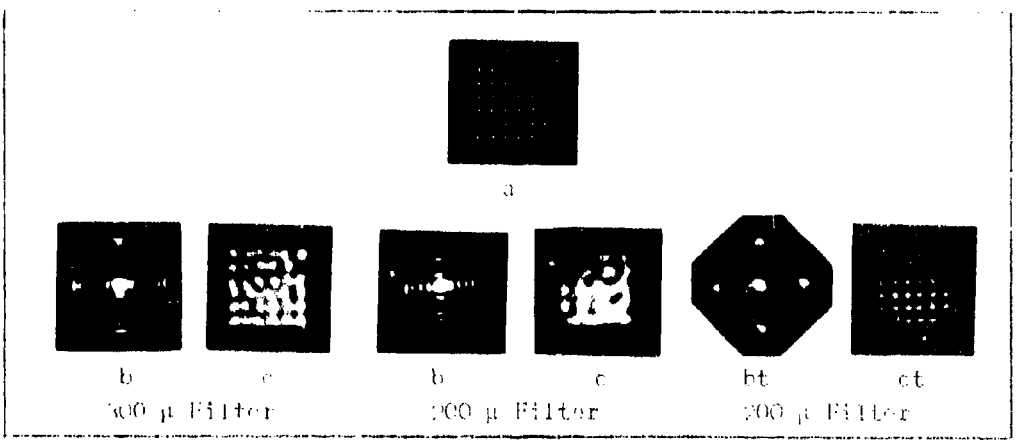


Fig. 13
Gestalt "Whole" Illustrated by Dot Pattern (Square Filter)

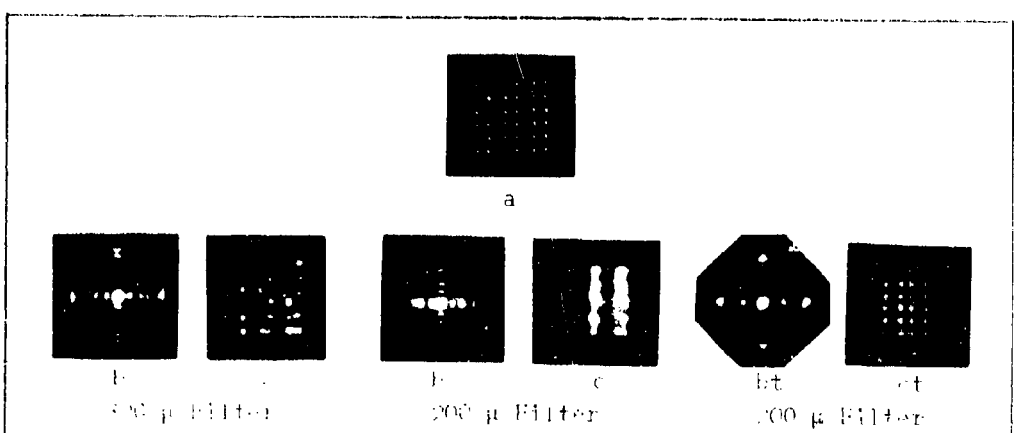


Fig. 14
Principle of Proximity Illustrated by Dot Pattern (Square Filter)

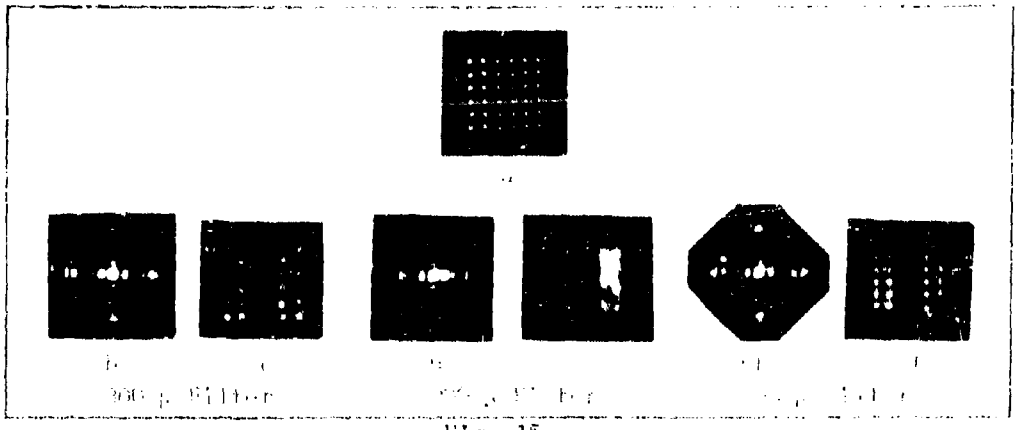

Fig. 15

Principle of Similarity Illustrated by Dot Pattern (Square Filter)

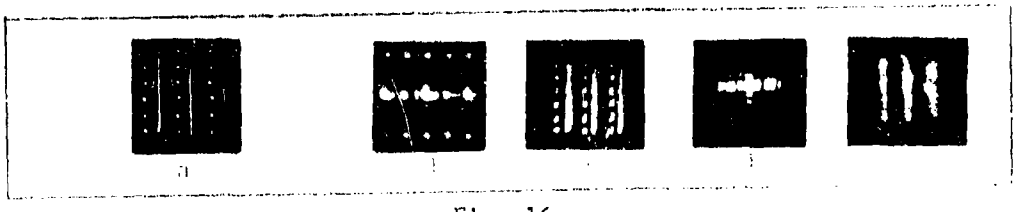

Fig. 16

Principles of Proximity and Similarity Illustrated by Dot and Line Pattern
(300 μ and 200 μ Square Filters)


Fig. 17

Figure-Ground Illustrated by Dot R in Dot Noise
(200 μ Square Filter)

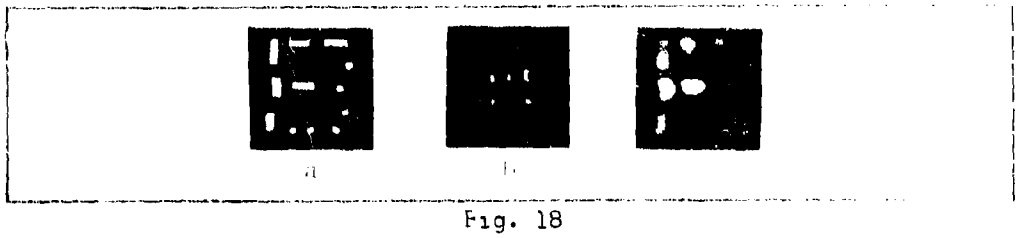

Fig. 18

Figure-Ground Illustrated by F/B Dot and Bar Pattern
(200 μ Square Filter)

These results strongly validate the model whereby illustrating the principles of perception that the Gestalt psychologists have been describing for almost 50 years. The grouping, closure, and figure-ground relationships have occurred not because of a specified algorithm for each of these tasks, but rather as an inadvertent concomitancy of processing for a pattern recognition algorithm, i.e., low-pass spatial filtering.

These results also suggest that the problem of describing perceived texture is amenable to low-pass spatial filtering techniques as well as being able to describe texture in terms of proximity, similarity, and brightness distribution. An obvious next question is: What are the parameters of low-pass spatial filtering that group and close pattern elements in terms of proximity and similarity? To answer this question requires a return to spatial filtering theory.

Spatial Filtering Revisited

As previously discussed, the reconstructed image from a spatially filtered transform can be interpreted as an interference pattern derived from summed, transformed, unfiltered spatial frequencies. Additionally, the Fourier transform spreads detail features primarily at the outer portion of the transform, whereas the gross features are primarily localized at the central portion of the transform. With pattern feature information arranged in this manner, the question arises: How does the spatial filter effect pattern features that will be reconstructed from a spatially filtered transform? There are several criteria which govern image feature resolution, e.g., the Rayleigh criteria of resolution for discriminating between two point sources. Nevertheless, to be consistent

with the filter properties of the model, image feature reconstruction will be interpreted in terms of spatial filter bandwidth (filter size).

Filter bandwidth is generally defined as the frequency distance between two half-power points where a half-power point is 0.707 of the maximum amplitude. Amplitude squared yields intensity, a term more commonly found in optics literature. Thus, the filter bandwidth may also be defined as the frequency distance between two half-intensity points, i.e., the half-width of the maximum, where the half-width is 0.5 of the maximum intensity (Ref 6:348).

The function of the filter bandwidth in resolving image features will be explained with the aid of Fig. 19. Consider two resolved image

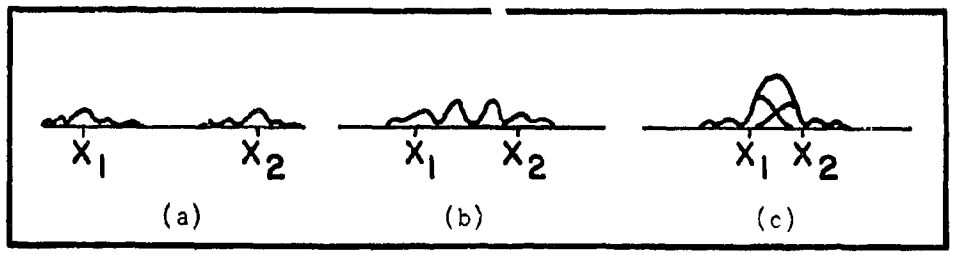


Fig. 19

Wave Patterns at $X_1$ and $X_2$

features represented by intensity wave patterns at $X_1$ and $X_2$, where the distance $X_1 - X_2$ is larger than the filter bandwidth (Fig. 19a). As the distance $X_1 - X_2$ decreases, the wave patterns re-enforce each other, the average intensities of $X_1$ and $X_2$ merge and the images at $X_1$ and $X_2$ cannot be resolved (Fig. 19b, c). The same effect of unresolved images will occur if the object positions remain fixed and the filter bandwidth is decreased. A decreased filter bandwidth blocks the higher spatial frequencies which contain the necessary intensity distribution required for image feature reconstruction, hence, image feature resolution.

This heuristic development can be quantified as follows: It is well known (Ref 17:63) that the width of the central maxima of the Faunhoffer diffraction pattern for a square aperture is given by

$$\Delta X = 2\frac{\lambda d}{\ell} \tag{15}$$

where $\lambda$ = wavelength of light source

$d$ = distance from aperture to the image plane

$\ell$ = aperture width

and the half-width of the central maximum is given by

$$\Delta X = \frac{\lambda d}{\ell} \tag{16}$$

Similarly, the half-width of the central maximum of the Airy diffraction pattern for a circle aperture is given by

$$\Delta X = 1.22\frac{\lambda d}{\ell} \tag{17}$$

where $\ell$ = diameter of the circular aperture

Consider the following parameters:

$\ell$ = 1/16 in. square or circle pattern feature

$\lambda = 6.328 \times 10^{-7}$ meters (for a neon-helium laser)

$d$ = 20 in.

Using these values for Eqs (16) and (17) results in the half-width of the central maximum

$\Delta X = 202 \times 10^{-6}$ meters for a square pattern feature.

$= 246 \times 10^{-6}$ meters for a round pattern feature.

It follows then that a 200 $\mu$ low-pass spatial filter would be expected to

resolve a 1/16 in. square pattern feature, although it would not be expected to resolve a 1/16 in. circular pattern feature using the half-width criteria. Therefore, equating spatial filter size ($f_X$) with the half-width of the central maximum results in

$$f_X = \frac{\lambda d}{\ell} \tag{18}$$

which is a generalized relationship between the spatial filter size and the resolvable pattern feature size in terms of the optical parameters.

It is desirable to quantize the resolvable pattern feature size in terms of spatial filter bandwidth. A convenient reference for pattern feature sizes would be the overall pattern size. Thus, for a 1/2 in. pattern ($\ell$) with the preceding optical parameters and a 200 μ low-pass spatial filter, the spatial filter bandwidth (BW) can be obtained by computing the width (W), the diffraction pattern zero crossings, from

$$\begin{aligned} W &= \frac{\ell f_X}{\lambda d} \\ &\approx 8 \end{aligned} \tag{19}$$

Let the harmonics passed by the spatial filter be obtained from

$$\begin{aligned} BW &= \frac{W}{2} \\ &= 4 \text{ spatial harmonics} \end{aligned} \tag{20}$$

Thus, the spatial filter bandwidth passes the dc and first three spatial harmonics, and is designated the 7×7 low-pass spatial filter of the Tallman-Radoy algorithm. In sum, a 200 μ low-pass spatial filter will pass the dc and first three spatial harmonics of a diffraction pattern

from a 1/2 in. object pattern and will resolve pattern features approximately greater than 1/16 in. in size using the preceding optical parameters. These are general solutions for simple cases; however, it does appear conceptually valid and desirable to quantify pattern features in the preceding manner.

Note that there is an inverse relationship between the feature size and the half-width of the central maximum from Eq (16). Thus, the larger feature size produces the smaller diffraction pattern, whereas the smaller feature produces the larger diffraction pattern as Fig. 20 illustrates.

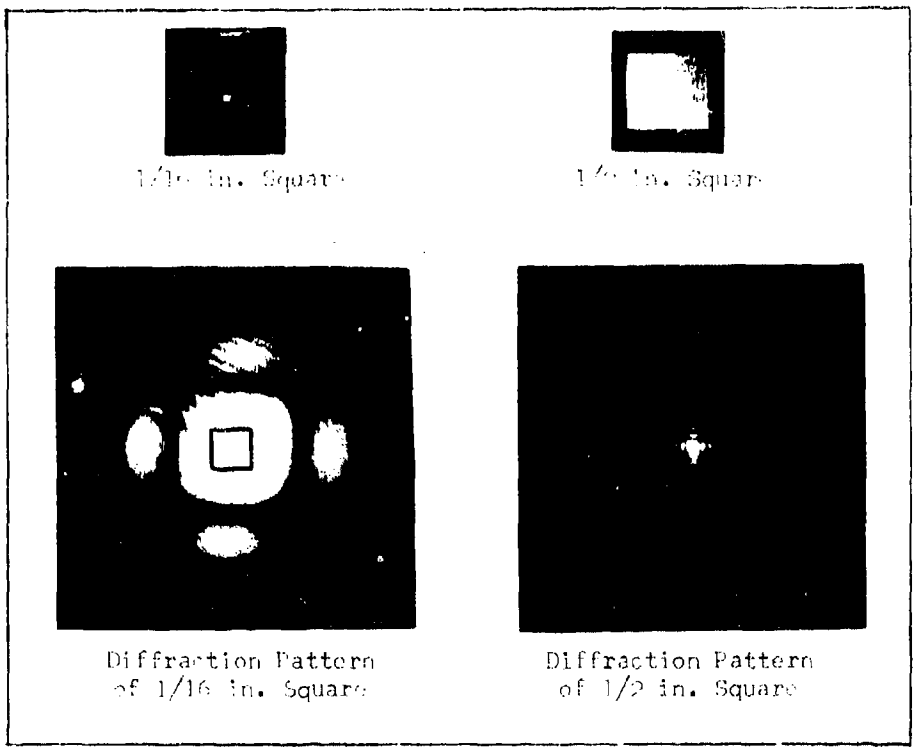


Fig. 20

Diffraction Patterns of a 1/16 in. Square and a 1/2 in. Square with Superimposed 100 μ Square Spatial Filter

Also note the superimposed 100 μ square spatial filter on these diffraction patterns. The 100 μ filter easily encloses the central maximum as

well as higher spatial frequencies of the smaller diffraction pattern, whereas the 100 μ filter does not even enclose the half-width of the central maximum of the larger diffraction pattern. Thus, the 1/2 in. pattern would be resolved; however, the 1/16 in. pattern would not be resolved. The cutoff of the spatial filters appears very sharp. Note the four dots that make up the upper curved portion of the R, reconstructed from a 200 μ spatial filter shown in Fig. 21. The resolved gap is slightly more than 1/8 in. apart, whereas the other two unresolved gaps are exactly 1/8 in. apart.

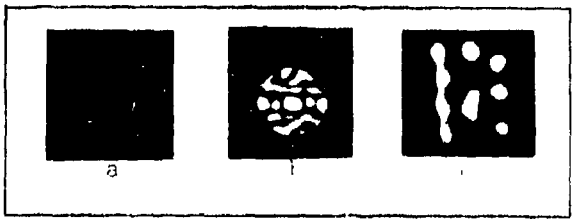

Fig. 21

Low-Pass Spatially Filtered Dot R
(200 μ Circle Filter)

In sum, it was the spatial filter bandwidth that blocked the spatial frequencies above the diffraction pattern central maxima of the Gestalt figure features that produced the grouping effects that the Gestalt psychologists term principles of perceptual organization.

Whereas the Gestalt principles, in terms of image resolution, can be considered to be a function of the spatial filter bandwidth, there appears to be other ramifications of the spatial filter. If pattern recognition is defined in terms of feature discrimination and the feature space is considered to be the transform domain, then feature discrimination

in terms of reconstructed image resolution can be described in terms of spatial filter bandwidth. It was illustrated that the larger the pattern feature, the smaller the transform diffraction pattern; conversely, the smaller the pattern feature, the larger the transform diffraction pattern. Therefore, if the discriminating pattern feature is large (contour), then a small filter size which allows only the half-power of the central maximum of that feature's diffraction pattern is required for image resolution. If the discriminating pattern feature is small (inflection), then a larger filter size must be used to allow the half-power of the central maximum of that feature diffraction pattern to pass for image resolution. It is realized that the preceding discussion has greatly simplified a complex human perceptual phenomenon. Whether the half-power criteris is valid for human feature discrimination remains to be proven. However, the concepts of object/image size in terms of spatial filter bandwidth appear to be a good starting point for quantifying the metrics of visual form in a manner that has been demonstrated to show psychological correlates. Quine is presently quantifying these concepts (Ref 41).

Now that image feature resolution in terms of spatial filter bandwidth is better understood, an investigation of geometric illusions with spatial filters will be pursued.

## Geometric Illusions

Introduction. Psychologists have been interested in geometric illusions mainly because perceptual failures, as well as perceptual successes, provide clues to the visual processes. While many theories have been proposed to explain the distortions of simple figures, none is widely accepted (Ref 18:141-150). As Ittelson points out, the current

status of visual illusions may be summarized best by a quote that Luckiesh wrote in his classic volume "Visual Illusions" 45 years ago: "Some theoretical aspects of the subject are still extremely controversial" (Ref 32:viii).

If the model postulated in this paper is valid, then it should provide insight into these perceptual abberations in terms of low-pass spatial filtering. Therefore, this section is concerned with an initial investigation to support this viewpoint.

Research Method. The geometric illusions investigated were constructed from black electrical tape, aluminum foil or exposed photographic film, and ranged in size from 0.5 in. to 0.75 in. The construction method depended primarily upon the complexity of the figure and ease of construction each material afforded. The geometric illusions were low-pass spatially filtered with the same Fourier optics techniques and spatial filters as were the Gestalt figures. As before, the letters a, b, and c will denote the object, spatially filtered transform, and reconstructed image, respectively, for the following photographs.

Results. Perhaps the best known man-made geometric illusion is the Muller-Lyer illusion illustrated in Fig. 22a, whereby equal line lengths are perceived as unequal. (This illusion, shown on the following page, was constructed from black electrical tape; thus the bottom line lengths are not exactly equal.) The reconstructed image of Fig. 22c illustrates the unequal line lengths resulting from low-pass spatial filtering. It is well known that the Muller-Lyer illusion does not depend upon the lines, whereas it does depend upon the angle of the arrow tips (Ref 18: 140). This fact is illustrated by Fig. 23. (This illusion was constructed by slitting aluminum foil; thus both spaces between the arrow tips are more equal than the preceding illusion.)

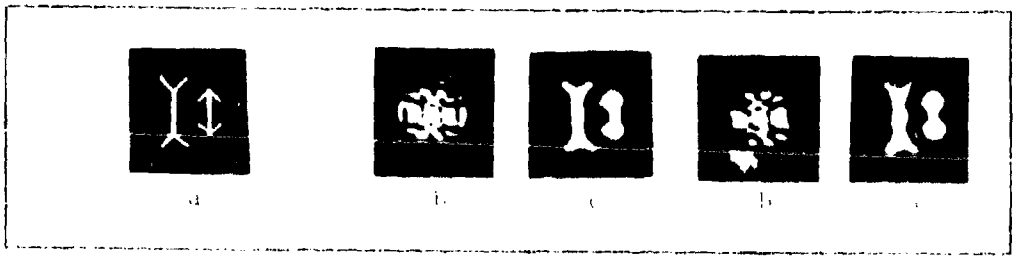

Fig. 22

Muller-Lyer Illusion with Lines
(200 μ Circle and Square Filters)

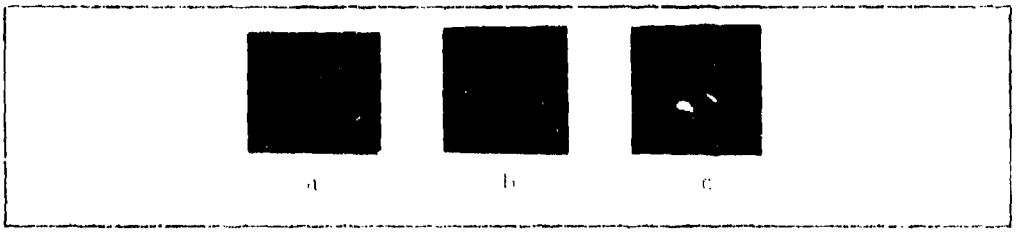

Fig. 23

Muller-Lyer Illusion without Lines
(200 μ Square Filter)

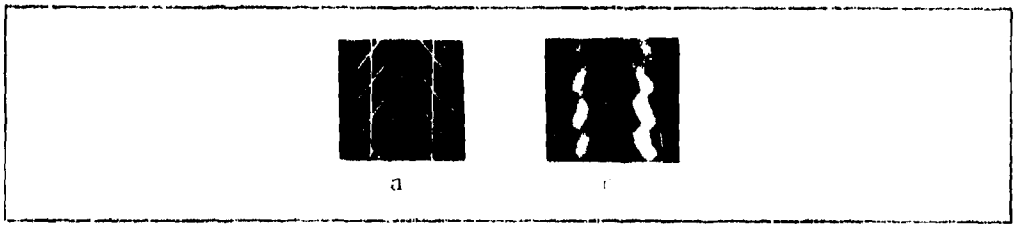

Fig. 24

Part of Herring Illusion
(200 μ Square Filter)

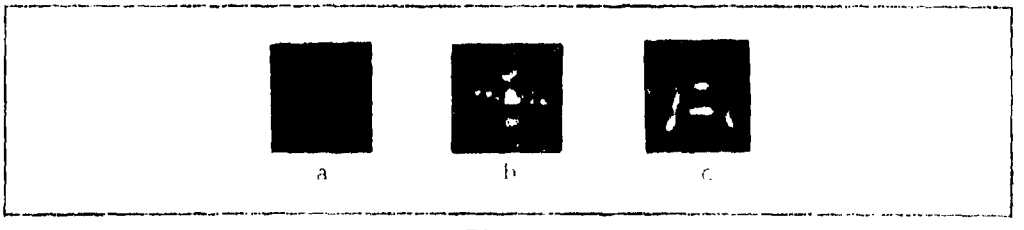

Fig. 25

Ponzo Illusion
(200 μ Square Filter)

The mechanism for the line length and distance changes in the Muller-Lyer illusion is the unresolved arrow tips resulting from low-pass spatial filtering. In the first illusion, the acute angles are smaller features than the obtuse angles and are resolved less, which results in line contractions; since the obtuse angles are unresolved also, line expansion results. The effect of the angle size is illustrated more effectively by the reconstructed image from part of a spatially filtered Herring illusion illustrated by Fig. 24. Note that the obtuse angles are more resolved than the acute angles. The distance changes of the second Muller-Lyer illusion are due to a slightly different reason. The point of the arrow tips is not resolved due to low-pass spatial filtering; thus, the reconstructed images favor the larger features of the arrow tips, located behind each arrow point.

The Ponzo illusion, illustrated by Fig. 25, also perceptually distorts equal line lengths, whereby the upper horizontal line is perceived as being longer than the lower horizontal line. This distortion is also accomplished by low-pass spatial filtering as Fig. 25c illustrates. In this illusion, it appears that proximity is the reason for the line length change. The smaller spaces between the horizontal and vertical lines cannot be resolved, thus extending the closest (upper) horizontal line tips to the vertical lines.

Discussion. It appears from this preliminary investigation that most geometric illusions can be explained by unresolved image features of low-pass spatially filtered transforms in terms of proximity and angle. Postulating the human perceptual space as the reconstructed image domain, it becomes apparent that the line length changes and the distance changes are perceived as such because they actually do occur. The model "fails" in the same way as humans "fail" with these illusions.

If one considers perceptual depth as a function of image intensity, then the preceding explanation of the Muller-Lyer and Ponzo illusions are not too unlike Gregory's explanation. Gregory considers the distortion of visual space to be due to inappropriate constancy scaling, whereby apparent depth from corners and angles is responsible for the illusion (Ref 18:147-160). Additionally, it is interesting to note that the different line lengths and distances of the reconstructed images would be amenable to the moment measurement techniques reported by Gill (Ref 15).

Now that the model appeared conceptually valid, another look was taken in regard to the spatial filter shape and perceptual organization.

# VI. Extensions of the Kabrisky Model

## Spatial Filter Shape Correlates

Introduction. This section is a post hoc analysis of the psychological correlates of the preceding investigations. The filter shape appeared to play a significant role in the letter identification under rotation experiment and the Gestalt principles of perceptual organization. Therefore, the filter shape is investigated further for additional psychological correlates of perceptual organization.

The Square Filter. It was noted that the square filter provided more significant correlations than the circle filter for the lower filter sizes in the letter identification under rotation experiment. The square filter accentuates the effect of the higher spatial frequencies at the diagonals of the square filter. Thus, the Euclidean distances for the letters did not monotonically increase as rotation increased and the square filter had more maximum Euclidean distances at 60° than the round filter had at 60°, as Table V illustrates.

Table V

Number of Maximum Euclidean Distances at 60°

| Spatial Filter Shape | 3×3 | 5×5 | 7×7 | 9×9 |
|---|---|---|---|---|
| Circle | 2 | 11 | 10 | 10 |
| Square | 12 | 15 | 14 | 10 |

As previously mentioned, the human visual system is spatially polarized with form recognition superior in the horizontal and vertical orientation as compared to oblique orientations. Arnoult showed graphs illustrating the accuracy and latency of shape discrimination with curvilinear shapes as a function of angular orientation to be non-monotonic through 0° to 180° clockwise and counter-clockwise (Ref 1). Discrimination times with lines and rectangles are reported by Attneave and Olson as being faster with horizontal and vertical orientation than with orientations 45° to the right or left (Ref 3). Taylor, in discussing several visual discrimination and orientation experiments, illustrates non-monotonic discrimination results with orientation as well as the non-monotonic ability to assess orientation (Ref 48). These parallel results from these two different tasks led him to suggest that meridional differences of discrimination may be due to the difficulty of orientation assessment. It will be assumed that the spatial filter shape of the model will be considered to play a significant part in meridional differences. The assumption will be re-enforced with the more basic psychological correlates concerning the Gestalt principles.

In reporting the results of the low-pass spatial filtering of the Gestalt patterns, it was also noted that the grouping effects due to proximity and similarity decreased when the patterns were rotated 45° with respect to the square filter. Hake has summarized Rush's experiments on the relative strength of the Gestalt principles of grouping with dot matrices by stating that the influence of proximity and similarity is affected by whether the dot matrix is horizontal, vertical, or oblique (Ref 21:57-58). By changing the distances between the dots of the dot matrices, Rush noted that proximity was slightly more effective in the vertical and oblique than in the horizontal, whereas similarity was more

effective in the oblique and least effective in the vertical. Olson and Attneave have reported similar results in that arrays of several figural or textural variables produced different similarity groupings which depended upon the orientation of the stimulus (Ref 36). The stimulus differed in slope and linearity of elements as well as combinations of slopes into angles. The effectiveness of similarity under these conditions was determined by subject reaction time in locating a disparate quadrant in a circular array with and without head tilt at 45°. The results were that slope differences produced better grouping than linearity and arrangements of slopes and when the whole array was oriented at different angles, the horizontal and verticals gave better groupings than diagonals. They further noted that the reaction time was a function of both retinal and gravitational orientation. Whereas the effect of gravitation orientation effects was more consistent than the effect of retinal orientation, the retinal orientation affected the mean reaction time more than twice as much as the physical orientation. The important points are that the retinal orientation of these stimuli do affect similarity grouping and cannot be accounted for entirely on a projection level but as Olson and Attneave suggest "... grouping and segregation depend on identities and differences between descriptors which in turn represent relationships between the stimulus array and an internal Cartesian reference system." It is suggested that this "internal Cartesian reference system" can be correlated to the Kabrisky model in terms of the horizontal and vertical axes of the spatial filter.

These psychological investigations just discussed suggest a correlate in terms of the model spatial filter shape. If one considers the change which the spatial transform undergoes during rotation in a square

filter, it becomes apparent that the maximum change of the vertical and horizontal components would occur at the diagonals of the square. Thus, for some forms, the image from the rotated object would have the largest deviation (in terms of spatial frequencies) from a stored prototype image. Additionally, the increased higher spatial harmonics from the diagonals would reduce the Gestalt groupings as previously illustrated. It is suggested that these factors could account for the non-monotonic discrimination ability as well as the changes in the Gestalt groupings under pattern rotation. However, the previous psychological investigations also note perceptual changes with horizontal versus vertical orientation that cannot be accounted for by a square filter that would resolve both the horizontal and vertical components of a bilaterally symmetrical pattern equally. An example of a non-symmetrical perceptual abberation is perhaps the simplest geometric illusion--the horizontal-vertical line illusion shown in Fig. 26. The vertical line appears to be longer than

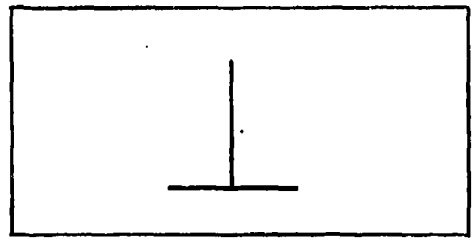

Fig. 26

Horizontal-Vertical Line Illusion

the horizontal line even though both lines are the same length. It is interesting to observe that the illusion is diminished if the figure is rotated by 90°. Clearly, with respect to the model, these effects cannot be explained in terms of a square shaped spatial filter.

The Rectangle Filter. It would appear that a rectangular spatial filter shape is required to solve the preceding problems. The disparate horizontal and vertical lengths of the rectangular spatial filter would resolve a pattern by different amounts depending upon pattern orientation. Additionally, diagonal pattern orientations would provide increased high spatial frequencies required for reducing the Gestalt groupings that correlate with previously discussed psychological experiments as well as large deviations from stored prototypes used to explain non-monotonic discrimination of forms. The rectangular spatial filter would also account for the horizontal-vertical illusion disparities as well as the decreased illusion effects when the figure is tilted 90°.

## Experiments with the Rectangle Filter

Introduction. The preceding discussion illustrated the failings of the square spatial filter in terms of basic psychological correlates and suggested a rectangular shaped spatial filter. This section concerns a preliminary investigation of the characteristics of a rectangular spatial filter in satisfying the previous psychological criteria.

Research Method. The pattern construction remained the same as outlined in previous sections. Low-pass spatial filtering was accomplished with a rectangle (1:0.6) filter using the same Fourier optics techniques previously used for the Gestalt figures and geometric illusions. Similarly, the letters a, b, and c will denote the object, spatially filtered transform, and reconstructed images for the following photographs. These photographs have been arranged to show the filter tilted--not the object--to allow a better comparison of the reconstructed images (Figs. 27 through 30 on pages 63 and 64).

Results. The effects of a rectangle 300μ×240μ low-pass spatial filter on the horizontal vertical illusion is illustrated in Fig. 27 on the following page. The equal object lines (3/8 in.) are now unequal in the reconstructed image. The vertical line is 1/16 in. longer than the horizontal line due mainly to the less resolved horizontal line. Figure 17 also illustrates the illusion turned 90° which resulted in making the vertical line 1/32 in. longer than the horizontal line. Also note that the vertical line is brighter than the horizontal line in both cases, again suggesting that brightness may play a part in geometric illusions. The illusion tilted 45° clockwise and counter-clockwise is illustrated in Fig. 27. Both the horizontal and vertical line lengths are approximately equally resolved and the brightness distribution is more uniform. It was noted that the tips of the lines were somewhat distorted. This observation prompted an investigation with a single line, illustrated in Fig. 28, oriented at 0, 45, 60, and 90 degrees, respectively. Note the line length changes as well as line tip distortion. These line tip distortions suggest gross distortions for complex line patterns such as letters. The rotated letter K at 0, 45, and 90 degree angles, illustrated in Fig. 29, demonstrates gross distortion at 45° with a 200μ × 120μ rectangle filter. The effect of the rectangle filter on the principle of similarity and proximity is demonstrated by Fig. 30, page 64. Especially note the increased resolution of the dots of this pattern at 45° as well as the dissimilar groups in the horizontal and vertical orientations.

Discussion. The results of this investigation with the rectangle filter correlate well to previous psychological findings of discrimination degradation upon rotation as well as the perceptual failure noted by the horizontal illusion. These results should only be considered to warrant further investigation. It was a difficult task in keeping the

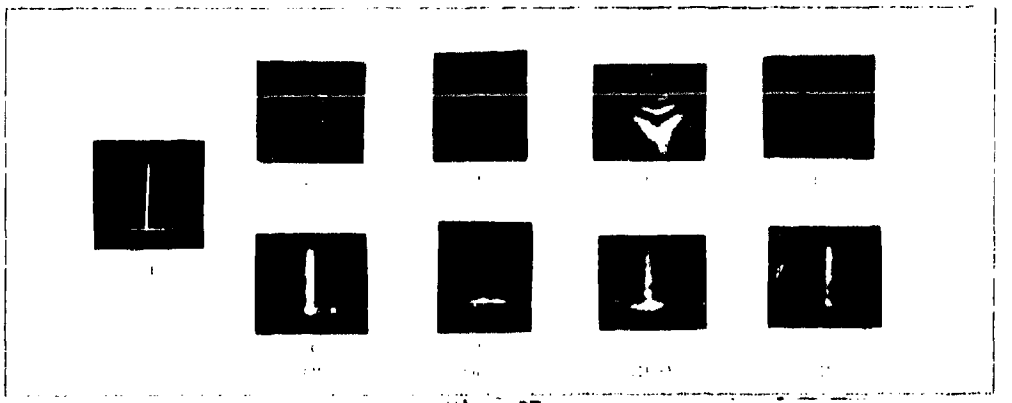

Fig. 27

Horizontal-Vertical Line Illusion
(300 μ × 180 μ Rectangle Filter)

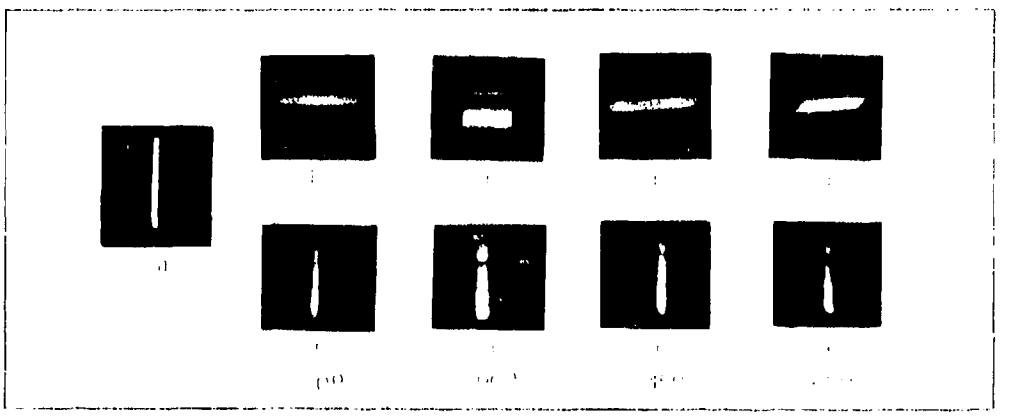

Fig. 28

Line (300 μ × 180 μ Rectangle Filter)

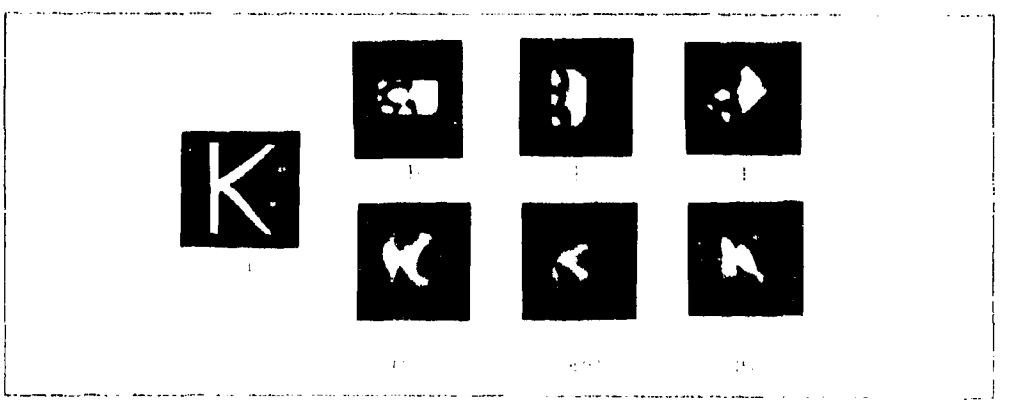


Fig. 29

Letter K (200 μ × 120 μ Rectangle Filter)

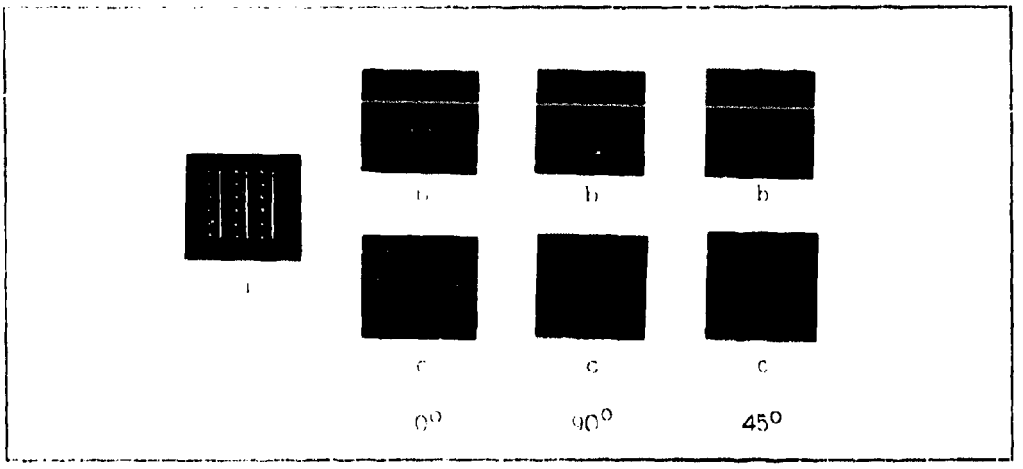


Fig. 30
Principles of Proximity and Similarity with Dot and Line Pattern
(300 μ × 180 μ Rectangle Filter)

transform centered during rotation and small changes in filter orientation somewhat disturb the reconstructed image. However, these results do validate the concepts and suggest that the Kabrisky model can be extended with a rectangular shaped spatial filter for additional psychological correlates.

It is well known that individuals from other cultures, e.g., the Zulu's, do not see many of the geometric illusions that Western man sees (Ref 18:160-163). In terms of the model, this fact suggests the existence of either an adaptive filter shape that is culturally conditioned or a selective attention mechanism that learns to "pay attention to" different parts of the cortical transform. Whereas the rectangular shaped spatial filter is mimicing, at least on a macroscopic level, human perceptual phenomenon, the shape and size ratios of the rectangular spatial filter should be considered tentative in lieu of a more accurate mapping of the visual space.

Comments on Parallel Processing

Although it is not intended to review the various theories of visual pattern recognition, there is one theory hypothesizing perceptual processing that greatly parallels the pattern recognition scheme of the model reported in this paper.

Neisser, a cognitive psychologist, asks a question much like Kabrisky, et al., have asked in the identification game: "How does the subject know an A when he sees one?" (Ref 35:102). Tempered with numerous psychological research studies, he suggests the following answer to his question: The A is segregated from the other simultaneously presented figures by pre-attentive processing mechanisms that emphasize the "whole" rather than the "part" in the figures that are constructed and reduplicated in parallel throughout the input field. Neisser further suggests focal attention devoted to the A which may lead to internal verbalization or a "sequence of comparisons with stored records of earlier synthesis to determine the proper classification for the present stimulus." Perhaps the weakest area of Neisser's theory is that he does not elaborate on possible cortical mechanisms to achieve focal attention and figural synthesis. However, there exists a striking parallel to his theory and the Kabrisky model, in that the low-pass spatial filtering of transformed patterns has been demonstrated to emphasize the whole rather than the part of the pattern.

Another question remains to be answered: How does one pattern become reduplicated throughout the input field? Consider a Mahaffey-type transform between cortical area 18 and 19. The Mahaffey transform maps the object at one plane into many smaller parallel areas in the next plane in a Fourier-like manner. If an assumption is made that the input pattern is spatially transformed at area 18, then by a Mahaffey-type transform,

area 19 could contain different spatially filtered images from the visual field as well as allow simultaneous attention of the visual field at one cortical level. This cortical scheme is illustrated by Fig. 31. Thus,

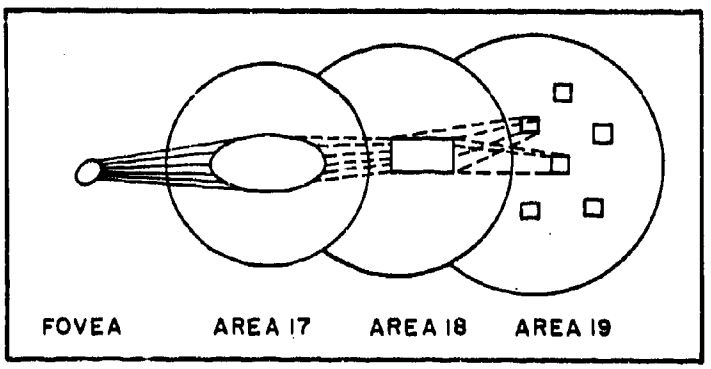


Fig. 31

Cortical Scheme of the Extended Model

the simultaneous foveal acuity as well as the gross features of the parafoveal visual field would be at the same cortical level for a selective attention mechanism. This point is important because if the reader will focus his visual attention on the period at the end of this sentence, it will be obvious that he can report surrounding features as well as the period without changing his external "look." Additionally, the human perceptual system can describe the Gestalt dot figures in terms of dots or groups--again, the need for simultaneous different spatially filtered pattern transforms at one cortical level.

Consider the figure-ground problem of the candle stick illusion shown in Fig. 32a on the following page. In viewing this object form, one may perceive two faces or a candle stick, depending upon the "internal set" that the viewer has chosen. If different spatially filtered images of this figure were available at one cortical level, as illustrated by Fig. 32 c1, c2, and c3, then a selective attention mechanism would "see"

whichever figure that corresponded to the spatial filter size that the viewer had brought to this perceptual task. Clearly, this concept allows simultaneous perceptual reports without changing the external viewing situation.

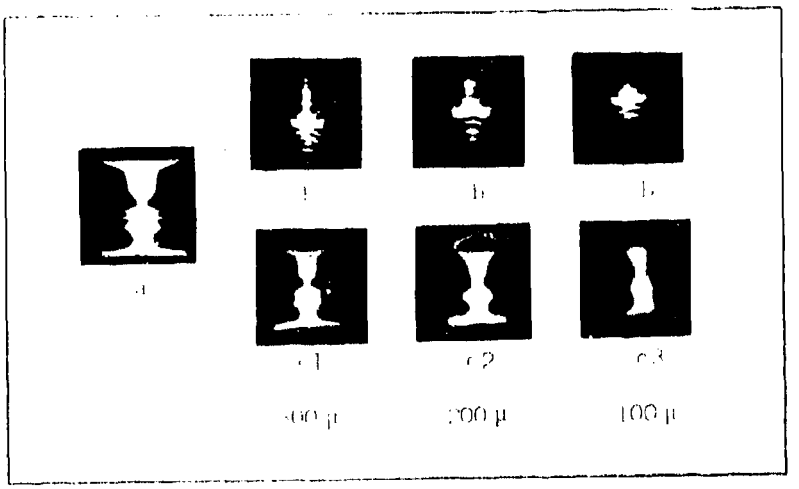


Fig. 32

Candle Stick Illusion (Square Filters)

A final concern of Neisser's theory is the classification scheme of stimulus. His letter classification scheme is very similar to the Euclidean distance technique employed by the Tallman-Radoy algorithm as previously discussed. However, it would be naive to assume that this is the only possible way to classify like stimuli. Whether the classification occurs by correlating reconstructed images with stored prototypes using a Euclidean distance type metric can only be conjectured at this time. Both forms of the spatially filtered pattern are equivalent and it is probable that perceptual classification may utilize both forms of the pattern depending upon the requirements of the classification task as well as memory storage. Whereas the reconstructed image offers a convenient perspective to what low-pass spatial filtering accomplishes to the

external observer, it would offer no additional information to an internal classification scheme as demonstrated by the Tallman-Radoy algorithm.

In sum, it appears that the extension of the Kabrisky model with a Mahaffey-type transform yields a model of the human visual system that correlates well with Neisser's theory of human pattern recognition.

## VII. Conclusions and Recommendations

An exploratory investigation has been undertaken to correlate the Kabrisky model of the human visual system, by the Tallman-Radoy computer algorithm and a Fourier optics homolog, to well-known psychological phenomena--identification of defocused letters and rotated letters, Gestalt principles of perception, and several geometric illusions. The following conclusions are supported by the results of this investigation:

1. The Kabrisky model of the human visual system embodied by the Tallman-Radoy computer algorithm and the Fourier optics homolog appears to be valid in providing a priori quantitative psychological metrics of visual perception.
2. Gestalt principles of proximity, similarity, closure, and figure-ground perception as well as several geometric illusions can be explained in terms of object/image feature size, spatial arrangement, and spatial-filter bandwidth.
3. The human perceptual decision space (feature space) is postulated to be the image domain from spatially filtered transforms of object forms.
4. The Kabrisky model can be extended with a rectangular spatial filter and a less densely connected Mahaffey-type transform for further psychological correlations.

Therefore, the general methodology of investigating models of the human visual system against well-known psychological correlates and, conversely, using psychological correlates to extend models appears to be

## Bibliography


1. Arnoult, M. D. "Shape Discrimination as a Function of the Angular Orientation of the Stimuli." J. Exp. Psy., 47:323-328 (1954).

2. Attneave, F. "Criteria for a Theory of Form Perception" in Models for the Perception of Speech and Visual Form (edited by W. Wathen-Dunn). Cambridge, Massachusetts: The M.I.T. Press, 1967.

3. -----, and R. K. Olson, "Discriminability of Stimuli Varying in Physical and Retinal Orientation." J. Exp. Phy., 74:149-157 (1967).

4. Averbach, E., and G. Sperling. "Short-Term Storage of Information in Vision" in Contemporary Theory and Research in Visual Perception (edited by R. N. Haber). New York: Holt, Rinehart, and Winston, Inc., 1968.

5. Blackford, C. W., Jr. Chromatic Pattern Recognition. MS Thesis GE/EE/71-4. Wright-Patterson AFB, Ohio: Air Force Institute of Technology, March 1971.

6. Born, M., and E. Wolf. Principles of Optics. New York: Pergamon Press, 1958.

7. Brown, D. R., and D. H. Owen. "The Metrics of Visual Form." Psy. Bull., 68:243-259 (1967).

8. Carl, J. W. Generalized Harmonic Analysis for Pattern Recognition: A Biologically Derived Model. MS Thesis GE/BE/70S-1. Wright-Patterson AFB, Ohio: Air Force Institute of Technology, June 1969.

9. Cochran, W. T. "What is the Fast Fourier Transform." Proc. IEEE, 55:1664-1674 (October 1969).

10. Conrad, R. "Acoustic Confusions in Immediate Memory." British J. Psy., 55:75-84 (1964).

11. Dodwell, P. C. Visual Pattern Recognition. New York: Holt, Rinehart, and Winston, Inc., 1970.

12. Dusser de Barenne, H. G., et al. The Isocortex of the Chimpanze. Urbana, Illinois: University of Illinois Press, 1951.

13. Evans, S. "Pattern Identification - A Review of Perceptual Research." A paper presented at the Army Numerical Analysis Conference at Fort Belvoir, Virginia, April 2-3, 1970.

14. Frederiksen, J. R. The Role of Cognitive Factors in the Recognition of Ambiguous Visual Stimuli. AD 473 580. Princeton, New Jersey: Educational Testing Service, July 1965.

15. Gill, R. A. The Scaling Problem in the Classification of Images by Spatial Filtering. MS Thesis GA/BE/70-1. Wright-Patterson AFB, Ohio: Air Force Institute of Technology, May 1970.

16. -----. "Recent Developments in Pattern Recognition using Spatial Filtering" in Proceedings 1971 National Aerospace Electronics Conference (NAECON). Dayton, Ohio: IEEE Transactions on Aerospace and Electronic Systems, May 1971.

17. Goodman, J. W. Introduction to Fourier Optics. New York: McGraw-Hill, 1968.

18. Gregory, R. L. Eye and Brain. New York: McGraw-Hill, 1966.

19. Guilford, J. P. Fundamental Statistics in Psychology and Education. New York: McGraw-Hill, 1965.

20. Hake, H. W. Contributions of Psychology to the Study of Pattern Vision. AD 142 035. WADC Technical Report 57-621. Wright-Patterson AFB, Ohio: Wright Air Development Command, October 1957.

21. -----. "Form Discrimination and the Invariance of Form" in Pattern Recognition (edited by L. Uhr). New York: John Wiley and Sons, Inc., 1966.

22. Hochberg, J. E., and D. Hardy. "Brightness and Proximity Factors in Grouping."Percept. Mot. Skills, 10:22 (1960).

23. Huble, D. H., and T. N. Wiesel. "Receptive Fields, Binocular Interaction, and Functional Architecture in the Cat's Visual Cortex." J. Psy., 160:106-154 (1962).

24. -----. "Receptive Fields and Functional Architecture of Monkey Striate Cortex." J. Psy., 195:215-243 (1968).

25. Kabrisky, M. "Feathers and Birds - Neurons and Nervous Systems." Unpublished lecture notes. Wright-Patterson AFB, Ohio: Air Force Institute of Technology.

26. -----. A Proposed Model for Visual Information Processing in the Human Brain. Urbana, Illinois: University of Illinois Press, 1966.

27. -----. "Visual Information Processing in the Brain" in Models for the Perception of Speech and Visual Form (edited by W. Wathen-Dunn). Cambridge, Massachusetts: The M.I.T. Press, 1967.

28. -----, et al. "A Theory of Pattern Perception Based upon Human Physiology" in Contemporary Problems in Perception (edited by A. T. Welford and E. H. Houssiadas). London: Francis and Taylor, Ltd., 1970.

29. -----, and J. W. Carl. "Sequency Filtered Densely Connected Transforms for Pattern Recognition" in Proceedings of the 4th Hawaii International Conference on Systems Science, Honolulu, Hawaii, January 1971.

30. Kolers, P. A. "Some Psychological Aspects of Pattern Recognition" in Recognizing Patterns (edited by R. A. Kolers and M. Eden). Cambridge, Massachusetts: The M.I.T. Press, 1968.

31. Lendaris, G. G., and G. L. Stanley. "Diffraction Pattern Sampling for Automatic Pattern Recognition." Proc. IEEE, 58:198-216 (February 1970).

32. Luckiesh, M. Visual Illusions. New York: Dover Publications, Inc., 1965.

33. Mahaffey, W. O., Jr. Pattern Recognition Model Based on Cortical Anatomy. MS Thesis GE/EE/71-18. Wright-Patterson AFB, Ohio: Air Force Institute of Technology, March 1971.

34. Maher, F. A. "A Correlation of Human and Machine Pattern Discrimination" in Proceedings 1970 National Aerospace Electronics Conference (NAECON). Dayton, Ohio: IEEE Transactions on Aerospace and Electronic Systems, May 1970.

35. Neisser, U. Cognitive Psychology. New York: Meredith Publishing Co., 1967.

36. Olson, R. K., and F. Attneave, "What Variables Produce Similarity Grouping." Am. J. Psy., 83:1-21 (1970).

37. O'Neill, E. L. "Spatial Filtering in Optics." IRE Trans. on Information Theory, 2:56-65 (1956).

38. Polyak, J. The Vertebrate Visual System. Chicago: University of Chicago Press, 1957.

39. Pratt, W. K., and H. C. Andrews. Optical Filtering by Digital Computer. AD 835 646. SAMSO-TR-68-179. Los Angeles, California: Space and Missile Systems Organization, June 1968.

40. -----."Digital Computer Simulation of Coherent Optical Processing Operations." Computer Group News (November 1968).

41. Quine, D. Optical Bandwidth Limitations for Visual Feature Recognition. Unpublished report. Wright-Patterson AFB, Ohio: Air Force Institute of Technology, May 1967.

42. Radoy, C. H. Pattern Recognition by Fourier Series Transformations. MS Thesis GE/EE/67A-11. Wright-Patterson AFB, Ohio: Air Force Institute of Technology, March 1967.

43. Roscoe, J. T. Fundamental Research Statistics. New York: Holt, Rinehart, and Winston, Inc., 1969.

44. Singh, J. Great Ideas in Information Theory, Language, and Cybernetics. New York: Dover Publications, Inc. 1966.

45. Stevens, S. S. Handbook of Experimental Psychology. New York: John Wiley and Sons, Inc., 1951.

46. Tallman, O. H., II. The Classification of Visual Images by Spatial Filtering. PhD Dissertation. Wright-Patterson AFB, Ohio: Air Force Institute of Technology, March 1967.

47. -----. Processing of Visual Imagery by an Adaptive Model of the Visual System: Its Performance and Its Significance. Aerospace Medical Research Laboratory Technical Report 70-45. Wright-Patterson AFB, Ohio: Aerospace Medical Research Laboratory, November 1970.

48. Taylor, M. M. "Visual Discrimination and Orientation," J. Opt. Soc. Am., 53:763-765 (1963).

49. Thompson, J. M. Foundations of Physiological Psychology. New York: Harper and Row, 1967.

50. Wertheimer, M. Principles of Perceptual Organization (edited by D. Beardsley and M. Wertheimer). Princeton, New Jersey: Van Nostrand, 1958.

51. Wiesel, T. N., and D. H. Huble. "Spatial and Chromatic Interaction in the Lateral Geniculate Body of the Rhesus Monkey." J. Neurophysiology, 29:1115-1156 (1966).

52. Zahn, C. T. "Graph-Theoretical Methods for Determining and Describing Gestalt Clusters." IEEE Trans. on Computers, C-20: 68-86 (1971).

# Appendix A

## Subject Data from the Identification of Defocused Letters Experiment

This appendix contains a table of the mean number of correctly identified letters per subject per trial for the identification of defocused letters experiment.

Table

**Mean Number of Letters Identified Correct for The Identification of Defocused Letter Experiment**

| | Subjects | | | | | | | | | | | |
|---|---|---|---|---|---|---|---|---|---|---|---|---|
| | Normal Group | | | | | | Defocused Group | | | | | |
| | LA | RN | PP | LB | MK | | TG | AG | JS | JG | WF | |
| Trial Number | | | | | | Mean | | | | | | Mean |
| 1 | 3.55 | 4.05 | 4.58 | 3.48 | 4.00 | 3.94 | 3.72 | 2.80 | 3.90 | 4.20 | 3.00 | 3.52 |
| 2 | 4.45 | 4.25 | 4.55 | 3.95 | 4.00 | 4.24 | 4.00 | 3.60 | 4.00 | 4.90 | 3.55 | 4.01 |
| 3 | 4.05 | 4.45 | 4.95 | 4.15 | 3.75 | 4.27 | 4.15 | 3.75 | 4.15 | 5.25 | 3.60 | 4.18 |
| 4 | 4.25 | 4.60 | 4.75 | 4.20 | 4.80 | 4.52 | 4.75 | 4.35 | 4.40 | 5.25 | 3.85 | 4.52 |
| 5 | 4.25 | 4.45 | 4.55 | 4.15 | 4.45 | 4.37 | 5.10 | 4.40 | 4.48 | 5.20 | 4.10 | 4.69 |
| 6 | 4.45 | 4.85 | 4.85 | 4.25 | 4.60 | 4.60 | 4.95 | 4.60 | 4.52 | 5.20 | 4.10 | 4.67 |
| 7 | 4.45 | 4.50 | 5.20 | | | 4.72 | 4.80 | 4.40 | 4.35 | | | 4.52 |
| 8 | 4.80 | 4.50 | 5.15 | | | 4.82 | 5.00 | 4.75 | 4.70 | | | 4.82 |
| 9 | 5.00 | 4.60 | 4.80 | | | 4.80 | 4.95 | 4.45 | 4.80 | | | 4.73 |
| 10 | 4.95 | 4.80 | 5.20 | | | 4.98 | 5.35 | 4.85 | 4.95 | | | 5.05 |
| 11 | 5.35 | 4.55 | 5.40 | | | 5.10 | 4.95 | 4.80 | 4.75 | | | 4.83 |
| 12 | 5.40 | 4.55 | 5.30 | | | 5.08 | 5.15 | 5.00 | 5.10 | | | 5.08 |
| 13 | 5.10 | 4.85 | 5.00 | | | 4.98 | 5.00 | 4.90 | 5.05 | | | 4.98 |
| 14 | 5.40 | 4.80 | 5.40 | | | 5.20 | 5.30 | 4.95 | 5.15 | | | 5.13 |
| 15 | 5.35 | 4.85 | 5.45 | | | 5.22 | 5.55 | 5.15 | 5.05 | | | 5.25 |
| 16 | 5.40 | 4.95 | 5.50 | | | 5.28 | 5.65 | 5.20 | 5.40 | | | 5.42 |
| 17 | 5.00 | 4.95 | 5.40 | | | 5.12 | 5.75 | 5.20 | 5.65 | | | 5.53 |
| 18 | 5.20 | 4.80 | 5.55 | | | 5.18 | 5.80 | 5.10 | 5.70 | | | 5.53 |
| 19 | 5.05 | 4.80 | 5.40 | | | 5.08 | 5.75 | 5.15 | 5.60 | | | 5.50 |
| 20 | 5.30 | 5.00 | 5.75 | | | 5.35 | 5.85 | 5.20 | 5.75 | | | 5.60 |

## Appendix B

## Confusion Matrices of Letter Identification Errors under Rotation

Confusion matrices of the human identification errors from the identification of rotated letters experiment at presentation angles of 0, 30, 60, 90, 120, and 150 degrees are contained in this appendix.

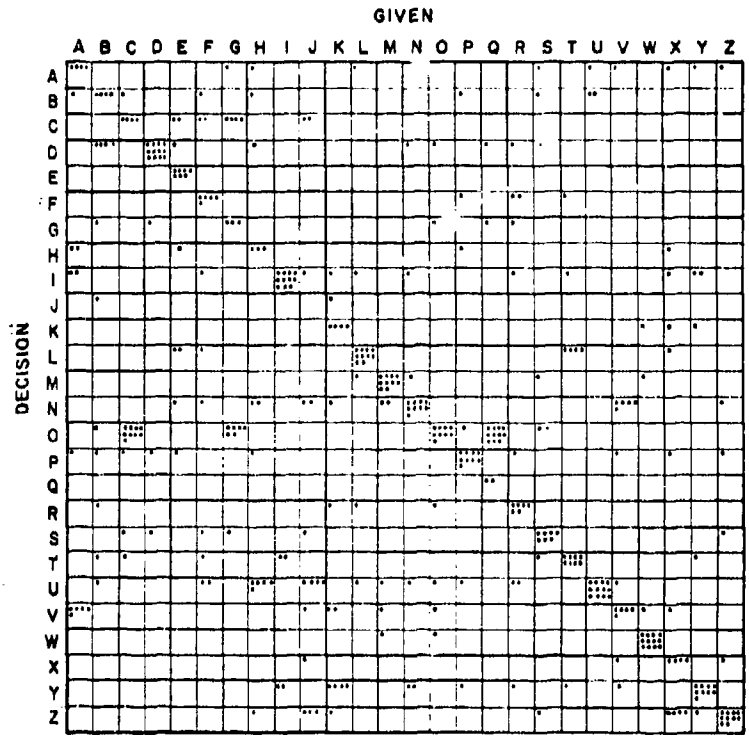


Confusion Matrix from
Identification of Rotated Letters Experiment at 0°

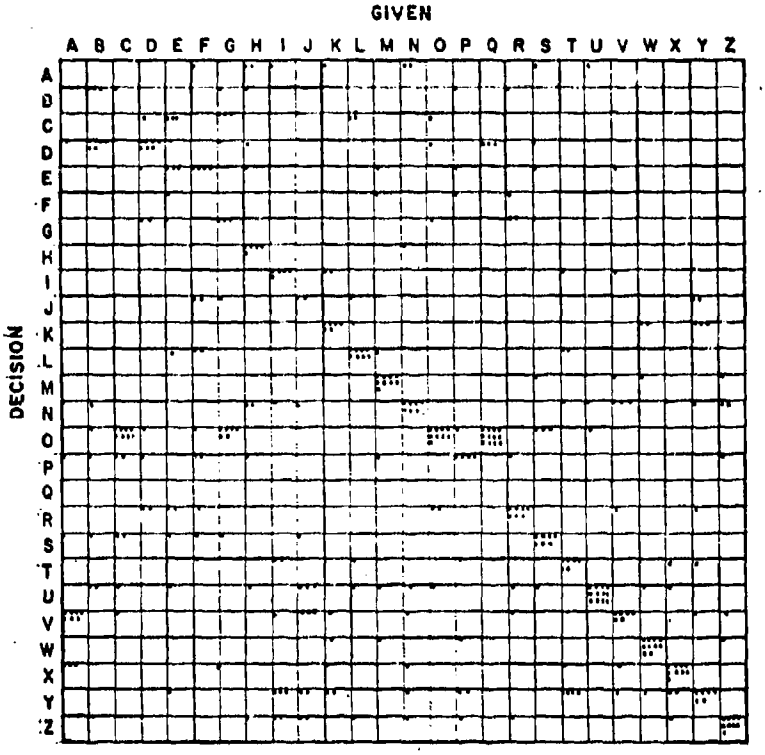


Confusion Matrix from
Identification of Rotated Letters Experiment at 30°

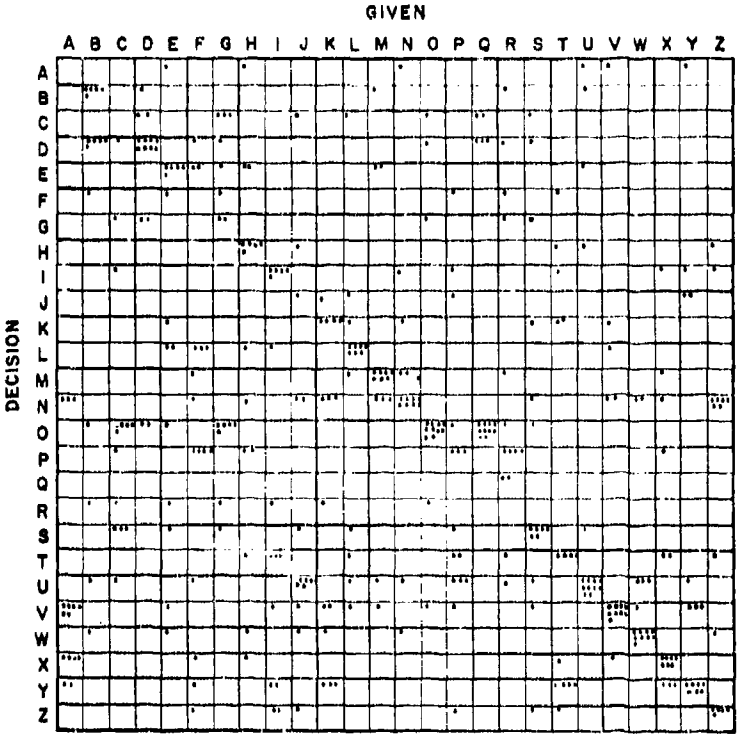


Confusion Matrix from
Identification of Rotated Letters Experiment at 60°

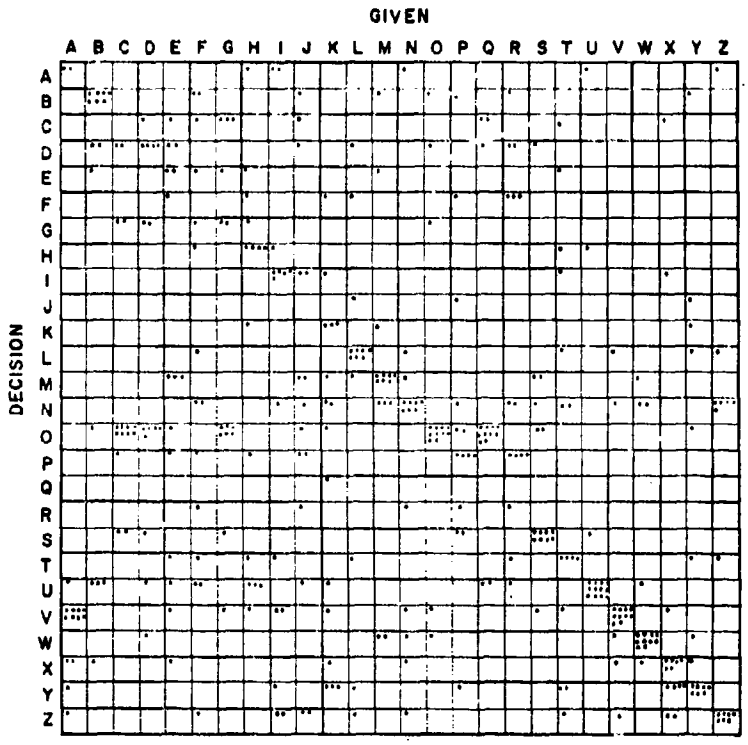


Confusion Matrix from
Identification of Rotated Letters Experiment at 90°

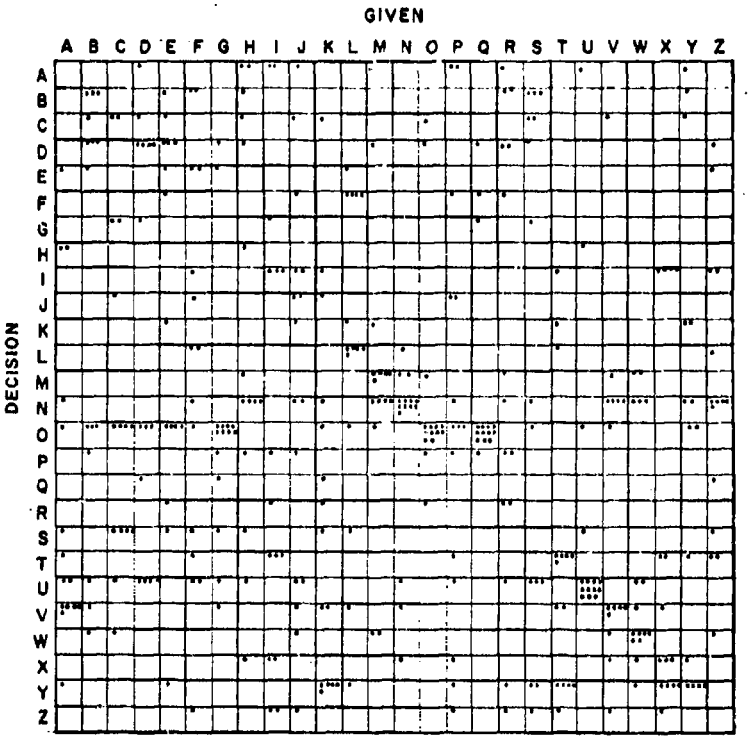


Confusion Matrix from
Identification of Rotated Letters Experiment at 120°

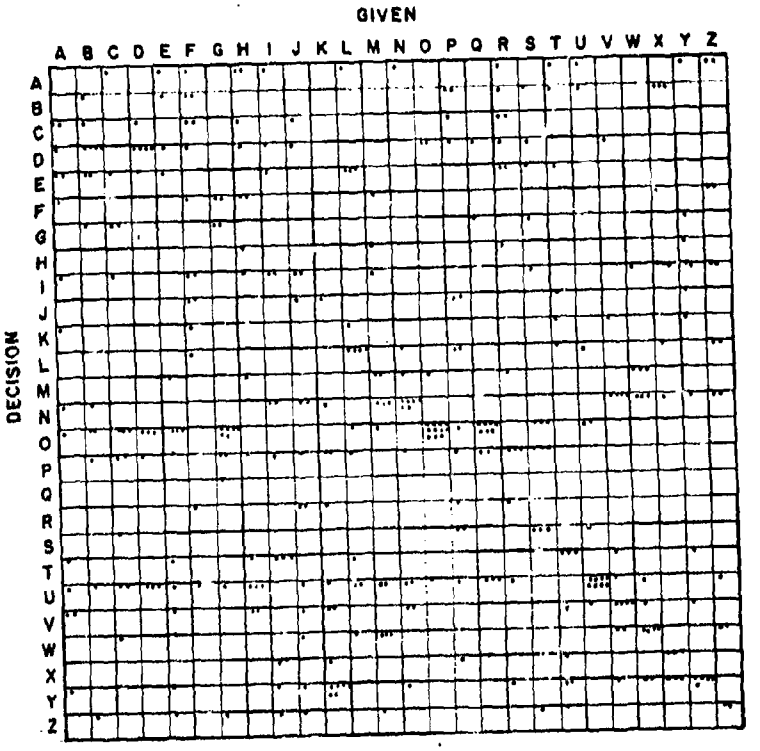


Confusion Matrix from
Identification of Rotated Letters Experiment at 150°

# Appendix C

## Tables of Euclidean Distance for Rotated Alphabet Letters

The Eudlidean distance for each letter at each angle referenced to itself at 0 degrees from 3×5, 5×5, 7×7, 9×9 square and circle spatial filters is given in this appendix in table form.

| LETTER | ANGLE (DEGREES) | | | | | |
|---|---|---|---|---|---|---|
| | 0 | 30 | 60 | 90 | 120 | 150 |
| A | 0. | 3.18 | 4.80 | 6.57 | 4.91 | 2.26 |
| B | 0. | 2.45 | 7.09 | 8.75 | 6.09 | 1.56 |
| C | 0. | 3.16 | 8.76 | 11.85 | 9.66 | 4.32 |
| D | 0. | 2.85 | 7.00 | 9.72 | 7.07 | 2.72 |
| E | 0. | 3.02 | 11.20 | 15.66 | 12.73 | 5.73 |
| F | 0. | 2.19 | 3.87 | 8.70 | 9.48 | 6.57 |
| G | 0. | 2.73 | 7.11 | 8.99 | 5.96 | 1.90 |
| H | 0. | 1.70 | 3.01 | 3.77 | 3.23 | 1.75 |
| I | 0. | 2.71 | 8.20 | 11.03 | 8.91 | 3.29 |
| J | 0. | 2.13 | 2.11 | 7.64 | 9.69 | 6.54 |
| K | 0. | 2.07 | 4.39 | 5.08 | 4.03 | 2.20 |
| L | 0. | 7.46 | 13.73 | 12.88 | 6.02 | 5.97 |
| M | 0. | 2.41 | 5.07 | 5.46 | 4.54 | 2.46 |
| N | 0. | 2.89 | 3.22 | 2.59 | 3.62 | 2.72 |
| O | 0. | 1.86 | 4.66 | 6.75 | 4.32 | 1.43 |
| P | 0. | 2.71 | 2.84 | 2.84 | 4.77 | 4.59 |
| Q | 0. | 3.65 | 7.86 | 8.74 | 5.31 | 2.66 |
| R | 0. | 1.01 | 3.08 | 4.02 | 3.24 | 2.76 |
| S | 0. | 5.01 | 10.80 | 11.79 | 7.23 | 1.51 |
| T | 0. | 4.22 | 10.93 | 13.35 | 10.09 | 6.43 |
| U | 0. | 2.96 | 2.51 | 3.36 | 2.65 | 3.53 |
| V | 0. | 3.37 | 5.06 | 5.20 | 4.79 | 3.10 |
| W | 0. | 0.59 | 2.01 | 2.24 | 2.69 | 1.02 |
| X | 0. | 2.32 | 6.68 | 8.23 | 5.98 | 2.84 |
| Y | 0. | 2.43 | 7.01 | 7.94 | 5.03 | 3.19 |
| Z | 0. | 2.28 | 12.61 | 15.93 | 17.67 | 7.36 |

Euclidean Distance for Each Letter at Angles of 30, 60, 90, 120, and 150 Degrees Referenced to Zero Degrees for the 3×3 Circle Filter

| LETTER | ANGLE (DEGREES) 0 | 30 | 60 | 90 | 120 | 150 |
|---|---|---|---|---|---|---|
| A | 0. | 19.36 | 27.73 | 23.25 | 12.00 | 13.42 |
| B | 0. | 7.44 | 11.25 | 11.22 | 10.77 | 5.21 |
| C | 0. | 13.37 | 21.93 | 20.00 | 17.28 | 13.51 |
| D | 0. | 9.96 | 15.21 | 13.34 | 12.95 | 10.04 |
| E | 0. | 16.35 | 24.04 | 23.37 | 21.43 | 20.00 |
| F | 0. | 15.07 | 24.51 | 20.19 | 24.04 | 19.50 |
| G | 0. | 8.70 | 14.24 | 13.75 | 14.33 | 10.13 |
| H | 0. | 18.31 | 24.41 | 23.12 | 20.21 | 17.82 |
| I | 0. | 17.44 | 30.33 | 33.13 | 32.42 | 19.31 |
| J | 0. | 14.04 | 22.45 | 22.77 | 30.55 | 24.39 |
| K | 0. | 13.34 | 16.04 | 13.02 | 17.96 | 13.49 |
| L | 0. | 23.46 | 33.03 | 33.32 | 33.74 | 32.05 |
| M | 0. | 18.51 | 23.41 | 20.95 | 21.78 | 20.79 |
| N | 0. | 19.20 | 24.34 | 19.21 | 23.03 | 13.45 |
| O | 0. | 4.49 | 7.68 | 9.64 | 5.89 | 3.59 |
| P | 0. | 12.32 | 14.99 | 13.93 | 12.24 | 13.10 |
| Q | 0. | 9.35 | 16.44 | 13.42 | 15.47 | 14.93 |
| R | 0. | 14.27 | 21.00 | 7.03 | 13.34 | 11.34 |
| S | 0. | 12.38 | 22.95 | 25.09 | 22.56 | 13.05 |
| T | 0. | 25.91 | 37.01 | 33.07 | 32.06 | 27.09 |
| U | 0. | 12.96 | 16.46 | 17.19 | 17.36 | 13.21 |
| V | 0. | 12.67 | 23.25 | 24.31 | 19.67 | 23.93 |
| W | 0. | 10.77 | 14.14 | 7.59 | 20.91 | 10.43 |
| X | 0. | 17.43 | 21.75 | 21.21 | 22.27 | 13.92 |
| Y | 0. | 20.45 | 28.49 | 25.28 | 17.51 | 19.49 |
| Z | 0. | 23.14 | 41.71 | 47.65 | 40.20 | 23.42 |

Euclidean Distance for Each Letter at Angles of 30, 60, 90, 120, and 150 Degrees
Referenced to Zero Degrees for the 5×5 Circle Filter

| LETTER | ANGLE (DEGREES) | | | | | |
|---|---|---|---|---|---|---|
| | 0 | 30 | 60 | 90 | 120 | 150 |
| A | 0. | 28.51 | 38.24 | 30.40 | 18.45 | 26.96 |
| B | 0. | 18.04 | 29.99 | 35.09 | 29.38 | 19.59 |
| C | 0. | 15.56 | 27.12 | 31.99 | 31.91 | 28.63 |
| D | 0. | 16.18 | 24.75 | 29.16 | 24.01 | 16.69 |
| E | 0. | 21.71 | 34.91 | 40.43 | 36.03 | 30.17 |
| F | 0. | 24.71 | 32.00 | 33.47 | 33.54 | 29.81 |
| G | 0. | 13.01 | 23.71 | 27.95 | 24.38 | 16.53 |
| H | 0. | 35.06 | 45.01 | 43.54 | 46.39 | 35.31 |
| I | 0. | 27.28 | 43.20 | 47.23 | 44.44 | 30.60 |
| J | 0. | 24.43 | 36.18 | 40.04 | 37.90 | 33.21 |
| K | 0. | 28.51 | 29.97 | 19.97 | 31.66 | 32.06 |
| L | 0. | 31.77 | 41.79 | 46.68 | 47.18 | 42.32 |
| M | 0. | 29.05 | 36.54 | 28.13 | 31.44 | 32.04 |
| N | 0. | 33.62 | 38.19 | 30.38 | 39.55 | 33.18 |
| O | 0. | 8.35 | 17.58 | 21.96 | 16.24 | 8.47 |
| P | 0. | 20.46 | 27.36 | 26.06 | 22.08 | 26.24 |
| Q | 0. | 14.36 | 23.31 | 25.64 | 24.64 | 19.60 |
| R | 0. | 24.68 | 28.51 | 28.65 | 31.44 | 28.79 |
| S | 0. | 16.44 | 28.84 | 33.39 | 30.56 | 19.73 |
| T | 0. | 33.46 | 45.02 | 48.78 | 42.05 | 34.13 |
| U | 0. | 25.89 | 31.57 | 31.83 | 31.53 | 27.51 |
| V | 0. | 36.69 | 42.49 | 34.30 | 28.46 | 39.03 |
| W | 0. | 27.14 | 25.86 | 23.50 | 23.70 | 22.01 |
| X | 0. | 32.16 | 34.32 | 24.15 | 34.37 | 31.72 |
| Y | 0. | 33.51 | 41.63 | 34.75 | 22.04 | 29.26 |
| Z | 0. | 29.64 | 46.00 | 51.18 | 42.63 | 25.84 |

Euclidean Distance for Each Letter at Angles of 30, 60, 90, 120, and 150 Degrees Referenced to Zero Degrees for the 7×7 Circle Filter

| LETTER | ANGLE (DEGREES) 0 | 30 | 60 | 90 | 120 | 150 |
|---|---|---|---|---|---|---|
| A | 0. | 35.36 | 43.14 | 34.80 | 27.72 | 31.20 |
| B | 0. | 28.55 | 45.07 | 51.72 | 45.61 | 31.40 |
| C | 0. | 23.37 | 38.63 | 43.56 | 43.23 | 35.34 |
| D | 0. | 23.58 | 35.42 | 41.23 | 35.55 | 27.07 |
| F | 0. | 34.52 | 52.01 | 60.01 | 50.10 | 41.35 |
| F | 0. | 36.90 | 46.20 | 47.36 | 47.86 | 44.82 |
| G | 0. | 23.95 | 38.88 | 44.73 | 40.80 | 29.82 |
| H | 0. | 39.98 | 50.01 | 47.92 | 50.90 | 40.73 |
| I | 0. | 37.26 | 51.99 | 51.21 | 51.78 | 41.46 |
| J | 0. | 31.89 | 42.34 | 48.90 | 47.80 | 45.50 |
| K | 0. | 43.50 | 41.71 | 33.50 | 42.39 | 44.62 |
| L | 0. | 42.13 | 49.81 | 53.26 | 53.81 | 49.75 |
| M | 0. | 36.35 | 41.57 | 33.60 | 35.75 | 36.99 |
| N | 0. | 40.49 | 43.38 | 33.65 | 43.51 | 40.32 |
| O | 0. | 13.93 | 24.76 | 28.16 | 23.28 | 14.06 |
| P | 0. | 26.89 | 35.65 | 39.63 | 36.53 | 42.99 |
| Q | 0. | 18.81 | 29.09 | 31.28 | 30.03 | 24.83 |
| R | 0. | 34.60 | 40.89 | 46.04 | 45.94 | 44.57 |
| S | 0. | 29.63 | 45.46 | 50.26 | 47.68 | 32.02 |
| T | 0. | 42.86 | 51.07 | 57.74 | 50.96 | 41.89 |
| U | 0. | 32.93 | 37.95 | 40.23 | 40.31 | 36.07 |
| V | 0. | 43.59 | 49.53 | 41.91 | 35.41 | 43.78 |
| W | 0. | 45.85 | 41.05 | 37.35 | 36.95 | 37.14 |
| X | 0. | 45.76 | 41.01 | 34.42 | 40.68 | 45.45 |
| Y | 0. | 45.18 | 49.13 | 40.89 | 32.26 | 38.05 |
| Z | 0. | 38.31 | 50.29 | 60.51 | 48.17 | 35.81 |

Euclidean Distance for Each Letter at Angles of 30, 60, 90, 120, and 150 Degrees Referenced to Zero Degrees for the 9×9 Circle Filter

| LETTER | ANGLE (DEGREES) | | | | | |
|---|---|---|---|---|---|---|
| | 0 | 30 | 60 | 90 | 120 | 150 |
| A | 0. | 6.88 | 9.50 | 7.78 | 5.91 | 5.93 |
| B | 0. | 5.74 | 8.33 | 7.03 | 6.49 | 5.95 |
| C | 0. | 8.10 | 12.86 | 13.67 | 12.79 | 11.24 |
| D | 0. | 6.55 | 9.54 | 10.17 | 9.23 | 7.16 |
| E | 0. | 11.29 | 17.29 | 17.10 | 15.79 | 12.73 |
| F | 0. | 8.80 | 13.92 | 13.40 | 10.34 | 8.14 |
| G | 0. | 5.70 | 8.50 | 8.63 | 9.79 | 6.93 |
| H | 0. | 4.78 | 5.82 | 7.03 | 6.05 | 5.20 |
| I | 0. | 8.70 | 12.18 | 11.77 | 12.58 | 8.03 |
| J | 0. | 9.57 | 16.00 | 15.38 | 12.53 | 9.57 |
| K | 0. | 4.50 | 6.62 | 6.81 | 7.24 | 7.49 |
| L | 0. | 9.59 | 15.59 | 19.50 | 20.82 | 14.82 |
| M | 0. | 6.27 | 8.80 | 7.47 | 7.91 | 7.27 |
| N | 0. | 4.75 | 9.40 | 10.31 | 8.17 | 5.44 |
| O | 0. | 3.57 | 5.45 | 6.83 | 5.52 | 3.60 |
| P | 0. | 5.76 | 9.84 | 10.25 | 7.74 | 5.67 |
| Q | 0. | 5.55 | 8.52 | 10.19 | 10.76 | 7.54 |
| R | 0. | 2.18 | 4.86 | 4.96 | 4.74 | 6.31 |
| S | 0. | 7.56 | 11.22 | 14.05 | 15.01 | 9.70 |
| T | 0. | 11.40 | 14.90 | 13.49 | 14.54 | 12.63 |
| U | 0. | 4.02 | 6.20 | 7.65 | 5.64 | 7.73 |
| V | 0. | 6.25 | 10.13 | 9.78 | 7.27 | 10.62 |
| W | 0. | 4.04 | 5.22 | 4.48 | 4.45 | 4.88 |
| X | 0. | 6.36 | 9.30 | 8.29 | 8.42 | 5.65 |
| Y | 0. | 7.59 | 9.61 | 8.47 | 7.59 | 7.71 |
| Z | 0. | 10.54 | 25.15 | 22.92 | 18.12 | 11.59 |

Euclidean Distance for Each Letter at Angles of 30, 60, 90, 120, and 150 Degrees Referenced to Zero Degrees for the 3X3 Square Filter

| | LETTER ANGLE (DEGREES) | | | | | |
|---|---|---|---|---|---|---|
| | 0 | 30 | 60 | 90 | 120 | 150 |
| A | 0. | 22.76 | 30.05 | 23.84 | 14.40 | 21.48 |
| B | 0. | 10.84 | 13.88 | 11.45 | 14.57 | 12.06 |
| C | 0. | 14.13 | 24.93 | 29.22 | 28.52 | 26.00 |
| D | 0. | 12.05 | 17.41 | 16.47 | 14.09 | 12.15 |
| E | 0. | 16.79 | 29.60 | 33.55 | 32.13 | 26.07 |
| F | 0. | 17.34 | 25.35 | 26.48 | 25.96 | 21.04 |
| G | 0. | 10.18 | 16.13 | 17.24 | 14.83 | 10.59 |
| H | 0. | 24.49 | 30.57 | 23.22 | 30.48 | 25.08 |
| I | 0. | 21.31 | 34.81 | 36.17 | 35.56 | 24.50 |
| J | 0. | 19.14 | 32.16 | 34.23 | 32.58 | 25.23 |
| K | 0. | 19.93 | 21.15 | 13.53 | 24.13 | 23.27 |
| L | 0. | 24.50 | 36.55 | 39.52 | 37.85 | 34.57 |
| M | 0. | 22.54 | 28.76 | 22.46 | 25.71 | 26.79 |
| N | 0. | 22.62 | 30.69 | 21.81 | 26.64 | 23.59 |
| O | 0. | 5.65 | 8.49 | 10.12 | 8.37 | 5.45 |
| P | 0. | 14.35 | 20.75 | 17.70 | 13.58 | 15.38 |
| Q | 0. | 11.15 | 19.16 | 20.11 | 20.30 | 17.52 |
| R | 0. | 15.03 | 17.00 | 9.92 | 17.46 | 17.35 |
| S | 0. | 13.30 | 24.53 | 27.31 | 23.65 | 14.21 |
| T | 0. | 26.62 | 38.39 | 38.12 | 34.88 | 31.05 |
| U | 0. | 17.30 | 20.55 | 17.29 | 21.51 | 21.77 |
| V | 0. | 24.36 | 33.51 | 26.34 | 21.12 | 32.59 |
| W | 0. | 14.51 | 14.73 | 7.68 | 14.04 | 15.17 |
| X | 0. | 21.97 | 27.29 | 21.30 | 26.16 | 22.97 |
| Y | 0. | 22.64 | 31.69 | 26.03 | 15.87 | 23.75 |
| Z | 0. | 25.59 | 43.96 | 50.24 | 41.29 | 23.52 |

Euclidean Distance for Each Letter at Angles of 30, 60, 90, 120, and 150 Degrees Referenced to Zero Degrees for the 5×5 Square Filter

| | LETTER ANGLE (DEGREES) | | | | | |
|---|---|---|---|---|---|---|
| | 0 | 30 | 60 | 90 | 120 | 150 |
| A | 0. | 33.75 | 41.10 | 33.07 | 23.90 | 29.87 |
| B | 0. | 24.87 | 35.75 | 36.38 | 36.89 | 27.37 |
| C | 0. | 20.31 | 31.78 | 34.12 | 35.86 | 32.53 |
| D | 0. | 19.33 | 29.69 | 30.12 | 29.34 | 23.79 |
| E | 0. | 28.01 | 42.46 | 41.41 | 39.38 | 36.43 |
| F | 0. | 31.78 | 37.70 | 37.25 | 39.77 | 35.49 |
| G | 0. | 19.34 | 30.40 | 31.73 | 30.60 | 23.92 |
| H | 0. | 38.40 | 47.64 | 43.73 | 46.72 | 39.01 |
| I | 0. | 32.34 | 48.03 | 47.33 | 44.16 | 36.47 |
| J | 0. | 27.27 | 38.24 | 41.83 | 40.99 | 37.69 |
| K | 0. | 38.07 | 35.65 | 24.03 | 38.06 | 33.25 |
| L | 0. | 36.24 | 45.32 | 47.69 | 50.45 | 44.73 |
| M | 0. | 31.23 | 39.06 | 30.29 | 32.65 | 34.29 |
| N | 0. | 38.98 | 41.91 | 32.64 | 42.41 | 37.32 |
| O | 0. | 12.89 | 20.72 | 21.64 | 20.09 | 12.64 |
| P | 0. | 25.87 | 30.71 | 30.95 | 29.41 | 34.51 |
| Q | 0. | 17.23 | 25.61 | 26.74 | 26.69 | 21.89 |
| R | 0. | 32.32 | 35.67 | 33.53 | 39.12 | 37.65 |
| S | 0. | 25.79 | 36.62 | 35.62 | 36.56 | 25.04 |
| T | 0. | 37.98 | 47.99 | 48.93 | 44.80 | 37.51 |
| U | 0. | 30.69 | 34.63 | 34.98 | 36.08 | 32.81 |
| V | 0. | 41.21 | 46.31 | 37.85 | 31.14 | 42.15 |
| W | 0. | 32.89 | 33.52 | 27.96 | 28.05 | 31.28 |
| X | 0. | 41.43 | 38.29 | 32.64 | 36.56 | 40.68 |
| Y | 0. | 39.53 | 46.22 | 37.83 | 26.35 | 35.82 |
| Z | 0. | 32.18 | 47.20 | 54.10 | 46.38 | 33.62 |

Euclidean Distance for Each Letter at Angles of 30, 60, 90, 120, and 150 Degrees Referenced to Zero Degrees for the 7×7 Square Filter

| | LETTER ANGLE (DEGREES) | | | | | |
|---|---|---|---|---|---|---|
| | 0 | 30 | 60 | 90 | 120 | 150 |
| A | 0. | 39.23 | 45.51 | 56.66 | 51.62 | 34.6[illegible] |
| B | 0. | 30.34 | 46.93 | 52.58 | 47.32 | 33.[illegible] |
| C | 0. | 26.32 | 41.01 | 46.56 | 47.76 | [illegible] |
| D | 0. | 26.[illegible]3 | 37.84 | 41.79 | 38.1[illegible] | [illegible] |
| E | 0. | 36.63 | 50.26 | 61.2[illegible] | 53.62 | 43.72 |
| F | 0. | 40.77 | 45.7[illegible] | 50.88 | 51.3[illegible] | [illegible] |
| G | 0. | 26.48 | 41.66 | 47.1[illegible] | 43.8[illegible] | 34.76 |
| H | 0. | 41.37 | 12.66 | 46.10 | 53.2[illegible] | [illegible] |
| I | 0. | 43.[illegible]7 | 54.21 | [illegible] | [illegible] | [illegible] |
| J | 0. | 36.32 | 46.71 | 51.24 | 51.96 | 41.44 |
| K | 0. | 49.54 | 45.67 | 44.[illegible]7 | 44.42 | 46.96 |
| L | 0. | 45.51 | [illegible]3.68 | 54.16 | 56.[illegible] | [illegible]2.30 |
| M | 0. | 42.61 | 45.1[illegible] | 35.6[illegible] | 41.[illegible]6 | 43.47 |
| N | 0. | 43.55 | 47.47 | 37.96 | 47.[illegible] | [illegible] |
| O | 0. | 15.[illegible]9 | 26.46 | 2[illegible].1[illegible] | 2[illegible].[illegible] | 16.81 |
| P | 0. | 30.66 | 39.21 | 41.74 | 4[illegible].9[illegible] | [illegible] |
| Q | 0. | 23.16 | 41.76 | [illegible].46 | 34.7[illegible] | 23.67 |
| R | 0. | 37.42 | 44.44 | [illegible].54 | 47.77 | [illegible] |
| S | 0. | 35.[illegible]3 | 4[illegible].[illegible]6 | 41.7[illegible] | [illegible].4[illegible] | [illegible].[illegible] |
| T | 0. | 45.[illegible]8 | [illegible]4.3[illegible] | [illegible]9.1[illegible] | [illegible].59 | [illegible].91 |
| U | 0. | 3[illegible].64 | 3[illegible].[illegible]2 | [illegible].[illegible]3 | 42.[illegible] | [illegible] |
| V | 0. | 47.23 | [illegible]2.7[illegible] | [illegible].87 | [illegible].[illegible] | [illegible].[illegible] |
| W | 0. | [illegible]6.26 | [illegible]3.26 | [illegible]3.17 | [illegible].[illegible] | [illegible].[illegible] |
| X | 0. | [illegible]3.38 | 42.[illegible] | [illegible].[illegible] | [illegible].[illegible] | [illegible].[illegible] |
| Y | 0. | [illegible]2.6[illegible] | [illegible].[illegible] | [illegible].[illegible] | [illegible].[illegible] | [illegible].[illegible] |
| Z | 0. | 41.[illegible]6 | [illegible].[illegible] | [illegible].[illegible] | [illegible].[illegible] | [illegible].[illegible] |

Euclidean Distance for Each Letter at Angles of 30, 60, 90, 120, and 150 Degrees Referenced to Zero Degrees for the 9×9 Square Filter

Appendix D

## Graphs of Euclidean Distance for Rotated Alphabet Letters

The Euclidean distance for each letter at each angle referenced to itself at 0 degrees from 3×5, 5×5, 7×7, 9×9 square and circle spatial filters is given in this appendix in graph form.

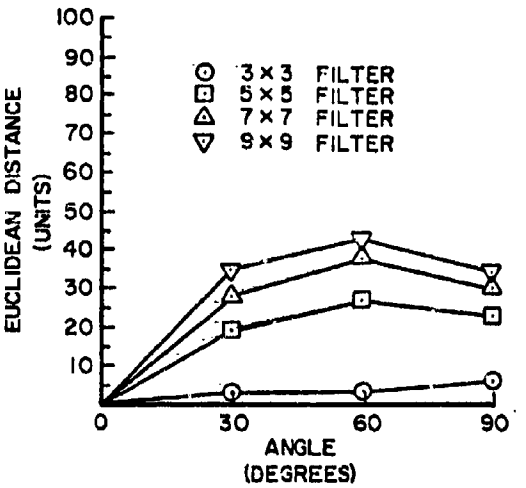


Circle Filter

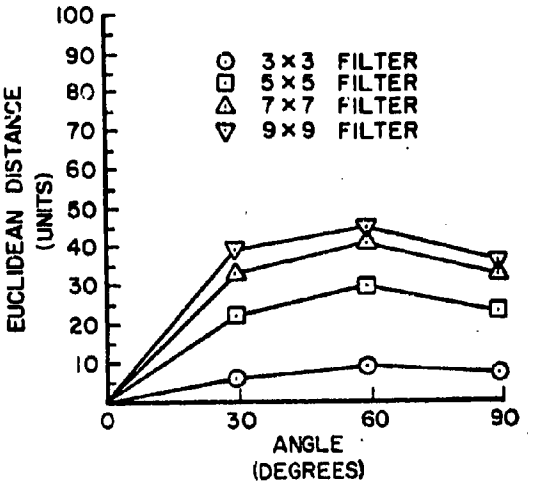


Square Filter

Letter A

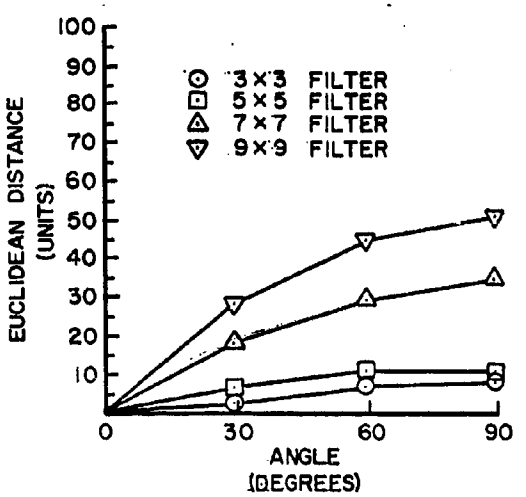


Circle Filter

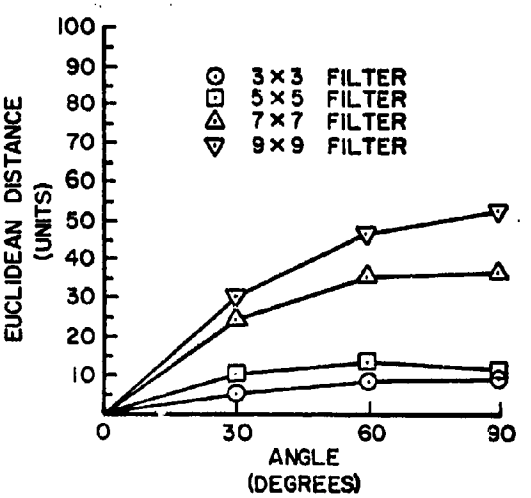


Square Filter

Letter B

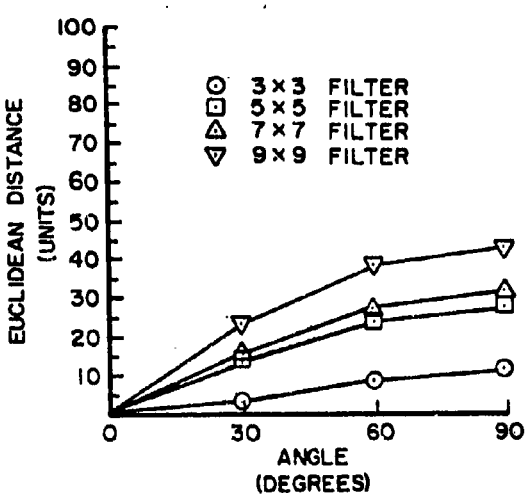


Circle Filter

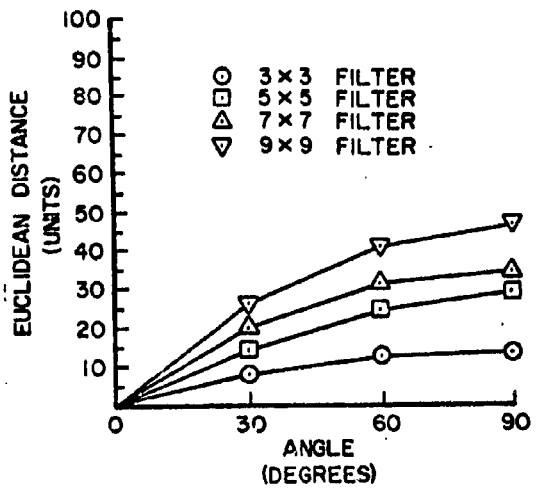


Square Filter

Letter C

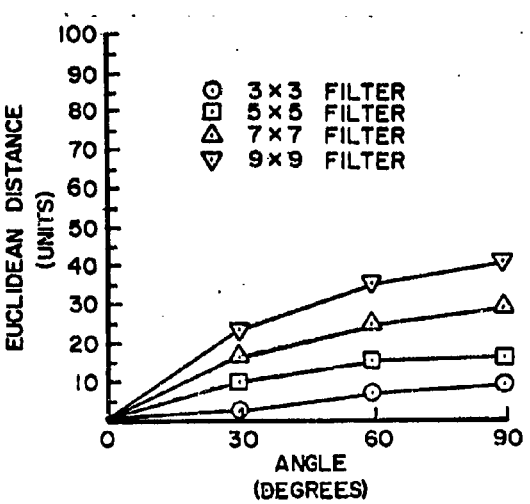


Circle Filter

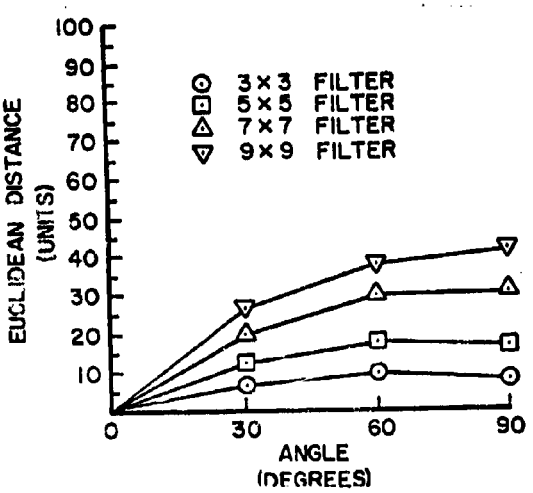


Square Filter

Letter D

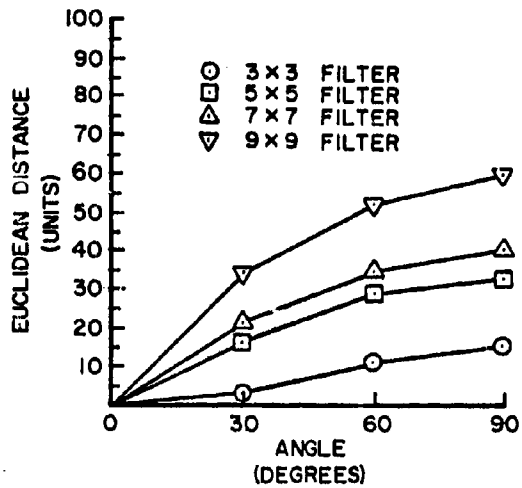


Circle Filter

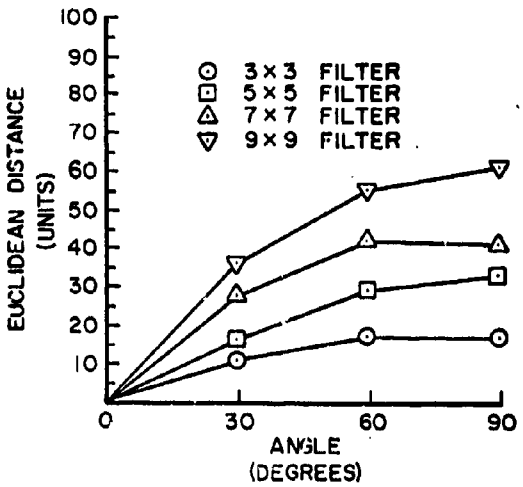


Square Filter

Letter E

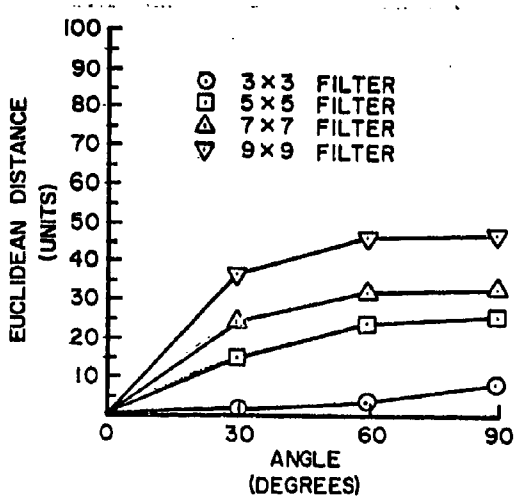


Circle Filter

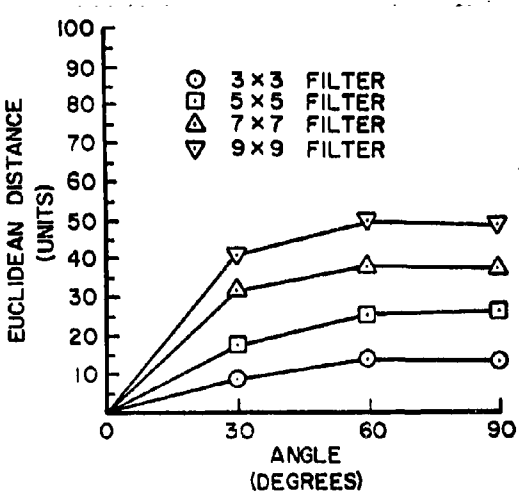


Square Filter

Letter F

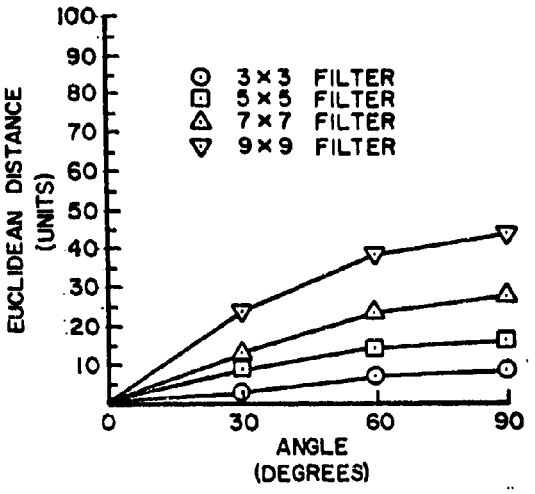


Circle Filter

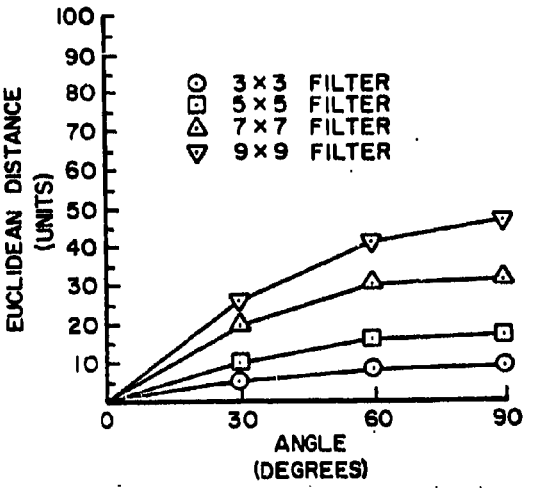


Square Filter

Letter G

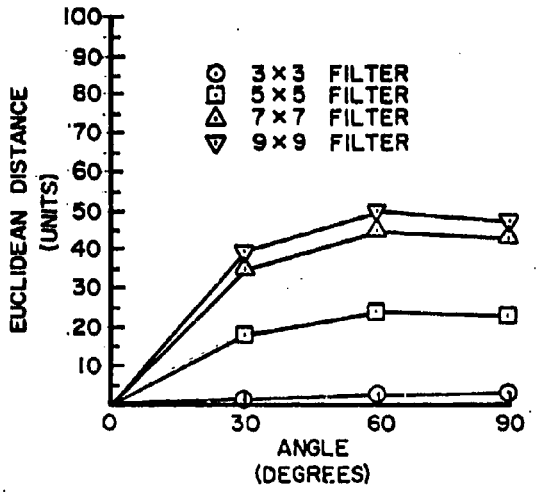


Circle Filter

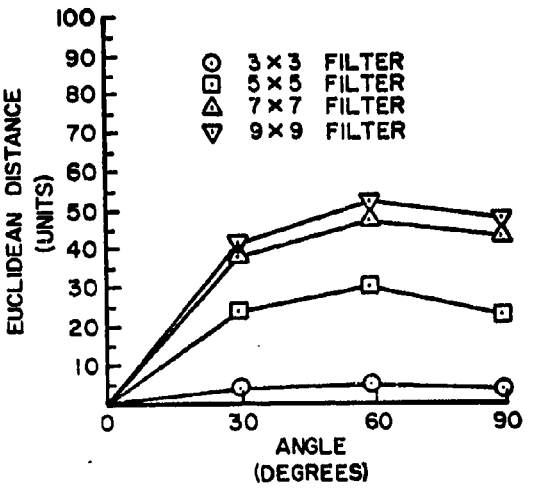


Square Filter

Letter H

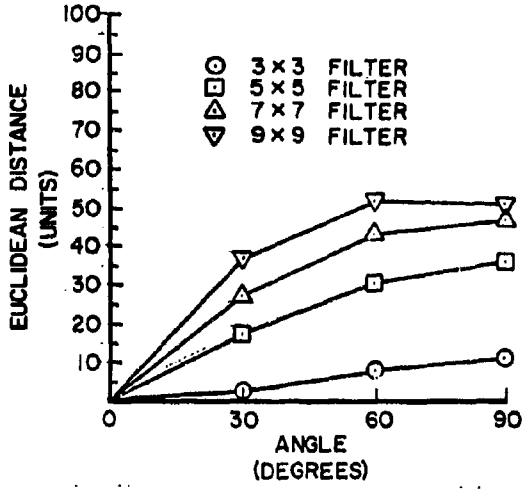


Circle Filter

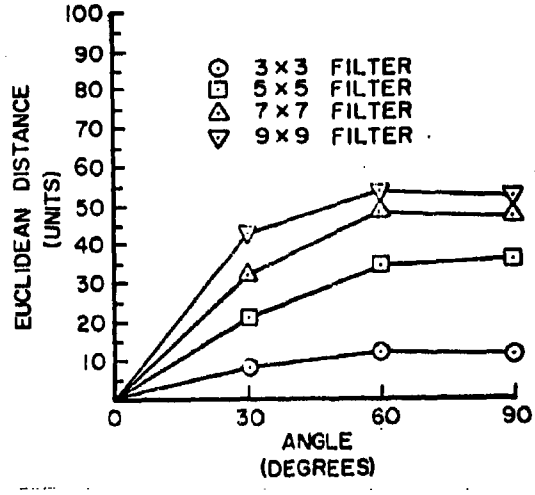


Square Filter

Letter I

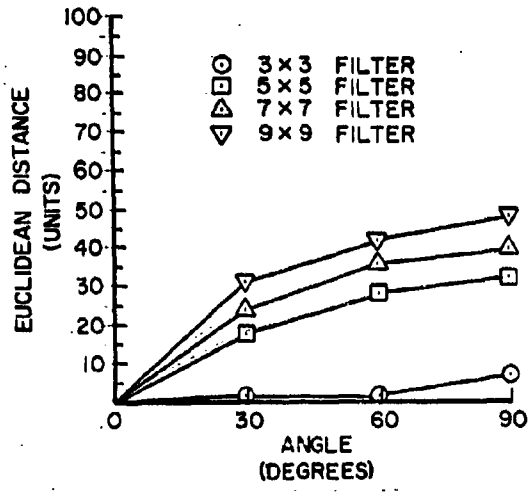


Circle Filter

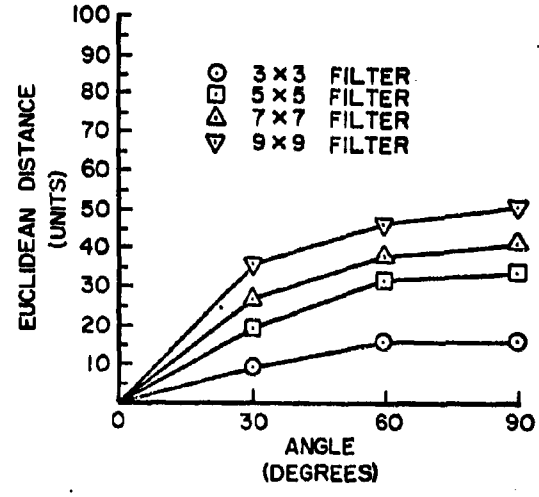


Square Filter

Letter J

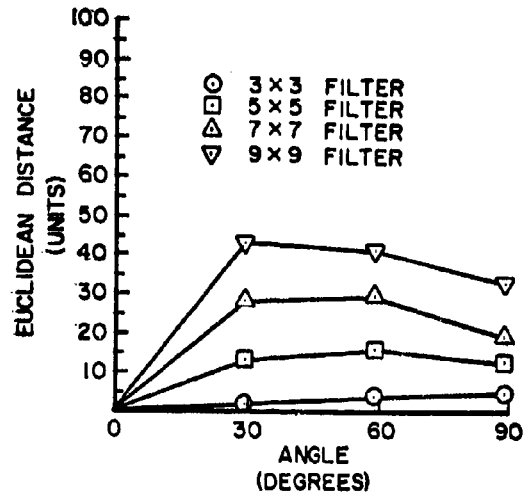


Circle Filter

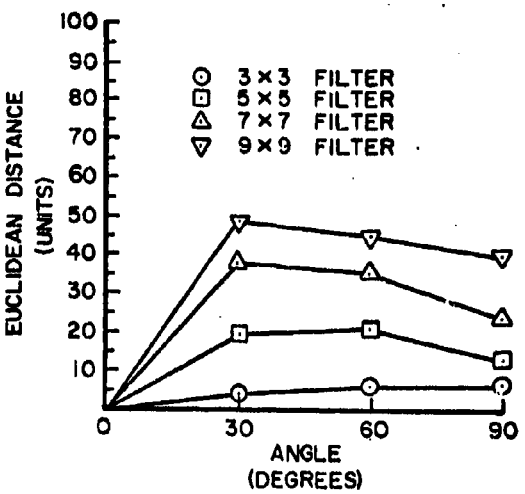


Square Filter

Letter K

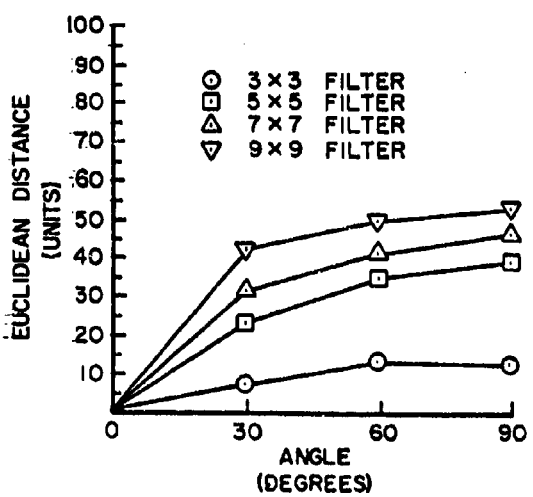


Circle Filter

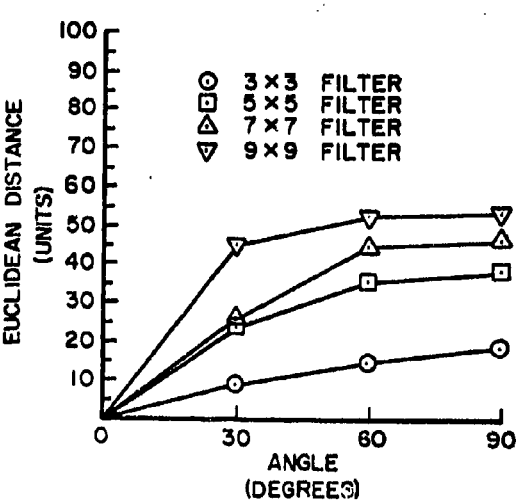


Square Filter

Letter L

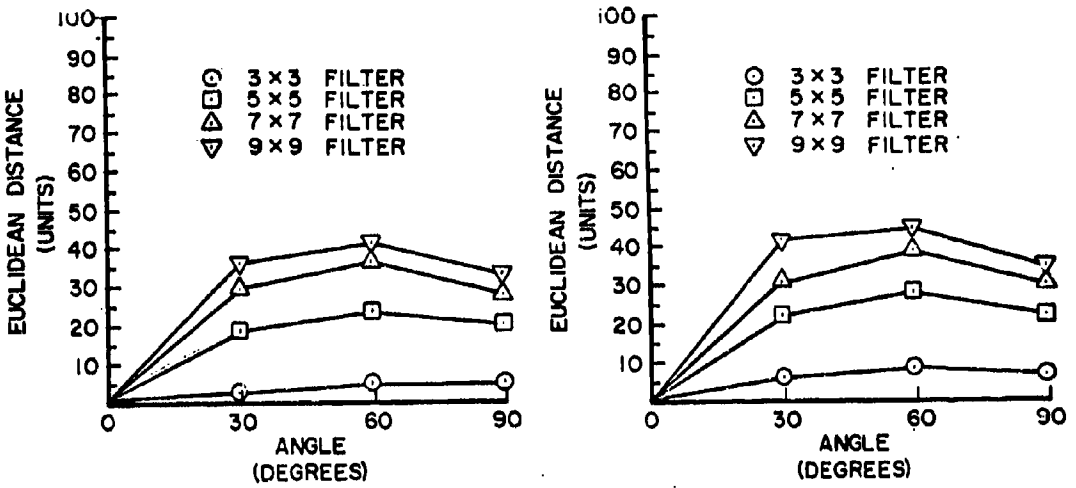


Circle Filter

Square Filter

Letter M

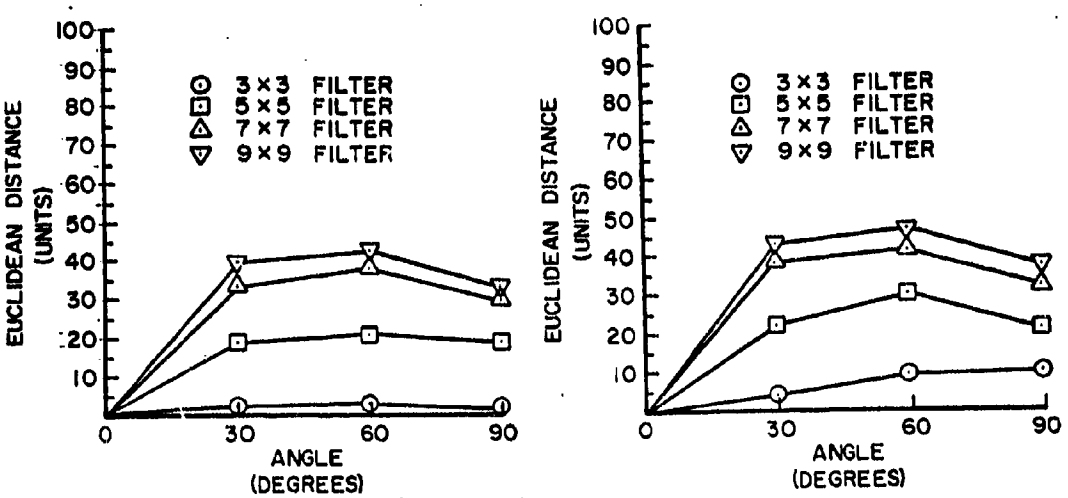


Circle Filter

Square Filter

Letter N

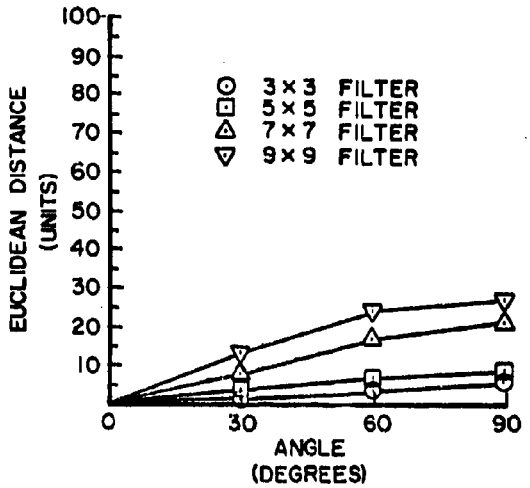


Circle Filter

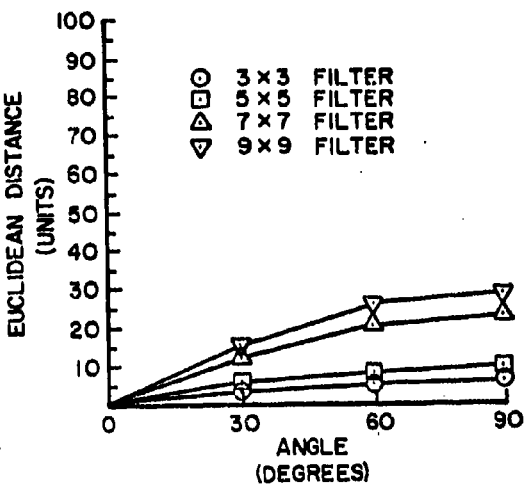


Square Filter

Letter O

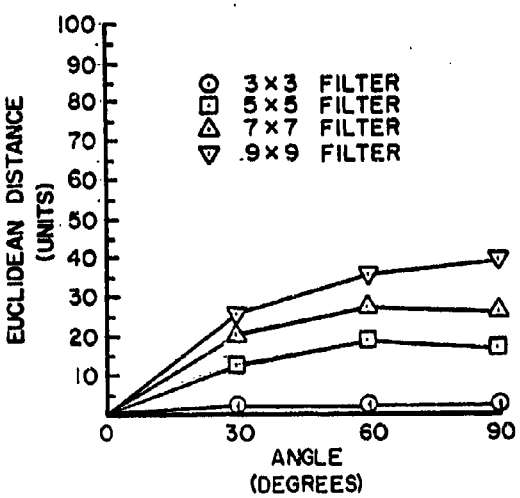


Circle Filter

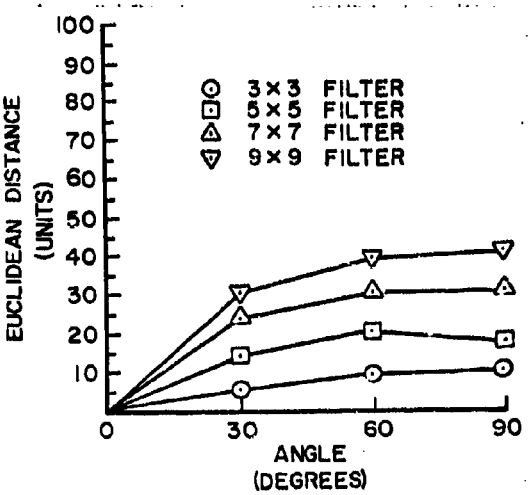


Square Filter

Letter P

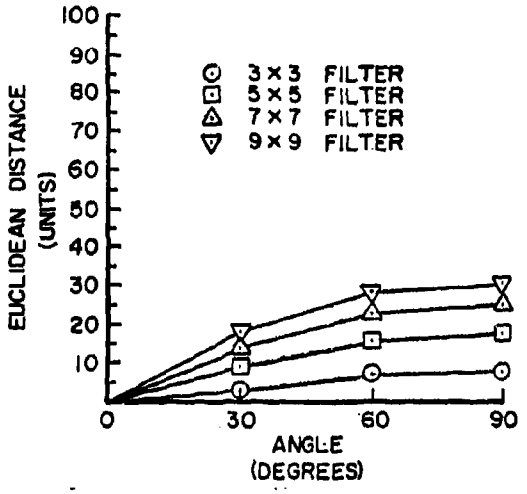


Circle Filter

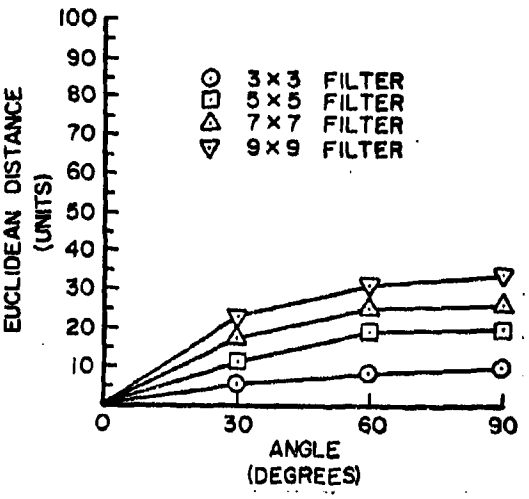


Square Filter

Letter Q

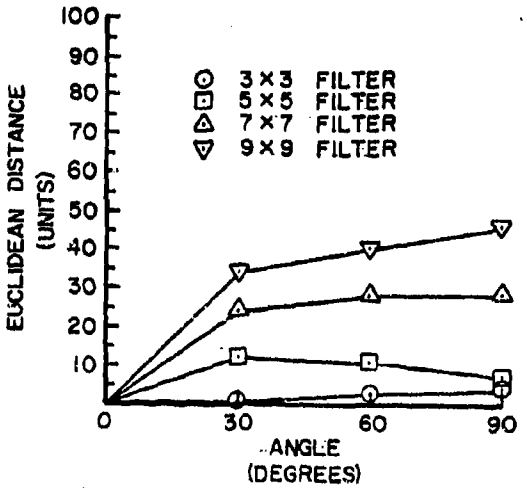


Circle Filter

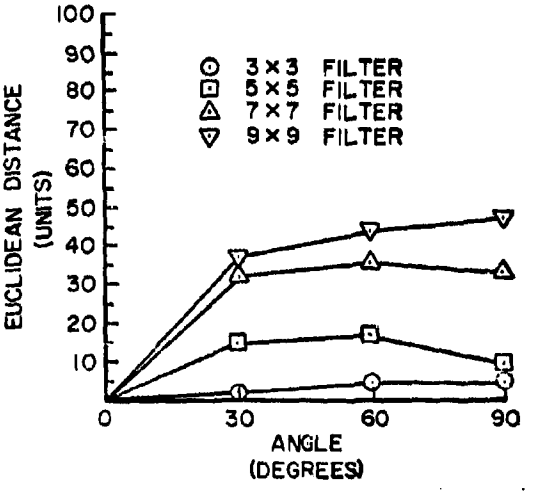


Square Filter

Letter R

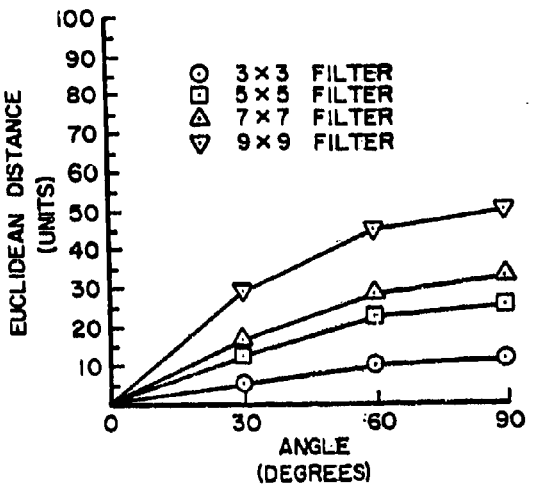


Circle Filter

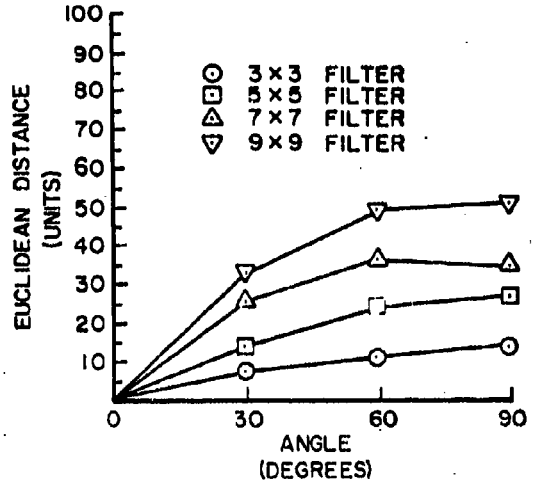


Square Filter

Letter S

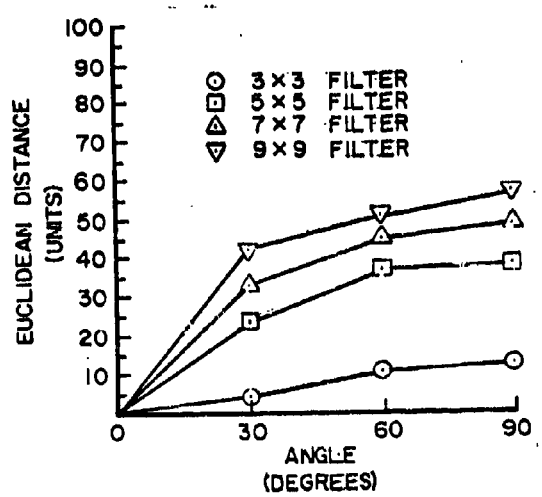


Circle Filter

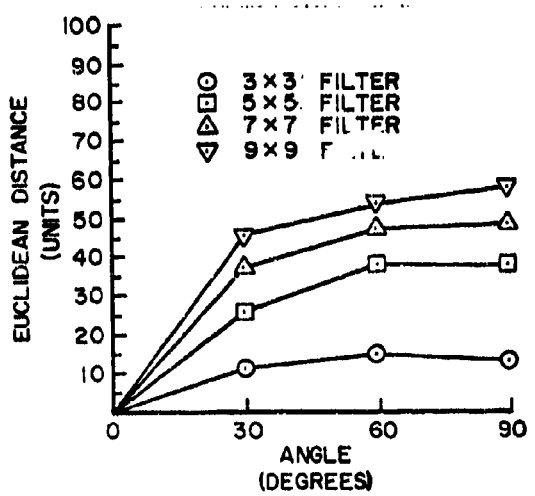


Square Filter

Letter T

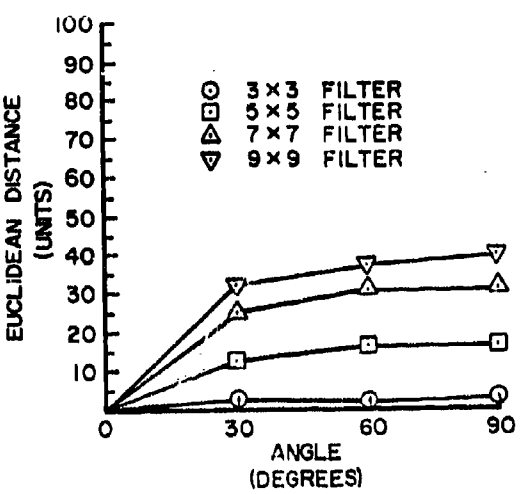


Circle Filter

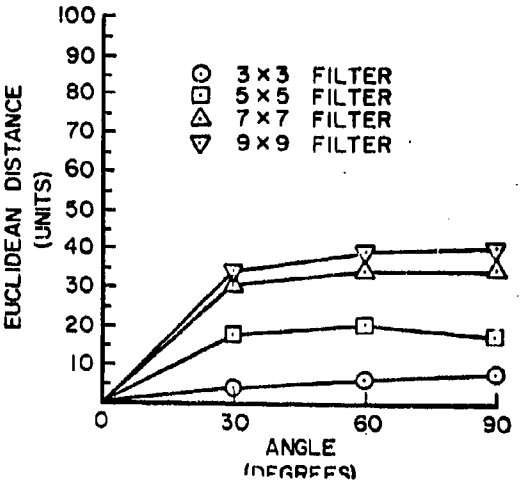


Square Filter

Letter U

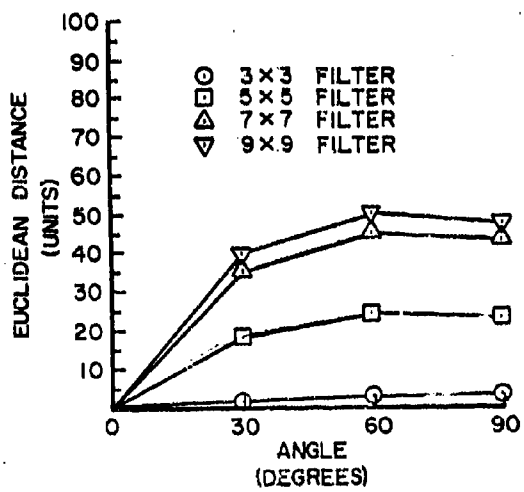


Circle Filter

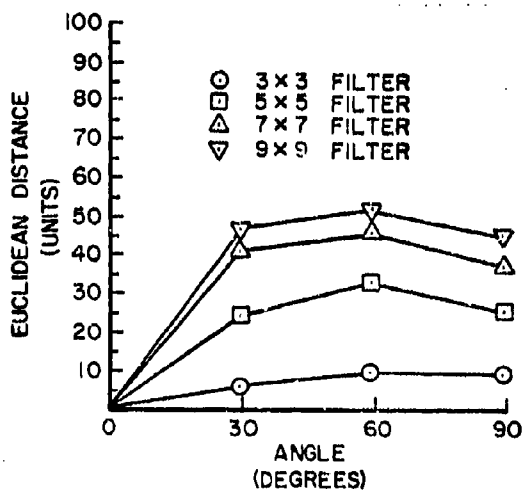


Square Filter

Letter V

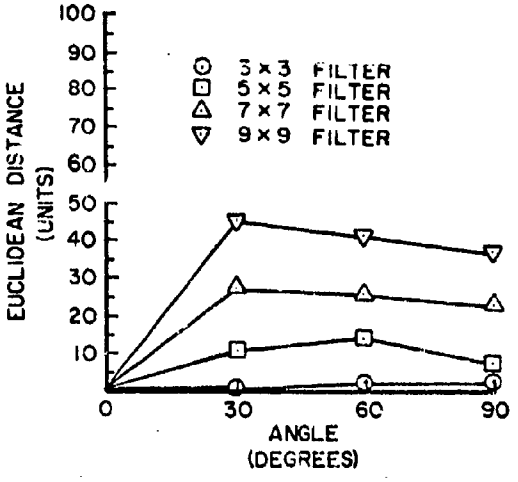


Circle Filter

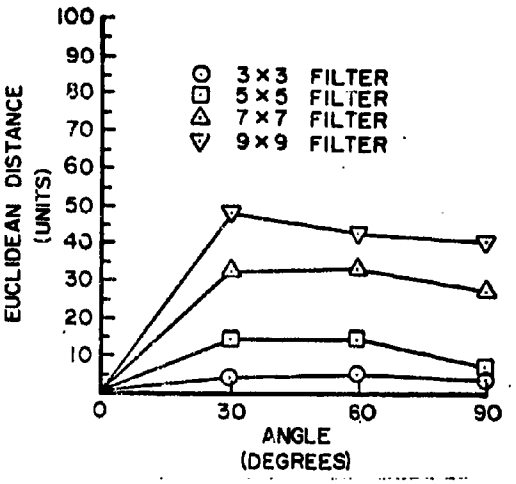


Square Filter

Letter W

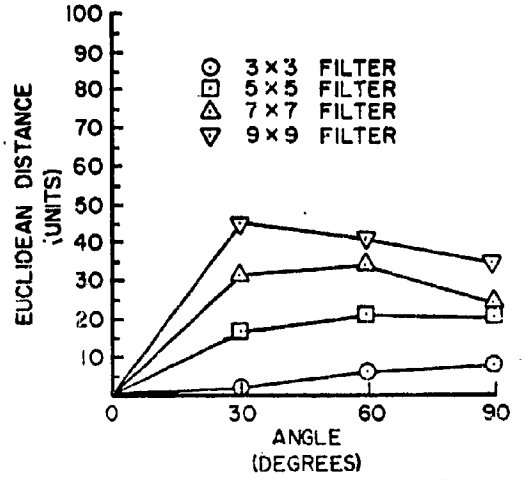


Circle Filter

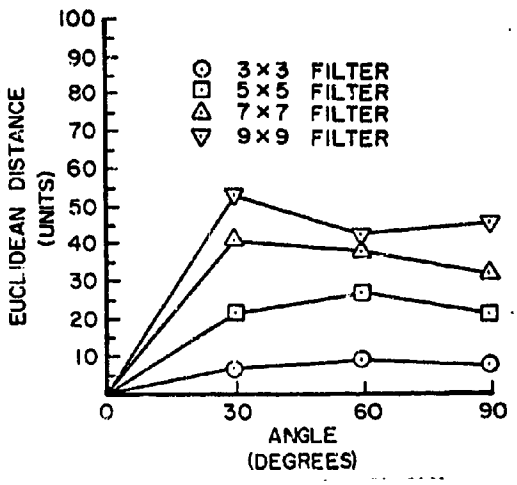


Square Filter

Letter X

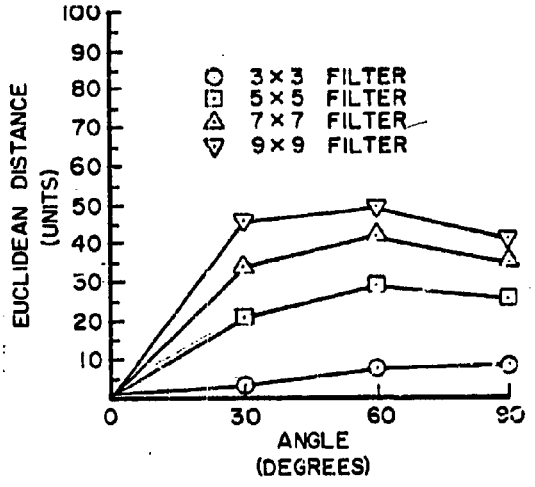


Circle Filter

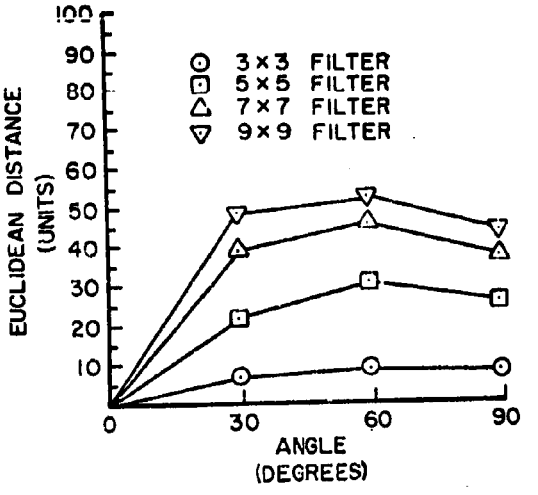


Square Filter

Letter Y

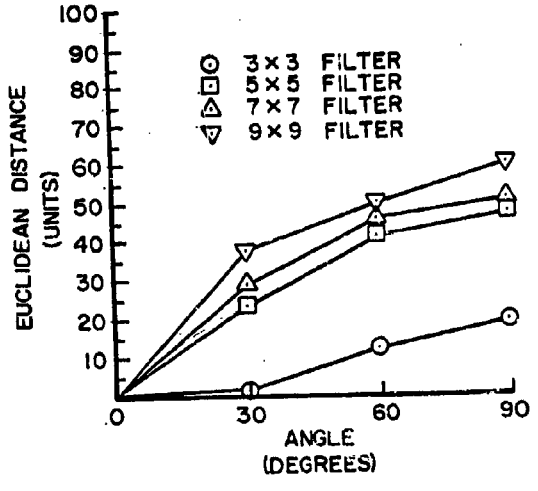


Circle Filter

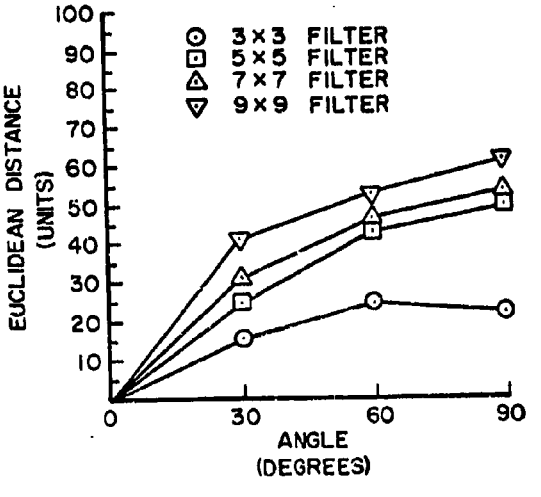


Square Filter

Letter Z